

JOURNAL OF LIQUID CHROMATOGRAPHY

VOLUME 6 NUMBER 10

1983

Special Issue

LIQUID CHROMATOGRAPHY

PART 1

ATES

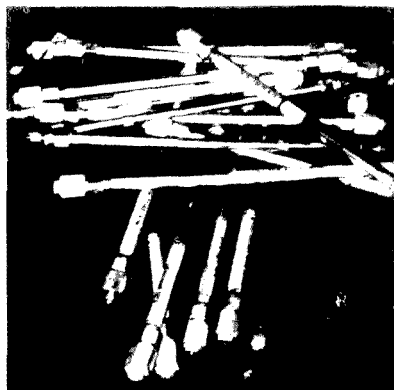
GPC

COLUMN REGENERATION SERVICE

μ STYRAGEL™
SHODEX

TOYO SODA
 μ BONDAGEL™

ULTRA STYRAGEL™
 μ SPHEROGEL™



All of these GPC columns give excellent performance. However, when they fail for various reasons (many of which are beyond your control) you must replace them at great expense. The GPC gels themselves NEVER WEAR OUT and may be used over and over as often as necessary!

ASI can clean and repack any 10 micron GPC packing to *exceed* new column specifications. All columns are unconditionally guaranteed for *in use* performance. Regardless of responsibility, if an ASI repacked column fails for *any reason* within the warranty period, it will be repaired at no additional cost.

Compare the performance, warranty and price and you will see that ASI offers a truly remarkable value.

REPACKED BY ASI

REPLACEMENT COST

PERFORMANCE	WARRANTY	PRICE	COLUMN TYPE	PERFORMANCE	WARRANTY	PRICE
20,000 μ m	120 days	\$250	WATERS ASSOC μ STYRAGEL™	9000-12000 μ m	?	\$595
30,000	90	\$350	WATERS ASSOC ULTRASTYRAGEL™	46,000	?	\$675
20,000	120	\$250-500	TOYO SODA (TS-7)	20,000	?	\$630-1050
20,000	120	\$250-500	SHODEX	20,000	30 DAYS	\$750-1080
20,000	120	\$250	BECKMAN μ SPHEROGEL™	20,000	30 ?	\$620
15,000	90	\$175	WATERS ASSOC μ BONDAGEL™	?	?	\$405-495



ANALYTICAL SCIENCES INCORPORATED

SUITE B-24, AIRPORT PARK • 1400 COLEMAN AVENUE • SANTA CLARA, CALIF. 95050 • (408) 779-0131

... THE WORLD'S FINEST LIQUID CHROMATOGRAPHY COLUMNS

Circle Reader Service Card No. 101

JOURNAL OF LIQUID CHROMATOGRAPHY

Editor: DR. JACK CAZES Editorial Secretary: ELEANOR CAZES
P. O. Box 1440-SMS
Fairfield, Connecticut 06430

Editorial Board

- E. W. ALBAUGH, *Gulf Research and Development Company, Pittsburgh, Pennsylvania*
K. ALTGELT, *Chevron Research Company, Richmond, California*
A. ASZALOS, *U.S. Food and Drug Administration, Washington, D. C.*
H. BENOIT, *Centre des Recherches sur les Macromolécules, Strasbourg, France*
W. BERTSCH, *University of Alabama, University, Alabama*
B. BIDLINGMEYER, *Waters Associates, Inc., Milford, Massachusetts*
P. R. BROWN, *University of Rhode Island, Kingston, Rhode Island*
J. A. CAMERON, *University of Connecticut, Storrs, Connecticut*
J. V. DAWKINS, *Loughborough University of Technology, Loughborough, England*
J. E. FIGUERUELO, *University of Valencia, Burjasot, Spain*
D. H. FREEMAN, *University of Maryland, College Park, Maryland*
R. W. FREI, *The Free University, Amsterdam, The Netherlands*
J. C. GIDDINGS, *University of Utah, Salt Lake City, Utah*
R. L. GROB, *Villanova University, Villanova, Pennsylvania*
E. GRUSHKA, *The Hebrew University, Jerusalem, Israel*
G. GUIOCHON, *Ecole Polytechnique, Palaiseau, France*
M. GURKIN, *E-M Science, Inc., Gibbstown, New Jersey*
A. E. HAMIELEC, *McMaster University, Hamilton, Ontario, Canada*
S. HARA, *Tokyo College of Pharmacy, Tokyo, Japan*
D. J. HARMON, *B. F. Goodrich Research Center, Brecksville, Ohio*
G. L. HAWK, *Zymark Corporation, Hopkinton, Massachusetts*
M. T. W. HEARN, *St. Vincent's School of Medical Research, Victoria, Australia*
E. HEFTMANN, *U.S. Department of Agriculture, Berkeley, California*
A. HEYRAUD, *Centre National de la Recherche Scientifique, France*
P. Y. HOWARD, *Micromeritics Instrument Corp., Norcross, Georgia*
H. J. ISSAQ, *Frederick Cancer Research Facility, Frederick, Maryland*
J. JANCA, *Institute of Analytical Chemistry, Brno, Czechoslovakia*
J. F. JOHNSON, *Institute of Materials Science - U. Conn., Storrs, Connecticut*
B. L. KARGER, *Northeastern University, Boston, Massachusetts*
P. T. KISSINGER, *Purdue University, West Lafayette, Indiana*
J. KNOX, *The University of Edinburgh, Edinburgh, Scotland*
J. C. KRAAK, *University of Amsterdam, Amsterdam, The Netherlands*
J. LESEC, *Ecole Supérieure de Physique et de Chimie, Paris, France*
B. MONRABAL, *Dow Chemical Iberica, S. A., Tarragona, Spain*
S. MORI, *Mie University, Tsu, Mie, Japan*
A. K. MUKHERJI, *Xerox Corporation, Webster, New York*
J. A. NELSON, *M. D. Anderson Hospital and Tumor Institute, Houston, Texas*
L. PAPAZIAN, *American Cyanamid Corporation, Stamford, Connecticut*
V. PRETORIUS, *University of Pretoria, Pretoria, South Africa*
QIAN RENYUAN, *Institute of Chemistry, Beijing, People's Republic of China*

(continued)

JOURNAL OF LIQUID CHROMATOGRAPHY

Editorial Board *continued*

- C. QUIVORON, *Ecole Superieure de Physique et de Chemie, Paris, France*
F. M. RABEL, *Whatman, Inc., Clifton, New Jersey*
J. RIVIER, *The Salk Institute, San Diego, California*
C. G. SCOTT, *Hoffman-LaRoche, Inc., Nutley, New Jersey*
R. P. W. SCOTT, *Perkin-Elmer Corporation, Norwalk, Connecticut*
H. SMALL, *Dow Chemical Company, Midland, Michigan*
E. SOCZEWSKI, *Medical Academy, Lubin, Poland*
E. STAHL, *Universitat des Saarlandes, Saarbrucken, West Germany*
B. STENLUND, *Abo Akademi, Abo, Finland*
J. C. TOUCHSTONE, *Hospital of University of Pennsylvania, Philadelphia, Pennsylvania*
S. H. WONG, *University of Connecticut School of Medicine, Farmington, Connecticut*

JOURNAL OF LIQUID CHROMATOGRAPHY

September 1983

Aims and Scope. The journal publishes papers involving the application of liquid chromatography to the solution of problems in all areas of science and technology, both analytical and preparative, as well as papers that deal specifically with liquid chromatography as a science within itself. Included will be thin-layer chromatography and all modes of liquid chromatography.

Indexing and Abstracting Services. Articles published in *Journal of Liquid Chromatography* are selectively indexed or abstracted in:

● Analytical Abstracts ● ASCA ● BioSciences Information Service of Biological Abstracts (BIOSIS) ● Chemical Abstracts ● Current Awareness in Biological Sciences ● Current Contents/Life Sciences ● Current Contents/Physical and Chemical Sciences ● Engineering Index ● Excerpta Medica ● Journal of Abstracts of the All-Union Institute of Scientific and Technical Information of the USSR ● Physikalische Berichte ● Science Citation Index

Manuscript Preparation and Submission. See the last page of this issue.

Subscription Information. *Journal of Liquid Chromatography* is published in fourteen numbers and two supplements in January, February, March (3 numbers), April, May, June (2 numbers), July, August, September (2 numbers), October, November, and December by Marcel Dekker, Inc., 270 Madison Avenue, New York, New York 10016. The subscription rate for Volume 6 (1983), containing fourteen numbers and two supplements, is \$298.00 per volume (prepaid). The special discounted rate for individual professionals and students is \$149.00* per volume. To secure this special rate, your order must be prepaid by personal check or may be charged to MasterCard or VISA. Add \$36.80 for surface postage outside the United States. For airmail to Europe, add \$72.32; to Asia, add \$91.52.

Mailing Address. Please mail payment with order to: Marcel Dekker Journals, P. O. Box 11305, Church Street Station, New York, New York 10249.

Copyright © 1983 by Marcel Dekker, Inc. All rights reserved. Neither this work nor any part may be reproduced or transmitted in any form or by any means, electronic or mechanical, microfilming and recording, or by any information storage and retrieval systems without permission in writing from the publisher.

Permission to photocopy for internal or personal use or the internal or personal use of specific clients is granted by Marcel Dekker, Inc. for libraries and other users registered with the Copyright Clearance Center (CCC), provided that the stated fee is paid directly (per copy) to the CCC, 21 Congress Street, Salem, MA 01970. Special requests should be addressed to Marcel Dekker, Inc., Permissions Dept., 270 Madison Avenue, New York, New York 10016.

Contributions to this journal are published free of charge. Second-class mailing permit pending at New York, New York and at additional mailing offices.

ADALAB™ & CHROMATOCHART™

Automate GCs, HPLCs For Less Than \$4,400*



PEAK INTEGRATOR operates 1 to 4 GC or HPLC systems simultaneously and unattended. Stores up to 64,000 raw data points per run in compressed format. Automatic baseline correction can be overruled manually and results can be recalculated. Supports internal and external standards calculations, and much more.

GRADIENT PROGRAMMER controls 2 pumps based on a variable profile of up to 200 points.

EVENT CONTROLLER detects or switches 8 input signals and 8 output signals at any time during a run. Run duration, sampling time and gradient duration are variable; each can be started or stopped independently.

CHART RECORDER plots a continuous chart on the screen (and optionally on the printer) as the data are collected and also during peak integration. Summary reports are also printed.

EASY TO USE: Menu-style operation is easy to learn. Methods can be stored on disk for repeated use.

*\$4315 price includes 64K Apple IIe, disk drive with controller card, 12" monitor, dot matrix printer and interface, IMI CHROMATOCHART software, plus IMI's ADALAB and CHROMADAPT interface hardware.

APPLE II OWNERS: Add-On Packages cost only \$1645 for HPLC (with CHROMADAPT) or \$1295 for GC (ADALAB and CHROMATOCHART only).



INTERACTIVE MICROWARE, INC.

P.O. Box 771, Dept. 205
State College, PA 16801

CALL (814) 238-8294 for IMMEDIATE ACTION!

Circle Reader Service Card No. 109

**LIQUID CHROMATOGRAPHY/ELECTROCHEMISTRY
PART 1***

Edited by

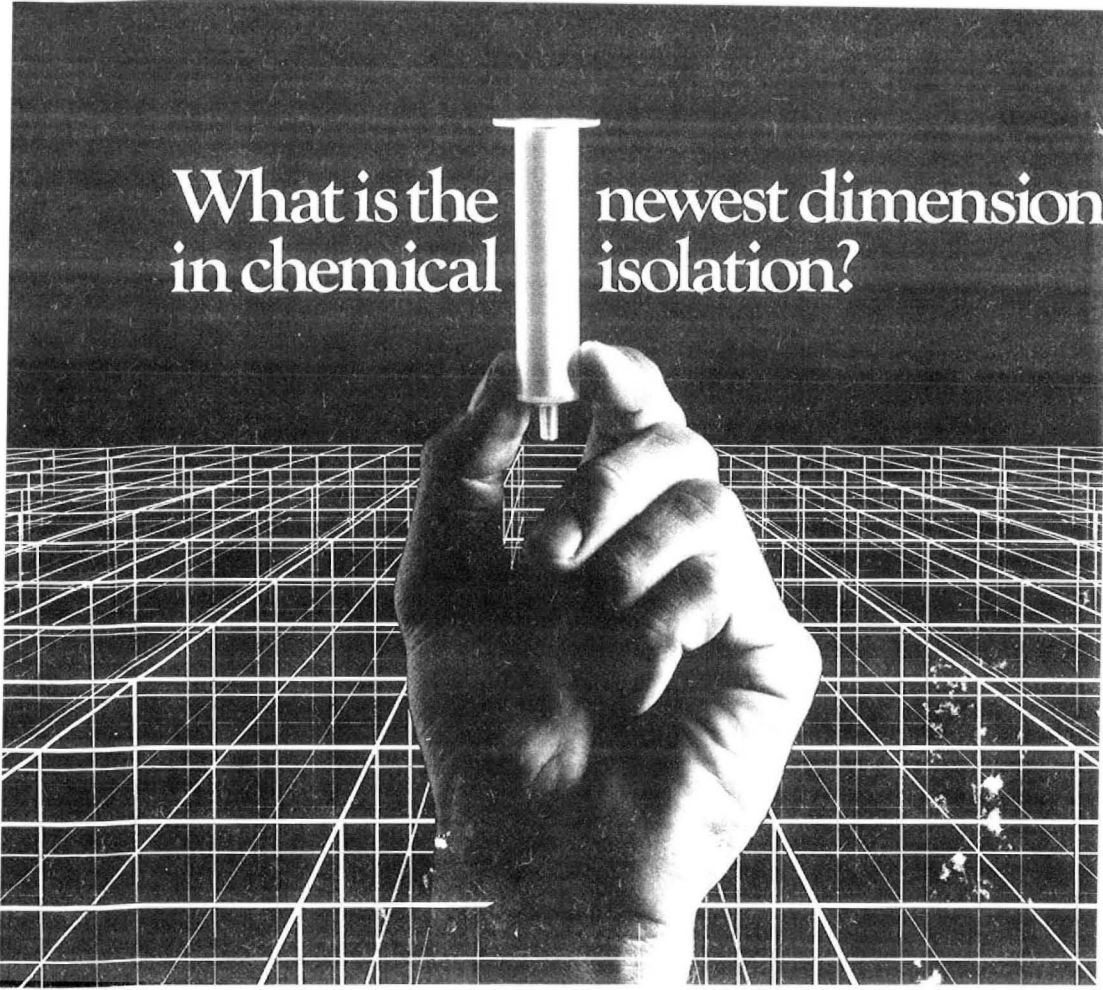
RONALD E. SHOUP
*Research Laboratories
Bioanalytical Systems Inc.
1205 Kent Avenue
West Lafayette, Indiana 47906*

and

R. W. FREI
*The Free University of Amsterdam
Department of Analytical Chemistry
Amsterdam, The Netherlands*

This is a special issue of *Journal of Liquid Chromatography*, Volume 6,
Number 10, 1983. *Part 2 will be published in Volume 6, Number 12, 1983.

MARCEL DEKKER, INC. New York and Basel

A black and white photograph of a hand holding a test tube. The hand is positioned in the center, with the test tube held vertically. The background is a perspective grid of white lines on a dark surface, creating a sense of depth and dimensionality. The lighting is dramatic, highlighting the contours of the hand and the test tube.

What is the newest dimension
in chemical isolation?

Analytichem introduces off-line Chromatographic Mode Sequencing.

Now there is a simple new bench technique that provides more efficient chemical isolation than any technology available today. In a fraction of the time. And at a fraction of the cost. It's called Chromatographic Mode Sequencing. The technique has been developed by Analytichem International for use with Bond Elut solid phase extraction columns.

Chromatographic Mode Sequencing (CMS) is a simple off-

line procedure that yields remarkably selective results. CMS allows the chemist to manipulate the interaction of various mobile and stationary phases to produce an almost limitless number of interactive modes. The result is that CMS, using Bond Elut, can solve virtually any chemical isolation problem. Yet it is disarmingly simple to perform.

The selectivity of this new technique is unsurpassed even by the most sophisticated column

switching procedures. And the simplicity of CMS means you can process a far greater volume of samples than with any other method available. CMS makes a totally new dimension in chemical isolation possible. And Bond Elut makes CMS possible. To learn how CMS can simplify your chemical isolation problems, call Analytichem today.



Analytichem International
24201 Frampton Ave., Harbor City,
CA 90710, USA (800) 421-2825.
In California (213) 539-6490
Telex: 664832 ANACHEM HRBO

Circle Reader Service Card No. 110

JOURNAL OF LIQUID CHROMATOGRAPHY

Volume 6, Number 10, 1983

Special Issue on Liquid Chromatography/Electrochemistry, Part 1

CONTENTS

- The Direct Electrochemical Detection of Amino Acids at a Platinum Electrode in an Alkaline Chromatographic Effluent** 1727
J. A. Polta and D. C. Johnson
- Tensammetric Detection in High Performance Liquid Chromatography. Application to Lynestrenol and Some Cardiac Glycosides** 1745
H. C. de Jong, W. H. Voogt, P. Bos, and R. W. Frei
- A New Polarographic Flow-Through Detector.** 1759
A. Trojánek and L. Křesťan
- Role of Interfacial Tension in Reverse Phase Liquid Chromatography** 1777
G. K. Vemulapalli and T. Gnanasambandan
- Liquid Chromatographic Behavior of Biological Thiols and the Corresponding Disulfides** 1785
L. A. Allison, J. Keddington, and R. E. Shoup
- Simultaneous Determination of Cadmium, Cobalt, Copper, Lead, Mercury and Nickel in Zinc Sulfate Plant Electrolyte Using Liquid Chromatography with Electrochemical and Spectrophotometric Detection.** 1799
A. M. Bond and G. G. Wallace
- Electrokinetic Detection in Reversed Phase High Performance Liquid Chromatography. I. Volatile Fatty Acids** 1823
W. Kemula, B. K. Głód, and W. Kutner
- Electrokinetic Detection in Reversed Phase High Performance Liquid Chromatography. II. Quaternary Ammonium Ion-Pairs of Some Volatile Fatty Acids** 1837
W. Kemula, B. K. Głód, and W. Kutner
- Fabrication and Characterisation of Leak-Tight Glassy Carbon Electrodes, Sealed in Glass Employing Silicon Coating, for Use in Electrochemical Detection.** 1849
J. C. Hoogvliet, J. A. G. van Bezooyen, A. C. J. Hermans-Lokkerbol, C. J. van der Poel, and W. P. van Bennekom

Determination of the Oxidized and Reduced Forms of Biopterin in Tissue Samples	1863
<i>C. E. Lunte and P. T. Kissinger</i>	
Interpretations of Voltammetry in the Striatum Based on Chromatography of Striatal Dialysate	1873
<i>J. B. Justice, Jr., S. A. Wages, A. C. Michael, R. D. Blakely, and D. B. Neill</i>	
High Performance Liquid Chromatographic Determination of Phenylenediamines in Aqueous Environmental Samples	1897
<i>R. M. Riggan and C. C. Howard</i>	
Dual Electrochemical Detection of Biogenic Amine Metabolites in Micro High-Performance Liquid Chromatography	1907
<i>M. Goto, E. Sakurai, and D. Ishii</i>	
Liquid Chromatography News	1927
Liquid Chromatography Calendar	1931

Liquid Chromatography / Electrochemistry

In 1974 BAS introduced the first commercial LCEC system. With over 5000 units installed and the largest research team to support them, it's not surprising that our nearest competitors are several generations behind us. Our thin-layer transducers lead the way with a wide selection of electrode materials in a variety of interchangeable configurations. The latest member of the family is the new LC4B/17 dual electrode amperometry package. Parallel and series amperometry can enhance selectivity, detection limits, speed and gradient compatibility. Let us show you how it's done, no one else can.

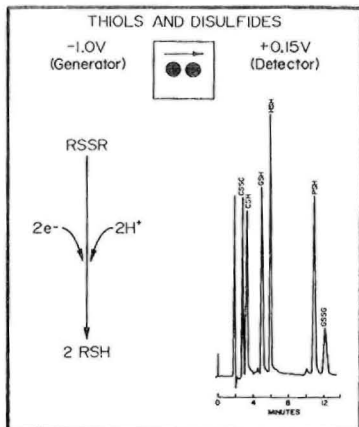
BAS

Purdue Research Park,
2701 Kent Avenue,
West Lafayette, IN. 47906
317-463-4527 TLX 276141

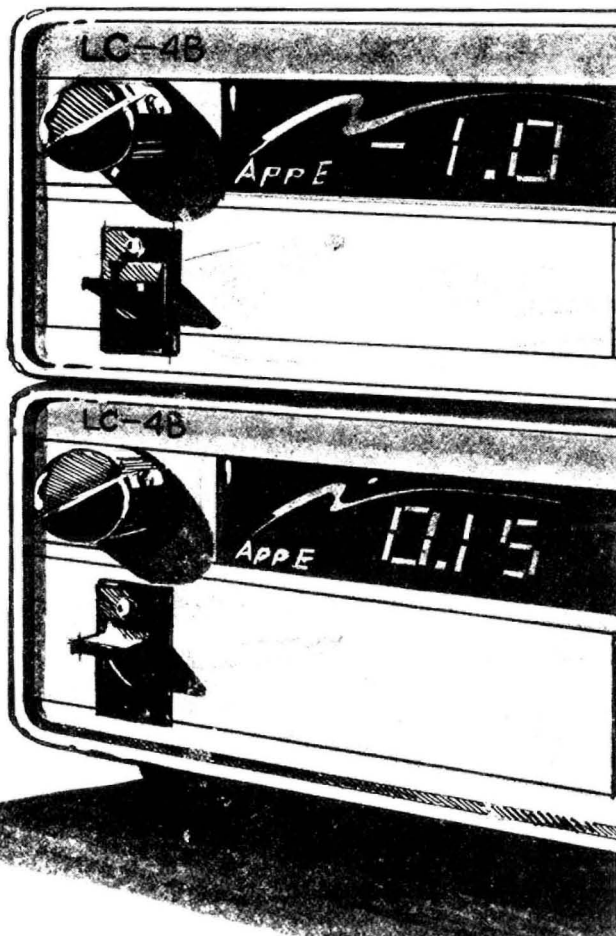
JAPAN: Tokai Irika Co. (Tokyo)

CANADA: Mandel Scientific

FRANCE: Biochrom s.a.r.l. (Vindelle)



Dual Electrode Detection: Standard mixture of Cystine, Cysteine, Glutathione, Homocysteine, Penicillamine, Glutathione Disulfide



THE DIRECT ELECTROCHEMICAL DETECTION OF
AMINO ACIDS AT A PLATINUM ELECTRODE IN
AN ALKALINE CHROMATOGRAPHIC EFFLUENT

J.A. Polta and D.C. Johnson*
Department of Chemistry
Iowa State University
Ames, Iowa 50011 U.S.A.

ABSTRACT

It is the general experience that most organic compounds including amino acids do not produce reversible or even quasi-reversible anodic waves at a Pt electrode under conditions of conventional cyclic voltammetry. Furthermore, amperometric detection of these compounds at a constant electrode potential is not successful because of the accumulation of adsorbed reaction products and/or an oxide film at the electrode surface. However, it is observed that a Pt electrode surface is cleaned quite effectively of adsorbed organic molecules and radicals simultaneously with the anodic formation of the oxide layer. This oxidation of adsorbed organic species is concluded to be electrocatalyzed by PtOH formed as the first step in the production of the oxide layer (PtO). A pulsed-potential waveform applied at a frequency of ca. 1 Hz is demonstrated to provide direct amperometric detection of adsorbed amino acids at a Pt electrode. Satisfactory analytical precision (i.e., < 3% rel. std. dev.) results because the waveform reproducibly generates the catalytically active surface state at the Pt electrode. Both primary and secondary amino acids are determined with satisfactory detection limits: e.g., ca. 13 ng for glycine, 7 ng for phenylamine and 23 ng for hydroxyproline in 50- μ L samples. Analytical response is concluded to depend on the adsorption isotherm of the amino acid being detected. Hence, the calibration plot of $1/I_{\text{peak}}$ vs. $1/C^0$ is linear for low surface coverages. Results are shown for amperometric detection of a synthetic mixture of amino acids by anion-exchange chromatography using NaOH as the eluent and supporting electrolyte.

INTRODUCTION

An extensive literature (1-5) has accumulated during the last three decades as a result of studies of the electrochemical oxidations of organic compounds at noble-metal electrodes, in general, and Pt electrodes, in particular. Nevertheless, comparatively few electroanalytical procedures have received wide acceptance for the anodic detection of organic compounds at noble-metal electrodes in aqueous solvents. The reasons are easily understood by observing that the anodic reactions generally yield voltammetric responses (e.g., I-E curves) characterized as being "surface-controlled". Surface-controlled reactions are those in which the total faradaic charge passed is controlled by the surface area of the electrode. Strong chemical interaction of the surface with the reactants and/or reaction products usually is concluded to exist for surface-controlled reactions. In the case of the anodic detection of simple alcohols at a Pt electrode, for example, a surface-catalyzed dehydrogenation occurs for the adsorbed molecules with the concomitant oxidation of the adsorbed hydrogen atoms, i.e. $(H)_{ads} \rightarrow H^+ + e$ (6,7). The remaining carbonaceous products of the dehydrogenation reaction are strongly adsorbed at the electrode, thereby blocking effectively those adsorption sites from further participation in the anodic dehydrogenation of unreacted molecules from the solution phase. Hence, the electrode current decays quickly to zero for the case of a constant applied potential. Surface-controlled anodic reactions of organic analyte previously have not found significant applications for detection in liquid chromatography.

It has long been the general experience in conventional voltammetric studies of inorganic systems that the presence of even trace levels of organic compounds can alter significantly the I-E response of electroactive species. As a result it has become standard practice to prescribe certain rites of surface pretreatment for noble-metal electrodes to insure the

reproducibility of voltammetric data (8). Pretreatment inevitably includes the alternate anodic and cathodic polarizations of the electrode at potential values near the limits for decomposition of the aqueous solvent to bring about the rapid, repeated formation and dissolution, respectively, of an oxide layer at the electrode surface. It is our premise that surface-controlled anodic reactions of organic compounds at Pt and other noble-metal electrodes can be applied for amperometric detection with satisfactory sensitivity and precision if the active surface-state of the electrode can be reproduced exactly prior to each measurement of the faradaic signal. We conclude further that the oxide-catalyzed oxygenation reactions responsible for the anodic cleaning of Pt electrodes can be used as the basis for amperometric detection of those compounds in aqueous chromatographic effluents.

Traditional procedures for voltammetric analysis of large volumes of solution in conventional cells have required potential waveforms which were designed to provide resolution of the separate I-E responses for each component of a mixture of electroactive species. Hence, the various waveforms (e.g., linear sweep, normal pulse, differential pulse, etc.) were required to produce a plot of the electrode current over a substantial portion of the available potential range for the particular electrode material in use. In applications of amperometric detection to LC, we develop our waveforms on the premise that the chromatographic system is responsible for resolution of mixtures. Furthermore, the background signal is easily determined in LC/EC from the detector response between elution peaks. Consequently, extensive freedom is allowed in the design of the waveforms to maximize the beneficial electrocatalytic properties of the electrode surface.

There have been a few observations of greater stability in the electrochemical response of solid electrodes resulting from application of pulsed-potential waveforms. Brown [9] expressed

the observation that for anodic organic electrolysis, the "coating of the anode with insoluble, insulating, polymeric films is a common hazard but it can be alleviated by use of periodic polarity reversal techniques." Clark, *et al.*, [10] applied pulsed voltammetry for oxidation of propylene at a Pt electrode to maintain electrode surface activity. MacDonald and Duke [11] observed an improvement in stability for the anodic detection of p-aminophenol at a Pt flow-through electrode when normal pulse amperometry was used instead of DC amperometry. Stulik and Hora [12] applied periodic potential pulses during the cathodic detection of Fe^{3+} and Cu^{+2} at a Pt electrode and reported improved stability of the cathodic signal when the pulse amplitude was sufficiently large to result in formation and subsequent dissolution of the oxide film on the electrode surface. In previous work from our laboratory (13-16), a triple-step potential waveform was applied successfully for the anodic detection of the C-OH moiety of alcohols and carbohydrates at a Pt electrode in alkaline solutions. According to this waveform, see Fig. 1 of (15), the faradaic current for oxidation of adsorbed molecules is measured using an analog sample-hold circuit in the last few milliseconds of the detection period at potential E_1 . The potential then is stepped to a value E_2 near the limit for anodic breakdown of the aqueous solvent which causes the formation of an oxide layer at the electrode surface with simultaneous oxidative removal of the adsorbed organic radicals which had been produced during the detection period. Further anodic detection of molecules from the solution does not occur at the oxide-covered surface and the subsequent step of potential to E_3 is necessary to bring about cathodic reduction of the oxide layer. Molecules of unreacted analyte from the solution phase are adsorbed at E_3 which, in turn, are detected following the subsequent potential step to E_1 . The electrical current corresponding to the "residual" surface processes following the step to E_1 (i.e., double-layer

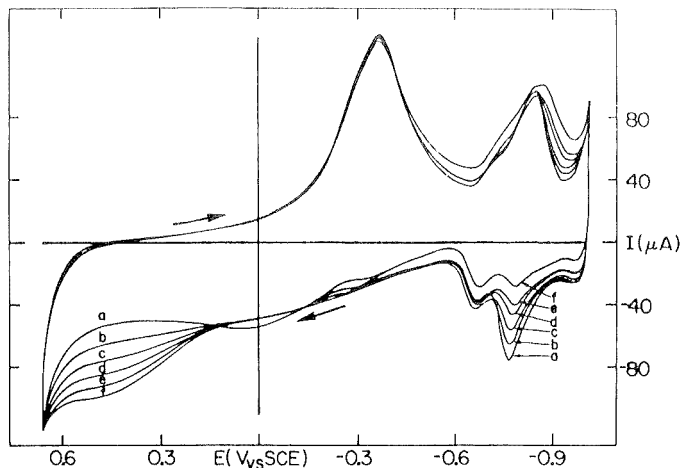


FIGURE 1.

Current-potential curves for glycine by cyclic linear scan voltammetry at a Pt RDE.

Conditions: 0.25 M NaOH, $\varnothing = 7.2 \text{ V min}^{-1}$, $\omega = 168 \text{ rad sec}^{-1}$.
 Concentrations (mM): a - 0.00, b - 0.050, c - 0.15, d - 0.35,
 e - 0.70, f - 1.20.

charging, anodic dissolution of adsorbed hydrogen atoms produced at E_3 , and the formation of a small amount of PtOH) decays more quickly than the current for oxidation of the adsorbed alcohols and carbohydrates. Hence, measurement of the desired analytical signal can be made accurately after a delay of only a few milliseconds. The use of a pulsed-potential waveform for detection of alcohols and carbohydrates at Au electrodes has also been demonstrated recently for detection in LC (17).

The general experience among electroanalytical chemists that the quantitative determination of aliphatic amines and amino acids in aqueous solutions cannot readily be achieved by conventional voltammetry and amperometry is illustrated here by selected quotations. Adams (18) stated: "...aliphatic amines are difficult to anodically oxidize in any quantitative

fashion." Malfoy and Reynaud (19) claimed: "Among the 20 amino acids present in the proteins only tryptophan and tyrosine are selectively oxidized at a gold, platinum or carbon electrode. Histidine is oxidizable only at a carbon electrode." Joseph and Davies (20) reported: "Most amino acids are not electroactive..." They proceeded to describe the a priori derivitization of amino acids to enable their electrochemical detection in LC.

The direct anodic detection of amino acids at a constant electrode potential has been reported recently by Huber et al. (21,22) at an oxide-covered Ni electrode in alkaline solutions. The detection reaction has been diagnosed by Fleischman et al. (23) to occur with direct involvement of the oxide. The amino acids reduce $\text{NiO}(\text{OH})_2$ to $\text{Ni}(\text{OH})_2$ with subsequent anodic oxidation of $\text{Ni}(\text{OH})_2$ back to $\text{NiO}(\text{OH})_2$. Disadvantages of using the Ni electrode result from 1) a long start-up time, during which the thickness of the oxide layer is stabilized and the background current decays to a steady value; and 2) the finite solubility of the oxides in the alkaline electrolyte solutions.

Here we report on the successful testing of triple-step potential waveforms for the direct anodic detection of primary and secondary amino acids at a Pt electrode in 0.25 M NaOH.

MATERIALS

Current-potential curves (I-E) were obtained by cyclic, linear scan voltammetry at a Pt rotated disk electrode (RDE, 0.460 cm^2 ; Pine Instrument Co., Grove City, PA) using a model PIR rotator and a model RDE3 potentiostat (Pine Instrument Co.). The I-E curves were recorded by an X-Y recorder (model RE0074, EG&G Princeton Applied Research). The chromatographic system consisted of a CMA-1 chromatographic module and a PMA-1 pumping module (Dionex Corp., Sunnyvale, CA). Separations were achieved with an anion-exchange column (model 48F, Dionex Corp.;

10- μm , 1 cm i.d. x 25 cm) at 40°C using 0.25 M NaOH as the eluent at a flow rate of 0.6 mL min⁻¹. Sample volumes were 50 μL . Flow-injection detections were performed with the chromatographic instrumentation after removal of the anion-exchange column from the fluid stream.

The amperometric detector was constructed from 22-ga. Pt wire which was heat-sealed into a 100- μL disposable glass pipet. The flow-through detector cell was constructed in the Iowa State University Chemistry Shop according to a previous design (16). Glass-filled Teflon (Crown Plastic, Inc., St. Paul, MN) was used for the major portion of the detector body with PTX plastic (Mitsui Petrochemical Ind., Ltd., Tokyo, Japan) for the inlet system. Back pressure was applied to the solution in the detector cell by a needle-valve connected into the outlet tubing to eliminate eluent degassing and accumulation of bubbles at the detector electrode. The triple-step waveform was generated automatically by a microprocessor-controlled potentiostat (model UEM, Dionex Corp.). All electrode potentials are reported in volts (V) vs. the saturated calomel electrode (SCE) as a reference.

CHEMICALS

All chemicals were reagent grade. Water was distilled, demineralized, and passed through an activated carbon column prior to use. All eluent solutions of NaOH were prepared from a saturated stock solution (18.0 M) using freshly boiled water to minimize carbonate contamination. All eluents were passed through a 0.45- μm filter prior to use.

RESULTS AND DISCUSSION

The voltammetric responses of amino acids at Pt electrodes in 0.25 M NaOH are illustrated adequately by the I-E curves for glycine obtained for a cyclic, linear scan of potential as shown in Fig. 1 for the Pt RDE. The residual response of the

electrode (curve a) obtained in the absence of the amino acid is characterized by an anodic wave during the positive scan for $E > -0.3$ V which corresponds to the formation of the oxide layer (PtOH and PtO). Rapid evolution of $O_2(g)$ occurs for $E > 0.6$ V. The oxide layer is cathodically reduced on the negative potential scan to produce the peak at -0.3 V. The cathodic and anodic peaks in the region -0.6 to -0.9 V correspond to the electrochemical production and dissolution, respectively, of adsorbed atomic hydrogen. Rapid evolution of $H_2(g)$ occurs for $E < -0.9$ V. Additions of the amino acid result in a decrease in the quantity of adsorbed atomic hydrogen which can be produced during the negative potential scan. This is explained if the amino acid is adsorbed at the electrode surface thereby depleting the number of available Pt sites. Oxidation of the adsorbed amino acid produces an anodic wave on the positive potential scan in the region $E = 0.3 - 0.6$ V, with the current increasing as a nonlinear function of the bulk concentration of the amino acid (C^b). There is virtually no evidence for oxidation of the amino acid on the subsequent negative potential scan in the region $E = 0.6 - 0.3$ V.

The anodic wave for the amino acid obtained on the positive potential scan was determined to vary in height as a linear function of the rate of potential scan and to be virtually independent of the rotational velocity of the RDE. Such behavior is consistent with the conclusion that the oxidation is a surface-controlled reaction. Furthermore, the oxide film produced on the positive potential scan to 0.65 V prevents further detection of the amino acid on the negative potential scan.

Various triple-step potential waveforms were developed on the basis of the I-E curves in Fig. 1. Three such waveforms are described in Table 1. Anodic detection of the amino acids occurs at potential E_1 . The anodic signal is measured using an analog sample-hold circuit after the delay period t_d ; ca. 50

TABLE 1. Description of three triple-step potential waveforms for detection of amino acids at Pt electrodes in 0.25 M NaOH.

Waveform	Step	Potential (V)	Period (msec)	Function
A.	1	$E_1 = 0.50$	$t_1 = 580$ ($t_d = 530$)	anodic detection (delay before sampling)
	2	$E_2 = -0.89$	$t_2 = 750$	reduction/adsorption
	3	$E_3 = 0.78$	$t_3 = 50$	anodic activation
B.	1	$E_1 = 0.50$	$t_1 = 250$ ($t_d = 200$)	-as above-
	2	$E_2 = -0.89$	$t_2 = 650$	
	3	$E_3 = 0.78$	$t_3 = 50$	
C.	1	$E_1 = 0.50$	$t_1 = 510$ ($t_d = 460$)	-as above-
	2	$E_2 = -0.89$	$t_2 = 360$	
	3	$E_3 = 0.70$	$t_3 = 50$	

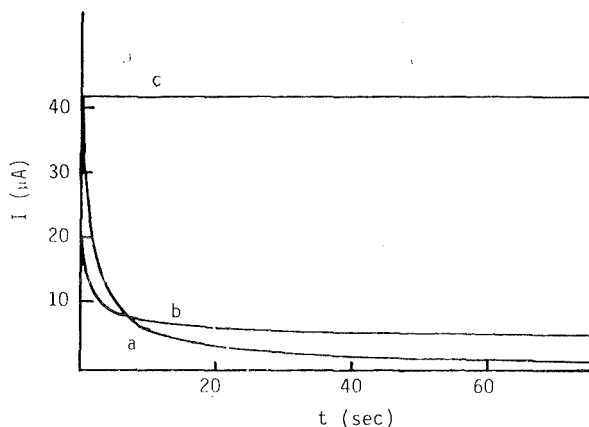


FIGURE 2.

Current-time curves for glycine at a Pt RDE.

Conditions: 0.25 M NaOH; $\omega = 41.9 \text{ rad sec}^{-1}$.

Curves: a - 0.00 mM glycine, $E = 0.50 \text{ V}$; b - 0.50 mM glycine, $E = 0.50 \text{ V}$; c - 0.50 mM glycine, waveform A.

msec was allowed for the sampling operation. The potential required to oxidize the amino acids is significantly more positive than required for alcohols and carbohydrates in the same alkaline medium. Hence, the coverage of the electrode surface by oxide at the respective detection potentials (E_1) is substantially greater for amino acids than for carbohydrates, and the corresponding residual current is slow to decay to a negligible value. The expected need for a long delay period (t_d) before the analytical signal sampled is obviated in the case of the amino acids by use of the large value for E_3 with the step back to the detection potential E_1 . For $E_3 > E_1$, the oxide coverage produced during the short period t_3 is greater than the equilibrium coverage for potential E_1 . Hence, the step from E_3 to E_1 results in the immediate cessation of oxide growth. Electrochemical reduction of PtOH and PtO does not occur at E_1 and, therefore, the residual current is negligible after several milliseconds. The potential step from E_1 to E_2 does result in the rapid reduction of the oxide layer followed by the adsorption of unreacted amino acids from the bulk solution. Clearly, the surface-controlled oxidation of amino acids commences immediately upon the potential step from E_2 to E_3 . The analytical success obtained for these waveforms results because the period for decay of the faradaic current for the amino acids is slow relative to the combined time periods $t_3 + t_d$. The waveforms are applied at a frequency of ca. 1 Hz which is sufficient for the "continuous" monitoring of a chromatographic effluent stream. Because the values of E_1 and E_3 are near the limit for anodic breakdown of the alkaline medium, retention on the electrode surface of free-radical products generated during the detection period does not persist substantially beyond the next repetition of the waveform.

The difficulty associated with application of surface controlled reactions for amperometric detection at a constant applied potential is illustrated for glycine in Fig. 2. Prior to recording the current-time ($I-t$) data, the potential of the

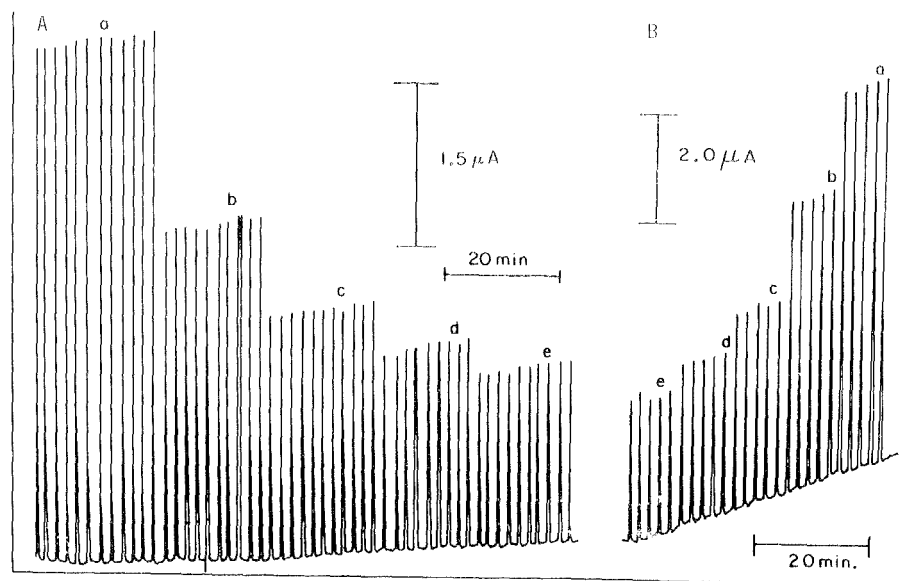


FIGURE 3.

Flow-injection detection peaks for glycine.

Conditions: 50- μ L injections; 0.25 M NaOH flowing at 0.80 mL min⁻¹; waveforms as indicated.

Concentrations(mM): a - 1.00, b - 0.50, c - 0.33, d - 0.25, e - 0.20.

Pt RDE was cycled repeatedly in the manner used for obtaining Fig. 1. The final scan was terminated at the negative limit, the potential was stepped to 0.50 V and the I-t curve recorded. The anodic signal in the presence of the amino acid (curve b) decreased rapidly. The residual response in the absence of the amino acid (curve a) is shown for comparison. The I-t curve for glycine is also shown in Fig. 2 which was obtained using the triple-step waveform A (curve c); no pretreatment of the electrode was needed in conjunction with curve c. No decrease of the signal was observed over a 10-min period.

Waveforms A and B in Table 1 were applied for the detection of various amino acids in the flow-through detector under conditions of flow-injection detection with repeated injections of 50- μ L samples of the amino acids. The concentration of NaOH in the samples and the carrier stream was 0.25 M. Representative results are shown in Fig. 3 for glycine. Baseline drift is less for waveform A, whereas sensitivity is greatest for waveform B. For the purpose of comparing the sensitivity of detection for various amino acids by the waveforms in Table 1, the average peak currents obtained by flow injection detection are given to Table 2 for 21 amino acids at a concentration of 5.0×10^{-4} M. Precision is satisfactory for all amino acids by the flow-injection technique with a relative standard deviation $< 3\%$.

Calibration plots for glycine (I_{peak} vs. C^b), prepared from data obtained by the flow-injection technique, approached linearity at low concentrations (i.e., $C^b < 0.6$ mM) but deviated significantly from linearity at higher concentrations. This behavior is the same as that observed for detection of alcohols and carbohydrates (13-16) by the triple-step technique and is concluded to be the consequence of a reaction mechanism in which only adsorbed species are detected. Hence, the anodic signal is proportional to the surface coverage (θ) by the adsorbed analyte. Based on the Langmuir isotherm, which is expected to be valid for $\theta \ll 1$ (i.e., small C^b), plots of $1/I_{\text{peak}}$ vs. $1/C^b$ are predicted to be linear. This prediction is verified by the data in Fig. 4 for glycine.

Detection limits (signal:noise = 2) for several amino acids using waveform B determined by flow-injection detection are given in Table 3.

The applicability of the triple-step waveform for amperometric detection of amino acids in the flow-through detector is further demonstrated in Fig. 5 for the chromatographic separation of a synthetic mixture of amino acids. The potential waveform was C (Table 1). Response for

TABLE 2. Average peak current (μA) obtained by flow-injection detection for 21 amino acids.

Electrolyte: 0.25 M NaOH at 0.50 mL min^{-1}
 Amino Acids: $50 \mu\text{L}$, $5.0 \times 10^{-4} \text{ M}$ in 0.25 M NaOH

Amino Acid	Waveform		Amino Acid	Waveform	
	A	B		A	B
alanine	6.44	13.9	leucine	4.32	8.13
β -alanine	10.46	17.8	lysine	18.6	22.7
arginine	26.9	32.0	methionine	23.7	26.5
asparagine	11.8	20.6	phenylalanine	23.5	30.3
cysteine	20.6	21.4	proline	2.19	5.19
cystine	13.6	16.7	serine	9.40	18.3
glutamic acid	3.92	7.19	threonine	10.38	18.3
glycine	8.58	16.4	tryptophan	25.9	31.6
Histadine	21.6	29.6	tyrosine	20.3	23.7
hydroxyproline	5.30	9.50	valine	3.56	6.53
isoleucine	3.86	7.68			

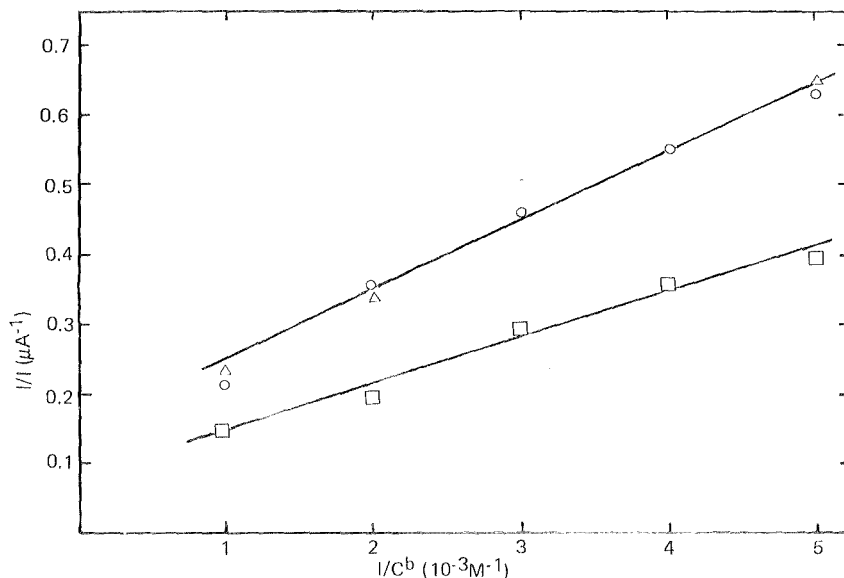


FIGURE 4.

Calibration curves ($1/I_{\text{peak}}$ vs. $1/C^b$) for glycine by flow-injection detection.

Conditions: $50\text{-}\mu\text{L}$ injections; 0.25 M NaOH flowing at 0.80 mL min^{-1} .

Curves: a - waveform A; b,c - waveform B.

TABLE 3. Detection limits for several amino acids using waveform B.

amino acid	ppm ($\mu\text{g mL}^{-1}$)	ng (50 μL sample)
phenylalanine	0.12	7
methionine	0.12	7
glycine	0.23	13
hydroxyproline	0.45	23
proline	0.86	43

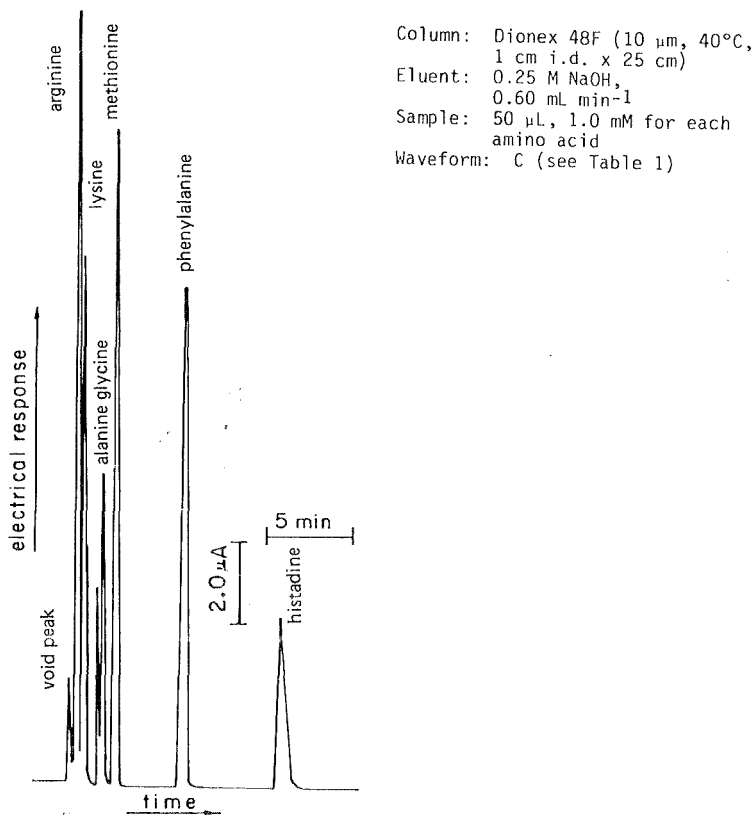


FIGURE 5.

Chromatogram of Selected Amino Acids Using Triple-Step Pulsed-Potential Amperometric Detection.

Peaks, in order of appearance: void, arginine, lysine, alanine, glycine, methionine, phenylalanine, histadine.

waveform C is similar to that for waveform A (i.e., low baseline drift); however, the frequency is somewhat larger (i.e., 1.1 Hz vs. 0.6 Hz for waveform A). The improvement in frequency came by a substantial decrease of period t_2 . Further decrease of t_2 resulted in a serious sacrifice of sensitivity, presumably because adsorption of the amino acids did not reach the equilibrium value of surface coverage. We hasten to emphasize with regard to Fig. 5 that we are stressing the feasibility of the amperometric detection system and not the quality of the separation. The Dionex 48F anion-exchange column was used for separations of carbohydrate mixtures under elution with dilute solution of NaOH and conditions were not optimized for separations of amino acids. The freedom to use alkaline solutions for elution is certainly advantageous, although use of post-column addition of the electrolyte can be successful (15,16).

We predict, on the basis of work with amino acids and carbohydrates, that triple-step potential waveforms will make available many additional surface-controlled anodic reactions of organic functional groups at noble-metal electrodes for amperometric detection in liquid chromatography.

ACKNOWLEDGEMENTS

The support of this research by Dionex Corp., Sunnyvale, CA, is gratefully acknowledged.

REFERENCES

1. Weinberg, N.L., and Weinberg, H.R., Electrochemical oxidation of organic compounds, Chem. Rev., 68, 449, 1968.
2. Tomilov, A.P., Mairanovskii, S.G., Fioshin, M. Ya., and Smirnov, V.A., Electrochemistry of Organic Compounds, Halsted Press, New York, 1972.
3. Baizer, M.M., ed., Organic Electrochemistry, Marcel Dekker, New York, 1973.
4. Ross, S.D., Finkelstein, M., and Rudd, E.J., Anodic Oxidation, Academic Press, New York, 1975.

5. Bard, A.J., and Lund, H., eds., *Encyclopedia of Electrochemistry of the Elements*, vol. XI-XIV (organic section), Marcel Dekker, New York, 1978-1980.
6. Breiter, N.W., Comparative voltammetric study of methanol oxidation and adsorption on noble metal electrodes in perchloric acid solutions, *Electrochim. Acta*, 8, 973, 1963.
7. Giner, J., The anodic oxidation of methanol and formic acid and the reductive adsorption of CO₂, *Electrochim. Acta*, 9, 63, 1964.
8. Adams, R.N., *Electrochemistry at Solid Electrodes*, Marcel Dekker, New York, 1969, pp. 206-207.
9. Brown, O.R., *Physical Chemistry of Organic Solvent Systems*, Covington and Dickinson, eds., Plenum Press, New York, 1973, p. 761.
10. Clark, D., Fleischman, M., and Pletcher, D., The partial anodic oxidation of propylene in acetonitrile, *J. Electroanal. Chem.*, 36, 137, 1972.
11. MacDonald, A., and Duke, P.D., Small-volume solid-electrode flow-through electrochemical cell; preliminary evaluation using pulse polarographic techniques, *J. Chromatogr.*, 83, 331 (1973).
12. Stulik, K., and Hora, V., Continuous voltammetric measurements with solid electrodes - Pt. I. A Flow-through cell with tubular electrodes employing pulse polarization of the electrode system, *J. Electroanal. Chem.*, 70, 253, 1976.
13. Hughes, S., Meschi, P.L., and Johnson, D.C., Amperometric detection of simple alcohols in aqueous solutions by application of a triple-pulse potential waveform at platinum electrodes, *Anal. Chim. Acta*, 132, 1, 1981.
14. Hughes, S., and Johnson, D.C., Amperometric detection of simple carbohydrates at platinum electrodes in alkaline solution by application of a triple-pulse potential waveform, *Anal. Chim. Acta*, 132, 11, 1981.
15. Hughes, S., and Johnson, D.C., High-performance liquid chromatographic separation with triple-pulse amperometric detection of carbohydrates in beverages, *J. Agric. Food Chem.*, 30, 713, 1982.
16. Hughes, S., and Johnson, D.C., The triple-pulse amperometric detection of carbohydrates: some results of chromatographic applications and the effect of variation of detector temperature, *Anal. Chim. Acta*, 000, 0000, 1983.
17. Rocklin, R.D., and Pohl, C.A., Determination of carbohydrates by anion exchange chromatography with pulsed amperometric detection, *J. Liq. Chromatog.*, in press.
18. Adams, R.N., op. cit., p. 375.

19. Malfroy, M., and Reynaud, J.A., Electrochemical investigations of amino acids at solid electrodes - Pt. II. Amino acids containing no sulfur atoms: tryptophan, tyrosine, histidine and derivatives, *J. Electroanal. Chem.*, 114, 213, 1980.
20. Joseph, M.H., and Davies, P., Electrochemical detection of amino acids, *Current Separations*, 4, 62, 1982. (Technical Bulletin, Bioanalytical Systems, W. Lafayette, IN)
21. Hui, B.S., and Huber, C.O., Amperometric detection of amines and amino acids in flow injection systems with a nickel oxide electrode, *Anal. Chim. Acta*, 134, 211, 1982.
22. Krafil, J.B., and Huber, C.O., Flow injection sample processing with nickel oxide electrode amperometric detection of amino acids separated by ion-exchange chromatography, *Anal. Chim. Acta*, 139, 347, 1982.
23. Fleischman, M., Korinek, K., and Pletcher, D., The kinetics and Mechanism of the oxidation of amines and alcohols at oxide-covered nickel, silver, copper, and cobalt electrodes, *J. Chem. Soc. Perkin II*, 1972, 1396.

TENSAMMETRIC DETECTION IN HIGH PERFORMANCE LIQUID
CHROMATOGRAPHY.
APPLICATION TO LYNESTRENOL AND SOME CARDIAC GLYCOSIDES

H.G. de Jong, W.H. Voogt, P. Bos and R.W. Frei*
Department of Analytical Chemistry, Free University,
De Boelelaan 1083, 1081 HV Amsterdam, The Netherlands

ABSTRACT

The application potential of tensammetric flow-through detection in high-performance liquid chromatography is studied. Batch experiments are performed to obtain optimal detection potentials. Lynestrenol, a steroid hormone used for birth control and the cardiac glycoside digoxin are used as model compounds. Detection limits have been found in the order of 20 ng per injection and permit the analysis of low dosage of pharmaceutical formulations. The operation of the flow-through tensammetric detection system is tested by detecting six cardiac-glycosides after reversed-phase chromatographic separation. For these analytes direct tensammetric detection has been shown to be a feasible technique. The use of such adsorption properties at a mercury electrode has potential as a complementary electrochemical detection technique for certain groups of compounds with no conventional electrochemical activity.

INTRODUCTION

The application of electrochemical flow-through detectors in HPLC based on the dropping mercury electrode (DME) has been demon-

*To whom correspondence is to be addressed.

strated by several workers [1-4]. These DME detectors were mostly used in the reductive mode. Some studies reported [5,6] on the application of tensammetry as detection technique in chromatographic systems. Tensammetry allows the detection of electro-inactive compounds that adsorb at the mercury electrode surface. In batch experiments a wide range of compounds have been studied [7-9]. Several theoretical aspects of tensammetry in non-flowing systems were subject to extensive treatment by various authors [7-12].

A classical tensammogram [7,8] is presented in Fig. 1, it shows two adsorption-desorption waves and baseline depression with respect to the blank electrolyte between these waves. Not only the heights but also the position of the adsorption-desorption waves in the tensammogram depends on the analyte concentration [7]. This makes the use of the adsorption-desorption process troublesome for detection in continuous flow systems when using commercially available AC polarographic equipment. By introducing computer operated devices or scan techniques as used in batch experiments on both capacitive and faradaic processes, this problem can be overcome [13,14]. However, the most straight forward approach to the application of tensammetry to continuous flow systems is the use of the properties in the adsorbed state. Adsorption of the analyte causes a depression in the electrochemical double layer capacity. This change can be measured by monitoring the double layer capacity on a display device [5,15] or by monitoring the capacity current [6]. When using the latter method calibration of the measuring device is not necessary. The double layer capacity depression can be observed over a wide potential range. The strongest depression is found in the neighbourhood of the electro-capillary maximum. This position is not specific for the analyte studied. Because of this property of the adsorption process, Kemula claimed tensammetry to be the most universal electrochemical detection technique [5].

Besides the usual limitations in eluent choice introduced by the demands of electrochemical detection, one is, when operating a ten-

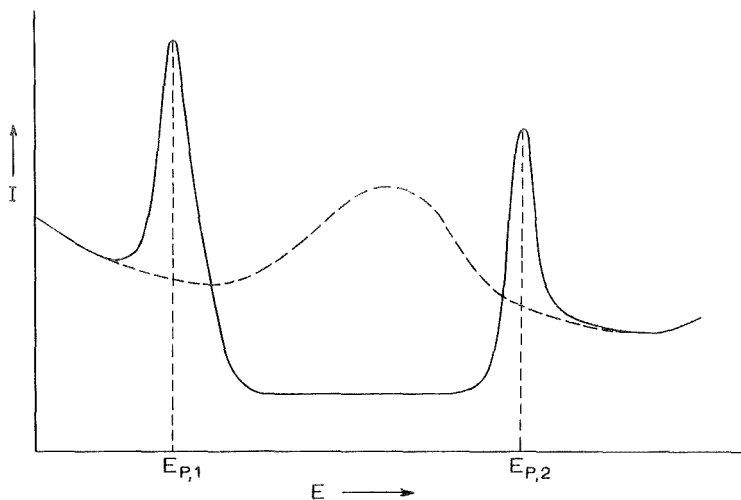


Fig. 1. Schematic representation of a tensammogram. $E_{p,1}$: peak potential of the positive tensammetric wave.

$E_{p,2}$: peak potential of the negative tensammetric wave.

— tensammetric curve

----- blank curve

sammetric detector in reversed-phase high-performance liquid chromatography (RP-HPLC), faced with adsorption of the polarity modifier at the electrode surface. Methanol and acetonitrile seem to be the most suitable modifiers in this context. Ethanol and higher alcohols adsorb so strongly that only a few percent in a RP-eluent can be tolerated. In general, addition of a polarity modifier gives rise to a loss in signal. A compromise is therefore often necessary between optimal separation and optimal detection conditions.

In this study the application of a tensammetry based detector is illustrated by the detection and separation of several cardiac glycosides and by the detection of lynestrenol (19-Nor-17 α -pregn-4-en-20-yn-17-ol), a steroid hormone used in formulations for birth regulation. In literature the chromatographic behaviour of cardiac glycosides was studied in both normal-phase and reversed-phase systems

[16-19]. Most determinations of lynestrenol were carried out with TLC and GC methods [20-23]. No HPLC data are available on lynestrenol because of detection problems. Using a tensammetric detector we shall demonstrate in this paper that RP-HPLC can be operated for the determination of the compounds mentioned in pharmaceutical formulations.

EXPERIMENTAL

For obtaining the most suitable detection potential complete tensammograms were recorded in batch with a classical polarographic setup. In continuous flow and chromatographic systems a PAR 310 electrode or a polarographic HPLC detector developed by Hanekamp et al. [24] was used. Both detectors enable synchronization of drop-time and electronics, hence sampled AC measurements can be performed.

Apparatus

A Princeton Applied Research (PAR) model 174 polarograph and a PAR 129A lock-in amplifier (EG & G, Princeton Applied Research Co., Princeton, NY, USA) both modified by our workshop for sampled AC operation were used with the PAR 310 static mercury drop electrode. These devices were interconnected with a PAR 174/50 AC polarographic interface. A Peekel 053A sinewave oscillator was used for generating the alternating voltage. The frequency of the alternating voltage was measured with a HP 5300A measuring system (Hewlett-Packard, Colorado, USA). A Fluke 8000A digital multimeter (John Fluke, MFG Co. Inc., Washington, USA) was used for checking the dc-detection potential. The overall current was monitored on a Tektronix 5103A oscilloscope (Tektronix, Beverton, OR, USA). The current was recorded on Kipp BD8 multirange recorder (Kipp en Zonen, Delft, The Netherlands).

In the second setup, the home-made detector [24] was connected with a Bruker E 310 modular research polarograph (Bruker Spectrospin

S.A., Brussels, Belgium). A PAR model 175 programmer was used for generating a drop dislodge pulse as described elsewhere [24]. The tensammograms were recorded on a HP 7046A XY-recorder (Hewlett-Packard). The chromatograms were recorded on a Servo 901 RE 571 Y-t recorder (Goerz Electro GmbH, Vienna, Austria). The overall current was monitored on a Tektronix type 502 oscilloscope. The applied potentials were always measured vs. a Ag/AgCl/1 M LiCl methanol-water 50/50% v/v reference electrode. In both chromatographic systems a PE 601 pump (Perkin-Elmer, Connecticut, USA), a Rheodyne 7120 injection valve (Rheodyne, Inc., Berkeley, CA, USA) and a stainless-steel column (10 cm x 4.6 mm I.D.) were used. The columns were packed with ODS Hypersil 5 μm (Shandon, Rumcorn, UK) or LiChrosorb RP-2 10 μm (Merck, Darmstadt, GFR).

Chemicals

The measurements were performed in water-methanol mixtures containing 0.1 M KNO_3 . The stock solutions were deaerated by purging with nitrogen (A28). Water was demineralized and distilled. The cardiac glycosides were supplied by Sandoz Ltd, Basel, Switzerland and Lynestrenol by Organon Ltd., The Netherlands. All other chemicals were analytical reagent grade (Baker "Analyzed" or Merck p.a.). The samples were deaerated by purging with nitrogen for about 10 minutes.

RESULTS AND DISCUSSION

Batch Experiments

Complete tensammograms of digoxin and lynestrenol were recorded as a function of the methanol-water ratio in the supporting electrolyte. In Fig. 2 some results obtained for digoxin are presented. The current depression (analytical signal) by adsorption of digoxin measured at a constant potential (-400 mV vs. Ag/AgCl) was observed to decrease considerably in going from 0% methanol ($\Delta I = 3.83 \mu\text{A}$) to 80% ($\Delta I = 0.54 \mu\text{A}$). This potential is chosen from

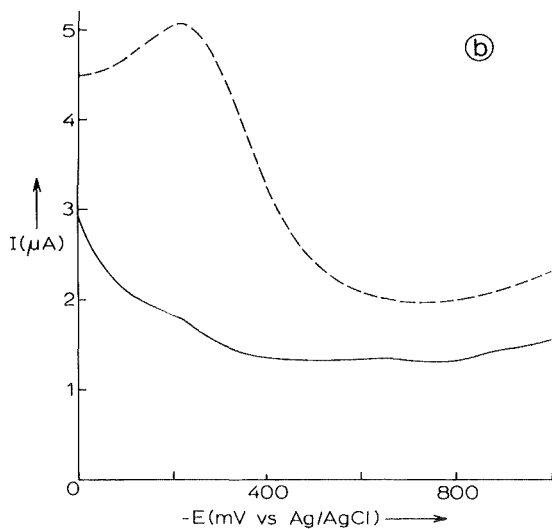
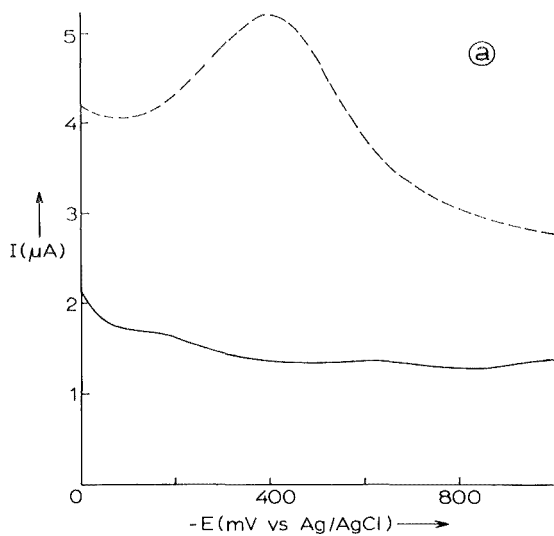
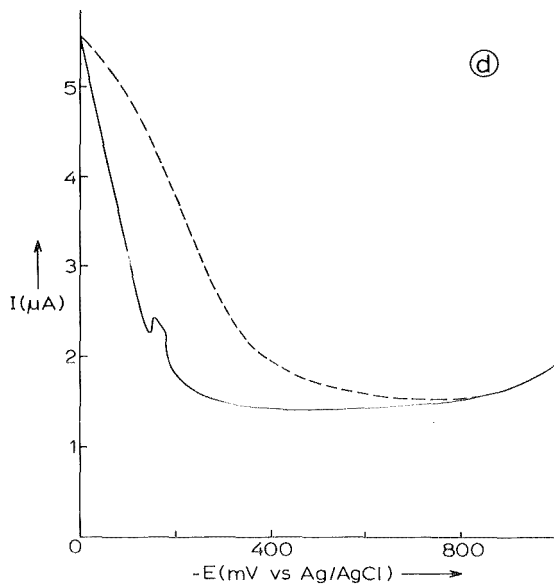
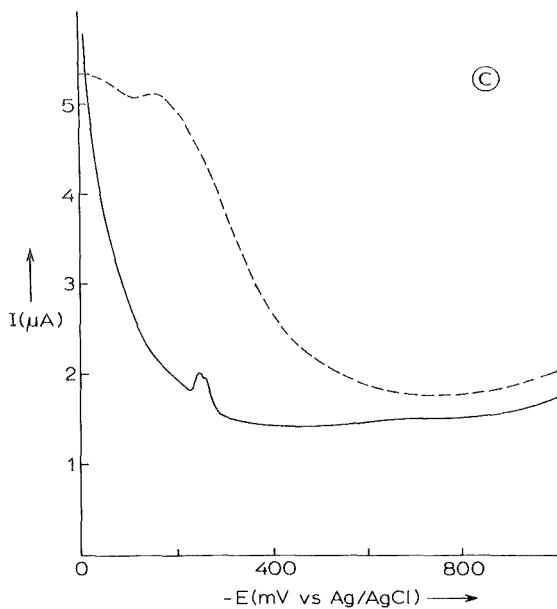


Fig. 2. Tensammograms of different electrolyte composition without (-----) and with (—) 10^{-4} M digoxin. Conditions: $f = 60$ Hz, amplitude 20 mV_{eff}, $\phi = 90$ degrees, $t_d = 1.0$ s, $h_{\text{Hg}} = 50$ cm, ϕ capillary = 0.010 cm (length 10 cm), scan



rate 2 mV s^{-1} . Electrolyte compositions: 0.1 M KNO_3 in various (v/v) ratios water-methanol:

- a. 100% water
- b. 70%-30% water-methanol
- c. 50%-50% water-methanol
- d. 20%-80% water-methanol

the tensammogram displayed in Fig. 2a. At this potential the current reaches a maximum value which is caused by a change of the double layer capacity due to specific adsorption and desorption of the anions from the supporting electrolyte [9].

Methanol addition to the electrolyte induces a change in position of this maximum in the tensammogram as can be seen from Fig. 2a and 2b. When the relative amount of methanol is increased even further the characteristic maximum disappears completely as can be seen from Fig. 2c and 2d. From Fig. 2 it can be concluded that various electrolyte compositions have different optimal detection potentials. Even at optimal detection potentials a net decrease in current depression and hence in sensitivity is observed when changing from a purely aqueous electrolyte towards larger amounts of methanol in the electrolyte. At methanol concentrations exceeding 60 percent (v/v) this effect is less obvious; then methanol adsorption is almost completely governing the capacity-potential curve. Lynestrenol qualitatively shows the same behaviour. The current depression is less strong as for digoxin in the potential range considered. The optimal detection potentials for lynestrenol in the electrolyte compositions studied differ approximately 50 millivolts from those for digoxin.

Continuous Flow Experiments

In a continuous flow system the peak height, which is actually the depression of the baseline was found to be linearly dependent on the applied modulation-frequency and the modulation amplitude. In Fig. 3 the peakheight (I_p) versus phase-angle (ϕ) is plotted for digoxin. From this graph it can be seen that the maximum current depression is observed at about 30 degrees with respect to the applied modulation voltage. This is a large deviation from the theoretical expected 90 degrees. In similar experiments with lynestrenol, performed with the PAR 310 detector, the maximum baseline depression was found between 80-100 degrees, which is more acceptable [9]. These observations suggests that the cell geometry might be responsible for the phase angle difference observed.

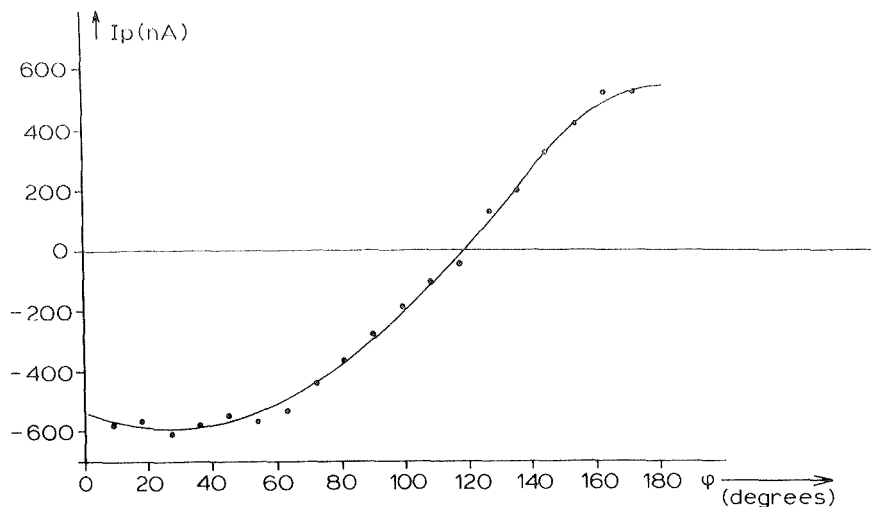


Fig. 3. Peak height (I_p) vs. phase-angle (ϕ) in continuous flow system with the home made DME detector for 200 μ l injections of 10^{-4} M digoxin. Conditions: $f = 35$ Hz, amplitude = 30 mV_{eff}, detection potential = -150 mV vs. Ag/AgCl, $t_d = 1$ s, $h_{Hg} = 30$ cm. Eluents: water-methanol 40%-60% (v/v) containing 0.1 M KNO_3 . Flow rate: 1 ml/min.

Application to HPLC

The application of continuous flow tensammetric detection was studied with two HPLC systems. Detection limits, linear dynamic range and precision were investigated with the PAR apparatus. Six cardiac glycosides were detected, after separation with the Bruker polarograph.

Results for lynestrenol: Lynestrenol was chromatographed in a RP-system using a LiChrosorb RP2 10 μ m packed column and a flow rate of 2 ml/min (30%-70% (v/v) water-methanol, 0.1 M KNO_3). The capacity factor k' was 3.2. The detection potential was chosen from batch experiments to be -150 mV vs. Ag/AgCl. From Fig. 2a it can

be seen that dI/dE is large at this potential in a blank electrolyte solution. Availability of a more stable potentiostat might have been resulted in a smaller baseline noise caused by potentiostat instability. Fig. 4 shows a logarithmic plot of the calibration curve for lynestrenol. In the range from 2×10^{-6} M, 2×10^{-4} M, a linear relationship exists between peak height and concentration. In this region a calibration line is calculated using the method of least-squares. The regression coefficient was 0.996 and the sensitivity was 8×10^{-4} AL/mole. At concentrations exceeding 2×10^{-4} M deviation from linearity is observed. In this region saturation of the electrode surface with lynestrenol starts to become important. In our setup a typical noise of 1 nA was observed. The detection limit for lynestrenol ($M = 284.42$) at a signal to noise ratio of 3:1 was calculated to be 1.0×10^{-6} M or 28 ng per injection. The standard deviation of peak height for 11 consecutive injections ($1.7 \mu\text{g}$ lynestrenol per injection) was 2.4%.

Results for Cardiac Glycosides: Cardiac glycosides were chromatographed in a RP system using an ODS Hypersil $5 \mu\text{m}$ packed column at a flow rate of 1 ml/min (40%-60% (v/v), water-methanol, 0.1 M KNO_3). The detection limit (conditions see Fig. 5) for digoxin ($M = 780.92$) was found to be 1.0×10^{-7} M or 16 ng per injection (with typical peak height 3 nA). The capacity factor for digoxin was 3.5. In Fig. 5 a HPLC separation of six cardiac glycosides is presented. Note the peak height differences between digitoxin and gitoxin on one hand and the other compounds on the other hand. These differences are caused by differences in adsorption strength at the detection potential chosen.

Application to Pharmaceutical Formulations: The potential of this detection technique for the analysis of pharmaceutical formulations was tested with digoxin ampoules and tablets. The chromatographic and detection conditions were the same as for Fig. 5. Ampoule solutions $20 \mu\text{l}$, were injected directly without any further pretreatment. The tablets containing 0.25 mg digoxine were pulverized with a mortar. After shaking for a few minutes with a mix-

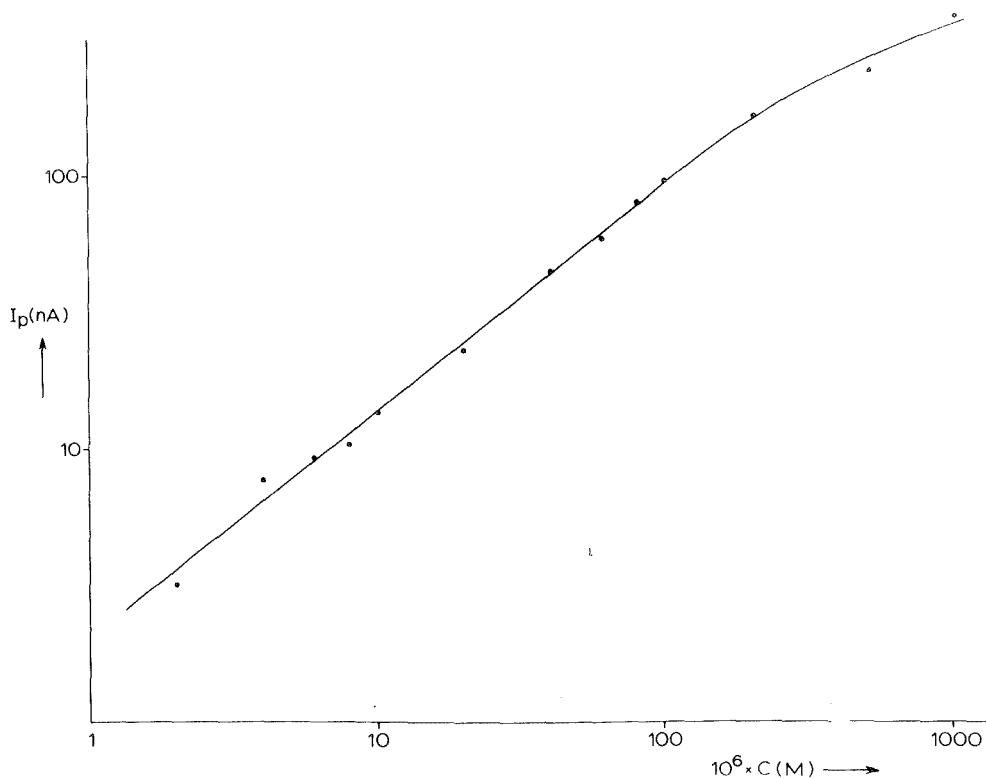


Fig. 4. Peak height (I_p) vs. concentration lynestrenol. Conditions: $f = 20$ Hz, amplitude 10 mV_{eff}, $\phi = 85$ degrees, detection potential -200 mV vs. Ag/AgCl, $t_d = 2$ s, drop size: large ($r = 0.0935$ cm), time constant = 3 s. Injection volume: 100 μ l. Eluent: water-methanol 30%-70% (v/v) containing 0.1 M KNO_3 . Flow rate = 2 ml/min.

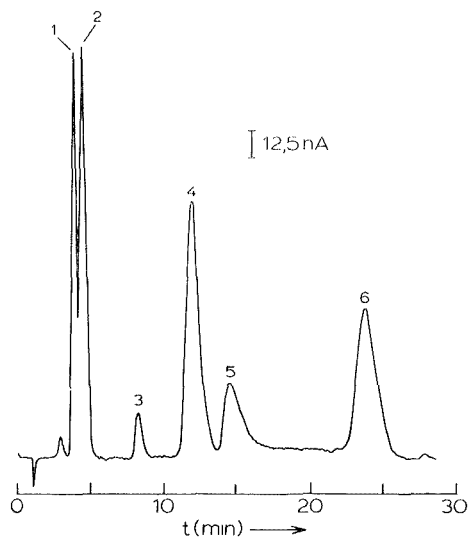


Fig. 5. Chromatogram of 6 cardiac glycosides: (1) digoxin, (2) digitoxin, (3) gitoxin, (4) lanatoside A, (5) lanatoside B, (6) lanatoside C. 20 μ l of a mixture containing 10^{-4} M of each compound was injected. Detection conditions: $h_{\text{Hg}} = 40$ cm, time constant 2.5 s. Further conditions see Fig. 3.

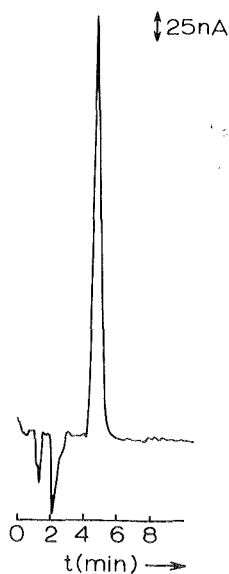


Fig. 6. Chromatogram of 0.25 mg digoxin tablet. Conditions: $h_{\text{Hg}} = 18$ cm, $t_d = 0.8$ s, further conditions see figure 5.

ture of EtOH 0.25 ml, MeOH 0.25 ml and H₂O 0.5 ml, 20 µl of the supernatant liquid were injected. A chromatogram for a digoxin tablet is shown in Fig. 6. Detection limits and reproducibility are comparable to those reported for standard solutions.

CONCLUSIONS

Tensammetric detection in HPLC is a feasible complementary technique to oxidative and reductive electrochemical detection. It is particularly favourable for groups of compounds which do not possess a strong chromophore. Lynestrenol is a good example in this regard. For cardiac glycosides the detection limits obtained are about comparable to UV detection at 220 nm [25] and thus no advantage would be gained by using this technique for formulations analysis, although some improvements could be made as to using more stable potentiostats. From the experience gained in this work we tend to agree with Kemula and Kutner [5] that tensammetric detection can be more universally applicable than other electrochemical detection modes. Further work is needed to explore other potentially interesting groups of compounds.

ACKNOWLEDGEMENTS

Dr. W.P. van Bennekom (State University, Leiden, The Netherlands) is thanked for supplying lynestrenol and for examining the manuscript.

Sandoz Ltd, Basel, Switzerland is to be thanked for a gift of cardiac glycosides and pharmaceutical formulations.

REFERENCES

1. Kutner, W., Debowski, J. and Kemula, W., *J. Chromatogr.*, 191, 47, 1980.
2. Michel, L. and Zatka, A., *Anal. Chim. Acta*, 105, 109, 1979.
3. Koen, J.G., Huber, J.F.K., Poppe, H. and Den Boef, G., *J. Chromatogr. Sci.*, 8, 192, 1970.
4. Hanekamp, H.B., Thesis, Free University, Amsterdam, 1981.
5. Kemula, W. and Kutner, W., *J. Chromatogr.*, 204, 192, 1981.

6. Lankelma, J. and Poppe, H., *J. Chromatogr. Sci.*, 14, 310, 1976.
7. Jehring, H., "Electrosorptions Analyse mit der Wechselstrom-Polarographie", Akademie Verlag, Berlin 1974.
8. Breyer, B. and Bauer, H.H., "AC polarography and tensammetry", Interscience, New York 1963.
9. Jehring, H., *J. Electroanal. Chem.*, 21, 77, 1969.
10. Berzins, T. and Delahay, P., *J. Phys. Chem.*, 59, 906, 1955.
11. Lorenz, W. and Möckel, F., *Z. Electrochem.*, 60, 507, 1956.
12. Lorenz, W. and Möckel, F., *Ibid.*
13. Wang, J., Ouziel, E., Yarnitzky, Ch. and Ariel, M., *Anal. Chim. Acta*, 102, 99, 1978.
14. Britz, D., *Anal. Chim. Acta*, 115, 327, 1980.
15. Rosen, J.M., Hua, X., Bratin, P. and Cohen, A.W., *Anal. Chem.*, 53, 232, 1981.
16. Nachtman, F., Spitzzy, H. and Frei, R.W., *J. Chromatogr.*, 122, 293, 1976.
17. Nachtman, F., Spitzzy, H. and Frei, R.W., *Anal. Chem.*, 48, 1576, 1976.
18. Nachtman, F., *Z. Anal. Chem.*, 282, 209, 1976.
19. Gfeller, J.C., Frey, G. and Frei, R.W., *J. Chromatogr.*, 142, 271, 1977.
20. Rizk, M. and Walash, M.I., *Pharmazie*, 33, 521, 1978.
21. Books, C.J.W. and Middleditch, B.S., *Clin. Chim. Acta*, 34, 145, 1971.
22. Verbeke, R., *J. Chromatogr.*, 177, 69, 1974.
23. Szekacs, I. and Klembala, M., *Z. Klin. Chem. Klin. Biochem.*, 8, 131, 1970.
24. Hanekamp, H.B., Voogt, W.H. and Bos, P., *Anal. Chim. Acta*, 118, 73, 1980.
25. Erni, F. and Frei, R.W., *J. Chromatogr.*, 130, 169, 1977.

A NEW POLAROGRAPHIC FLOW-THROUGH DETECTOR.

A. Trojánek and L. Křesťan,
J. Heyrovský Institute of Physical Chemistry
and Electrochemistry, Czechoslovak Academy
of Sciences,
Prague 1, Jilská 16, Czechoslovakia

ABSTRACT

The construction of a flow-through polarographic detector is described, based on introduction of the test solution into a space filled with mercury. Two variants of the detector have been developed, with the inlet jet placed vertically and horizontally. The dynamic properties of the two detector variants, the linear dynamic range and the response reproducibility were tested using o-nitrophenol as a model substance. The detector with the vertical jet has a wide linear dynamic range and that with the horizontal jet exhibits an extremely rapid response with a time constant of the order tenths of a second.

INTRODUCTION

Most practically used flow-through voltammetric detectors operate with solid electrodes and respond to anodically oxidizable substances. However, there exist many important compounds containing functional groups that can be cathodically reduced under certain conditions (nitro-, nitroso- and azo-compounds, aldehydes, oximes, hydrazones, etc.). To detect these compounds in flow-through instruments, a number of polarographic detectors have been constructed over last twenty years, employing the advantages of mercury electrodes and sup-

pressing to a varying extent their undesirable properties. All the polarographic detectors that have so far been described (1,2) are basically flow-through versions of a common polarographic cell, constructed so that the internal volume is as small as possible. They all contain a dropping mercury electrode consisting of a glass capillary, which is the most sensitive and most expensive part of the detector.

This paper describes the construction and properties of a flow-through polarographic detector based on a new principle, without a glass capillary.

EXPERIMENTAL

Chemicals

Methanol, acetic acid, sodium acetate, o-nitrophenol and 2,6-dinitrophenol (all from Lachema, Brno, Czechoslovakia) were of p.a. purity and were not further purified. The samples and the base electrolyte were deaerated prior to measurement by passage of argon.

Instruments

The detector was tested in a system consisting of a high-pressure linear pump (HPP 4001, Laboratorní Přístroje, Prague, Czechoslovakia) and a sampling valve whose construction is described below. For the connections, a stainless-steel capillary, 0.4 mm I.D., was employed.

The chromatographic measurements were carried out on an LC-XP liquid chromatograph (Pye Unicam, Cambridge, Great Britain), with a Separon C₁₈ column, 25 cm long, 0.8 cm I.D., 10 μ m (Laboratorní Přístroje, Prague, Czechoslovakia). Samples were injected through a 20 μ l sampling loop.

A three-electrode polarograph with circuits for handling the current signal and the circuit for the

measurement of electrolytic conductance were assembled from operational amplifiers. The conductance was measured with a large-area platinum electrode in the working electrode compartment at a frequency of 1 kHz.

The output signal was recorded using a TZ 4200 line recorder (Laboratorní Přístroje, Prague, Czechoslovakia) or a Tektronics 5103 storage oscilloscope (Tektronics, Beverton, USA).

Sampling Valve

One requirement of the sampling valve is to introduce the sample into the flowing stream as a zone with a sharp front edge. As the detectors tested do not cause a perceptible pressure gradient in the liquid stream, the sampling valve was constructed as a low-pressure device. The rotating sandwich valve with a rotor between two stators is made of plexiglass. The adjacent surfaces are lubricated with graphite and the bored channels are 0.4 mm in diameter. Fig. 1 depicts the valve in position "LOAD", when the sampling loop is filled with the sample using pressurized argon. On turning the rotor by 60° the loop content, including the rectangular channels, is swept into the stream between the pump and the detector.

Detector

The detector construction is schematically given in Fig. 2. The whole detector is also made of plexiglass and its body consists of two main parts, one containing the reference electrode and the other the mercury compartment. The two main parts are connected by a thread and the connection between them and between the jet holder and the front of the mercury compartment are sealed. The inlet channel (0.4 mm I.D.) and the jet are tightly and flexibly connected by a small seal at the channel circumference. The two

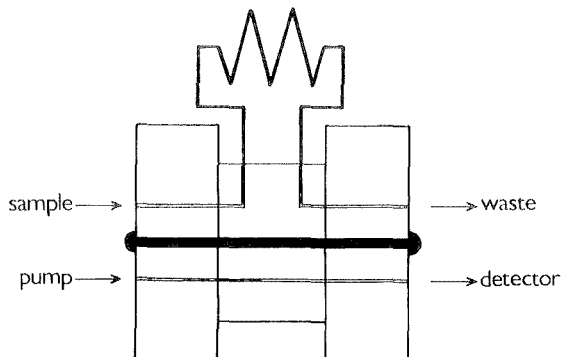


FIGURE 1. Sampling valve.

outlets in the mercury compartment permit the work with the detector in both vertical and horizontal position.

The most important part of the detector is the jet through which the test solution is introduced into the mercury. It is made of porous ceramics and pressed into the plexiglass holder. The jet has a channel 0.4 mm in diameter, and the jet is narrowed to 0.2 mm for 1 mm at the tip. The part of the jet that is in contact with mercury is covered with a protective lacquer (Brush-on Plastic Tape, No. 1572-20, TechSpray, USA). Common epoxide materials are unsuitable for the jet insulation, because they cannot resist prolonged action of methanol. After drying of the lacquer, the jet tip was ground with a fine emery paper, thus obtaining a non-insulated contact area with a diameter of about 0.7 mm with the 0.2 mm jet and about 1 mm with the 0.4 mm jet.

An Ag/AgCl reference electrode with 1M LiCl in 50% methanol was used.

RESULTS AND DISCUSSION

The principle of the detector is introduction of the test solution into a space filled with mercury.

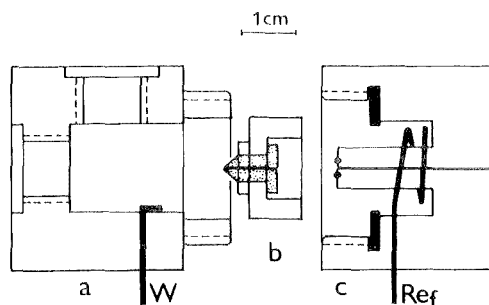


FIGURE 2. Schematic diagram of the detector. a) mercury compartment, b) porous jet in the plexiglass holder, c) reference electrode compartment. Contacts to the working (W) and reference electrodes (Ref) are depicted.

The working electrode is the mercury surface surrounding the drop or layer of the test liquid and can be connected with the other electrodes in various ways. To test the properties of this detector, we used the inlet stainless-steel capillary as the auxiliary electrode and the working and reference electrodes were connected by the jet made of a porous material.

Among the properties important for practical use, the response stability and rate, the linear dynamic range (the concentration range within which the response is linear) and the dependences of the measured quantities on the flow-rate were determined. As the model substance, *o*-nitrophenol (ONPh) was selected in a medium of 0.1M acetate buffer of pH 4.6 containing 50% vol. methanol. Thus the detector was intentionally tested under difficult chromatographic conditions with a low electric conductance. When the detector contained this electrolyte, a resistance of ca. 200 k Ω was measured between the tip of the jet and the auxiliary electrode. In the measurement, 400 μ l of the sample was

usually injected into the detector, thus ensuring that the amount injected was sufficient for the attainment of a steady-state current signal.

The axis of the detector jet can basically be oriented in two directions, vertically or horizontally. As will be seen below, different directions of the jet axis with respect to the direction of the gravitational force and buoyancy lead to detectors with different properties and thus they are discussed separately.

Detector with Vertical Jet Axis

Due to the formation of droplets of the liquid at the jet tip and their disconnection caused by buoyancy, the current signal obtained oscillates similar to that measured with a dropping mercury electrode. The oscillations cause difficulties in the evaluation of the current signal, especially at low concentrations of the electroactive substance (Fig. 3). The oscillations can be suppressed by using the sampling method based on a peak detector that does not require synchronization with the drop disconnection (3).

Response Rate

The response rate is an important property that is often used as the main criterion for the comparison of detectors of various designs. However, it is practically impossible to compare detectors on the basis of the data given in the literature in terms of geometric, response, internal, effective, rinse, hold-up, wash-out, dead, etc., volumes, as the relationships among these quantities are not unambiguously defined and their values variously depend on the experimental conditions.

A relatively reliable dynamic parameter is the response time constant, whose value generally depends on the flow-rate and possibly on other experimental parameters. The finding of these dependences can be

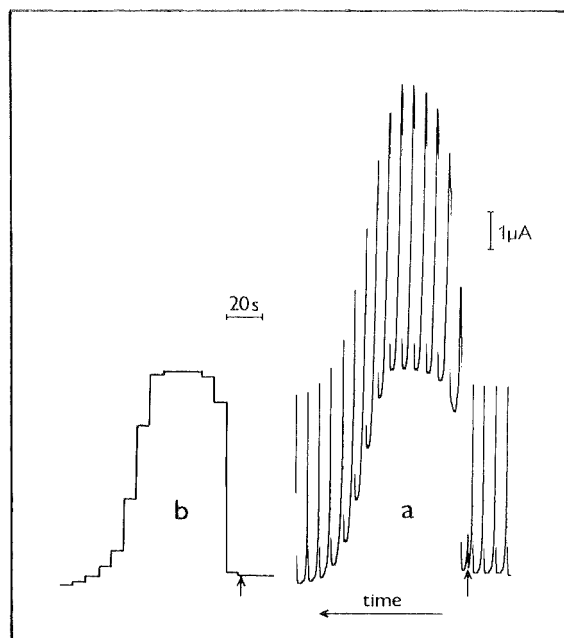


FIGURE 3. Response of the vertical jet detector; 400 μl of 2×10^{-5} M CNPh injected; Jet diameter 0.4 mm, flow-rate 0.5 ml/min. a) signal; b) sampled signal.

considered as a sufficient characteristic of the response rate of the detector or, more precisely, of the whole detection system. The time constant of the detector response can be determined from the output signal recorded after a stepwise change in the input concentration. It is often possible (and the present detectors are not an exception) to express the time-course of the output signal with a sufficient precision by the exponential equation, $S = S_M(1 - \exp(-t/\tau))$, where S is the signal amplitude at time t , S_M is the maximal amplitude and τ is the response time constant. Therefore, the τ value can be found from the known signal amplitude at any time after the beginning of the

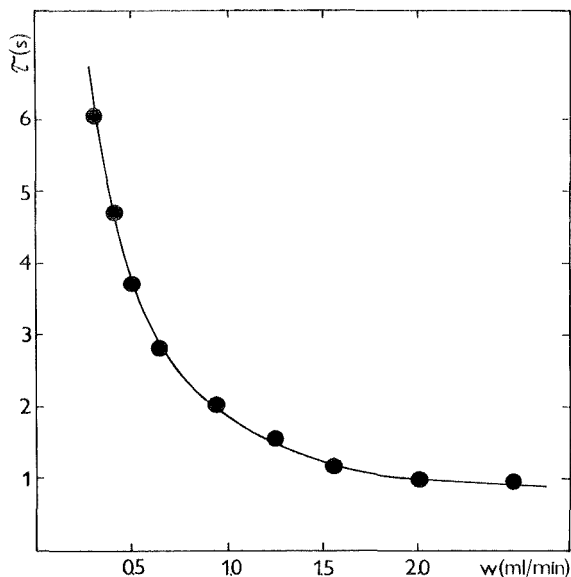


FIGURE 4. Dependence of the response time constant on the flow-rate. Vertical jet detector, jet diameter 0.2 mm. 400 μ l of 2×10^{-5} M ONPh injected.

signal growth and it can be used to compare the performance of various detectors under the same experimental conditions.

An accurate determination of the response time constant is somewhat difficult for the detector with the vertical jet axis, because the steepest part of the curve must be approximated by a straight line. The time constant values given in Fig. 4 were thus obtained from the above equation by evaluating the part of the curve between the points at which the detector signal attained 50 and 90% of the steady-state value.

The product of the volume flow-rate and the time constant, the response volume, V_r (4), remained virtual-

ly constant over the whole range of the flow-rates studied and amounted on average to 31.7 μl with a standard deviation of 1.8 μl . The droplet volume, V_d , found from the period of dropping at a known flow-rate, was also constant within this range. The mean droplet volume was 58.8 μl (standard deviation, 0.7 μl) for 0.2 mm jet and 52 μl for 0.4 mm jet.

It follows from the equation of the exponential response that 99.5% of the steady-state amplitude can, under optimal conditions, be attained after disconnection of the $5.3 V_r/V_d$ droplets, i.e. after about three droplets. However, a simple consideration shows that full deflection can be reached at the latest after two droplets on a step change in the concentration. The sample zone that just passed through the jet tip leads to a drop of electrolyte in which the zone is diluted, but the following drop is composed only of the sample zone and the detector should indicate the full deflection. The slower response observed can be explained by an assumption that the drops are imperfectly disconnected from the jet tip. It must be borne in mind that a spherical drop 60 μl in volume would have a diameter of almost 5 mm and the translational velocity of the liquid is more than half metre per second with a 0.2mm jet and a flow-rate of 1 ml/min. Thus the detector operates probably with elongated electrolyte drops, deposited along the external circumference of the jet, from which a part is always imperfectly separated.

Calibration Curve

When the 0.2 mm jet was used, a linear calibration curve was obtained from 5×10^{-6} to 10^{-4} M concentrations, at a flow-rate of 0.5 ml/min. The slope of the calibration straight line with a regression coefficient of 0.9994 was $2.26 \times 10^5 \text{ uA.l.mol}^{-1}$. The response non-line-

arity at higher current densities is most probably caused by a high potential gradient inside the electrolyte drop that cannot be compensated, even if a positive feedback is introduced. This is supported by the fact that when using an electrolyte with a higher conductance (0.2M acetate buffer containing 5% methanol, in which the measured resistance between the mercury and the auxiliary electrode was 65 k Ω) the linear section of the calibration curve is doubled with the positive feedback.

On the other hand, a linear calibration curve (with a regression coefficient of 0.9987) was obtained in a concentration range of 5×10^{-6} to 2.5×10^{-4} M even in a medium of 50% methanol, when using the 0.4mm jet. The upper limit of this interval was given by the operational range of the potentiostat that attained the saturation voltage at a current of ca. 55 μ A. The detection with the larger jet was virtually equally sensitive as that with the narrower jet, 2.23×10^5 μ A.l.mol $^{-1}$.

The Dependence of the Signal Amplitude on the Flow-Rate

The conditions of the transport of the electroactive substance toward the surface of a hollow drop electrode are very complicated. Convection caused by the growth of the drop and that caused by the flow of the electrolyte are combined and the situation is further complicated by the above mentioned inhomogeneity of the potential distribution over the working electrode surface. Therefore it will only be stated that the current signal increases linearly with increasing volume flow-rate (Fig. 5) and that the dependence deviates from linearity when using the smaller jet in the region of higher current densities, similar to the calibration curve.

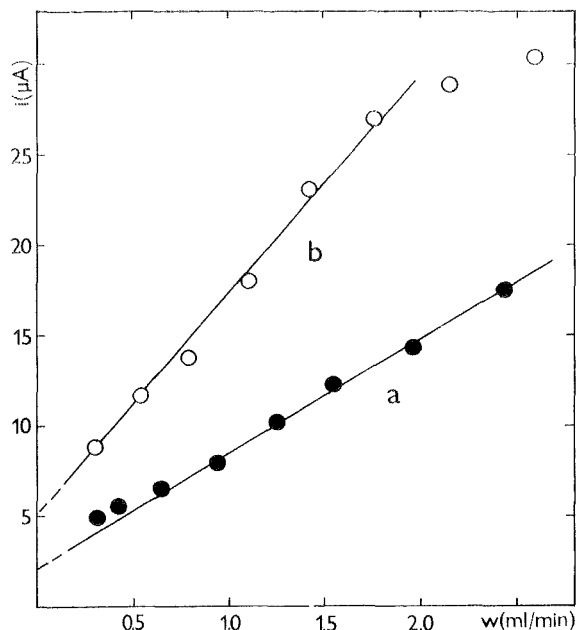


FIGURE 5. Dependence of the signal amplitude on the flow-rate. Vertical jet detector, jet diameter 0.2 mm, 400 μl of a) 2×10^{-5} M ONPh and b) 5×10^{-5} M ONPh injected.

Response Reproducibility

The detector response reproducibility is comparable to that of a classical dropping mercury electrode. Twenty measurements of samples at a concentration of 5×10^{-5} M at a flow-rate of 0.5 ml/min yielded a mean value of the current of 11.46 μA with a standard deviation of 0.08 μA .

Detector with Horizontal Jet Axis

In the detector with the horizontal jet axis the current signal has no oscillations, because the solution does not drop, but forms a thin layer between the external surface of the jet and the mercury. The effective

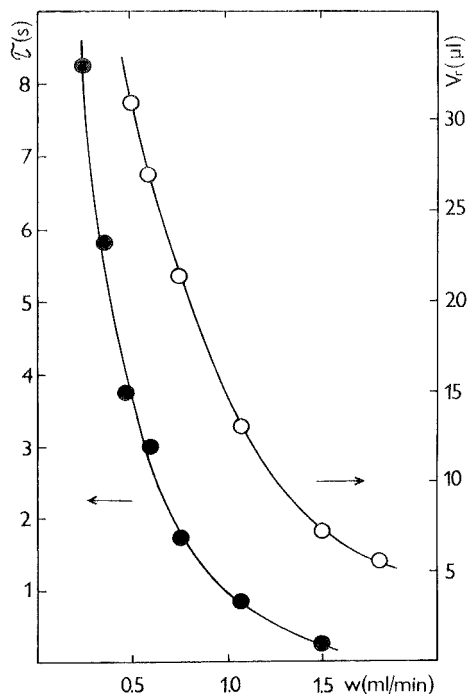


FIGURE 6. Dependence of the response volume and the time constant on the flow-rate. Horizontal jet detector, jet diameter 0.4 mm, 400 μ l of 2×10^{-5} M ONPh injected.

surface area of the working electrode (on which the electrochemical reaction can occur) is not exactly defined, which leads to certain peculiarities in the detector behaviour, as described below.

Response Rate

As can be seen from the time constants given in Fig. 6, the detector with the 0.4 mm jet exhibits a dynamic behaviour similar to that of the detector with the vertical jet. However, the response volume does not remain constant when the flow-rate is changed and relatively rapidly decreases with increasing flow-rate.

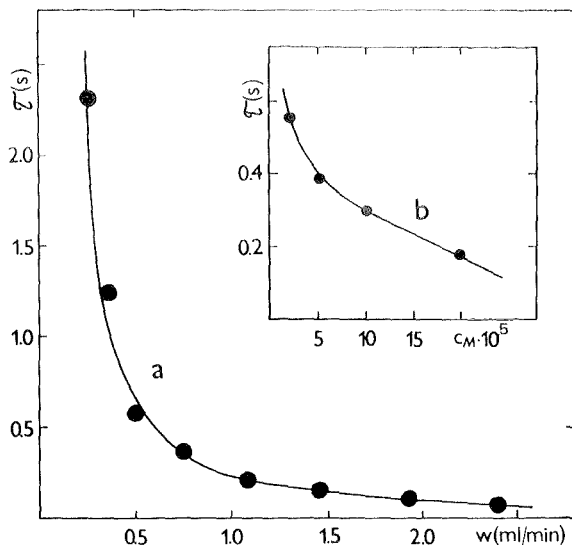


FIGURE 7. Horizontal jet detector: time constant vs. the flow-rate (a) and the concentration of o-nitrophenol (b). Jet diameter 0.2 mm, 400 μ l injected. a) constant concentration 2×10^{-5} M, b) constant flow-rate 0.5 ml/min.

When the 0.2 mm jet is used, the response rate is substantially increased and the time constant becomes to a certain extent dependent on the electroactive substance concentration (Fig. 7). This somewhat unexpected dependence can be understood when realizing that with increasing concentration, i.e. increasing electrolytic current, the inhomogeneity of the potential distribution over the working electrode surface also increases. Thus the electrode effective surface area decreases, leading to a decrease in the volume in which the detection takes place.

Calibration Curve

The deterioration of the geometry between the reference electrode tip and the working electrode sur-

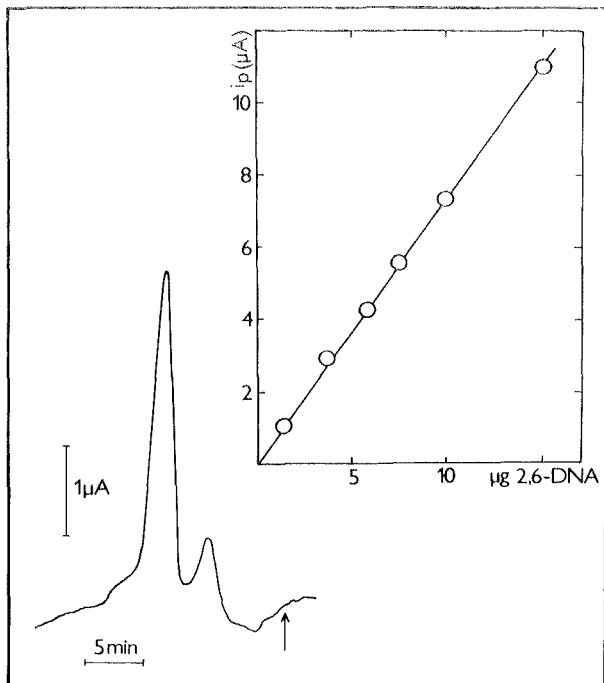


FIGURE 8. Horizontal jet detector: chromatogram of 5 μg of 2,6-dinitroaniline and the corresponding calibration curve. Jet diameter 0.2 mm, flow-rate 1.5 ml/min.

face (compared with the previous detector) causes a narrowing of the linear dynamic range. Even if the 0.4 mm jet was used, the linear calibration curve was only obtained from 5×10^{-6} to 10^{-4}M concentration at a flow-rate of 0.5 ml/min. and this interval could be extended to $2 \times 10^{-4}\text{M}$ by introducing positive feedback. The slope of the calibration curve with a regression coefficient of 0.9986 was $2.13 \times 10^5 \mu\text{A.l.mol}^{-1}$. Therefore the detection sensitivity was virtually the same as that for the detector with vertical jet.

When samples were injected in amounts corresponding to about one third of the stationary current signal (18.6 μl), a linear calibration curve was obtained in a concentration range of 10^{-6} to $3 \times 10^{-4}\text{M}$. The straight line with a regression coefficient of 0.9970 had a slope of $5.7 \times 10^4 \mu\text{A.l.mol}^{-1}$ for amounts of 25.8 to 775.5 ng of o-nitrophenol. For the detector with the 0.2 mm jet, a substantially narrower linear dynamic range was obtained with the same flow-rate, namely, from 5×10^{-6} to $2 \times 10^{-5}\text{M}$. The calibration curve obtained from four experimental points had a regression coefficient of 0.9983 and a slope of $4.3 \times 10^5 \mu\text{A.l.mol}^{-1}$. In spite of the discouragingly narrow linear dynamic range, this detector was tested in combination with a liquid chromatograph, as it could be expected that its rapid response would be favourable. Fig. 8 depicts the response in the detection of 2,6-dinitroaniline. The calibration curve, obtained intentionally for large amounts injected (1.5 to 15 μg) at -1.0V is reliably linear because of low concentrations of the electroactive substance in the eluted zone. It can be simply derived (5) that the concentration at the peak top was $1.2 \times 10^{-5}\text{M}$ for 10 μg of 2,6-dinitroaniline injected.

Dependence of the Signal Amplitude on the Flow-Rate

This dependence was again followed for the steady-state current signal at concentrations of 2×10^{-5} and $5 \times 10^{-5}\text{M}$, from 0.25 to 2.4 ml/min.

With the 0.4 mm jet, the plot in the logarithmic coordinates yielded straight lines with slopes of 0.47 and 0.52 and the respective regression coefficients, 0.9929 and 0.9983. The current signal amplitude thus increases with the square root of the flow-rate, similar to thin-layer detectors with solid electrodes. The dependence is complicated by the high potential

gradient when the small jet is used, and the dependence exhibits a negative deviation from the square-root dependence for high flow-rates.

Response Reproducibility

As mentioned above, the effective surface area of the working electrode is not exactly defined in this detector type. Therefore, certain rules must be observed to obtain reproducible results, in contrast to the detector with the vertical jet.

The detector exhibits optimal performance when the mercury surface is virtually dry, which can be attained by modifying the liquid outlet from the detector. The outlet to the waste that is lower than the detector is through a stainless-steel tube brought through the detector wall to a distance of about 1.5 cm above the jet base. After filling the compartment with mercury, the mercury is forced to the waste by the liquid; utilizing the siphon effect (for short-time opening of the upper closing), all excess mercury and electrolyte are removed. When the upper closing is again sealed, the absence of the electrolyte on the surface of the mercury and a constant mercury level are ensured. The detector prepared in this way yields well reproducible response after conditioning under flow conditions for several minutes. Twenty measurements on samples with a concentration of $2 \times 10^{-5} \text{M}$, using the 0.2 mm jet and a flow-rate of 0.5 ml/min., gave the mean current value of 8.83 μA with a standard deviation of 0.17 μA .

The results obtained in the testing of the detectors, some of which are given in the table, indicate that detectors of good properties can be constructed using this principle. The vertical jet detector is suitable e.g. for continuous analyzers, because of its slower response and a broad linear dynamic range. The construction with the closed mercury also ensures the

TABLE 1
Important Properties of Tested Detectors

Detector	Jet diameter (mm)	Time constant at 1ml/min. (s)	Response volume (μ l)	Linear dynamic range (mol.l^{-1})
Vertical jet	0.2	1.8	31.7	5×10^{-6} - 10^{-4}
	0.4	-	-	^a 5×10^{-6} - 2.5×10^{-4}
Horizontal jet	0.2	^b 0.22	4.0	5×10^{-6} - 2×10^{-5}
	0.4	1.0	15.0	5×10^{-6} - 10^{-4}

^aLimited by the operational range of the potentiostat

^bDependent on the electroactive substance concentration

safety of the operator during the measurement. The detector with a horizontal jet with a small diameter, which has some properties similar to those of solid-electrode thin-layer detectors, seems to be suitable for detection in liquid chromatography where small amounts are involved and a fast response is required. In a further development of detectors of this type, the attention should be directed to broadening of their linear dynamic range, which is directly connected with the geometry of the electrodes.

REFERENCES

1. Štulík, K. and Pěcáková, V., Electrochemical Detection Techniques in High - Performance Liquid Chromatography. *J. Electroanal. Chem.* 129, 1, 1981.
2. Trojánek, A., Elektrochemické detektory v analytických průtokových zařízeních, *Chem. Listy* 76, 695, 1982.

3. Trojánek, A. and Holub, I., Current Sampling in Polarography without Synchronization with the Drop Time. *Anal. Chim. Acta* 110, 161, 1979.
4. Hanekamp, H.B., Bos, P., Brinkman, U.A.Th. and Frei, R.W., A Comparison of Different HPLC Detector Designs Based on the Dropping Mercury Electrode Principle. *Fresenius Z. Anal. Chem.* 297, 404, 1979.
5. Scott, R.P.W., *Liquid Chromatography Detectors*, Elsevier, Amsterdam, Oxford, New York, 1977, p. 11.

ROLE OF INTERFACIAL TENSION IN REVERSE PHASE LIQUID CHROMATOGRAPHY

G.K. Vemulapalli and T. Gnanasambandan, Department of Chemistry,
University of Arizona, Tucson, Arizona 85721

ABSTRACT

A thermodynamic equation relating chromatographic equilibrium constant to the interfacial forces between the stationary phase and the mobile phase is derived from the first principles. Advantages of using this equation in the analysis of bonded phase chromatographic data are discussed.

INTRODUCTION

During the last decade chromatography with chemically bonded phases has evolved into an indispensable technique for chemical separation. It has been widely recognized that both kinetics and equilibrium thermodynamics control chromatographic separation process (1,2). Many attempts have been made to correlate equilibrium constants derived from liquid chromatography with the known solvent-solute interactions (3,4,5). Theoretical attempts have also been made to formulate the equilibrium constant expressions in terms of solvent and solute parameters (6,7,8).

In most of these studies it has been tacitly assumed that the thermodynamic equilibria involved in chromatographic separation are the same as those involved in liquid-liquid partition. However, we should expect interfacial forces to play a crucial role; yet there have been only sketchy discussions on this point

in liquid chromatographic literature and only empirical correlations between interfacial forces and retention times have been made with ad hoc theoretical machinery. The interfacial forces considered in previous investigations are between two solvents (9) or between solute and a solvent cavity (10). These are not as directly related to chromatographic equilibrium as the interfacial forces between the mobile and the stationary phases considered here.

In the following article we will show how interfacial tension directly enters into the liquid chromatographic equilibrium. We derive a general expression for the equilibrium constant for the distribution of solute between bulk phase, where surface forces may be safely ignored, and an interfacial phase, where surface forces dominate.

Even though the derivation given below is based on familiar theoretical procedures, it is not described in the literature. In tracing the expression for the equilibrium constant back to first principles, we have found that theory gives valuable insights into (a) the role of interfacial tension in the separation process, (b) the composition of the stationary phase and (c) the dependence of selectivity on length of carbon chains in the stationary phase. These are discussed in the last section of the article.

THEORY

Let the subscripts b and s represent bulk and surface phases respectively. The chemical potential of a solute at constant temperature and pressure in the bulk phase is given by

$$d\mu^b = RT d \ln a^b, \quad (1)$$

where a^b represents the activity of the solute. The chemical potential of the solute in the surface phase is given by (11)

$$d\mu^s = RT d \ln a^s + \gamma dA, \quad (2)$$

since the interfacial tension, γ , is given by

$$\gamma = \left(\frac{\partial \mu}{\partial A} \right)_{T, P, a}, \quad (3)$$

where A is the area of the interface. In the chromatographic experiments A is usually constant and γ varies with composition of the solution. Hence we need μ as an explicit function of γ . This is accomplished by the following Legendre transformation (12):

$$\hat{\mu} = \mu - A \left(\frac{\partial \mu}{\partial A} \right)_{T, P, a} = \mu - \gamma A \quad (4)$$

From the above expression it follows that

$$d\hat{\mu}^S = RT d \ln a^S - A d\gamma. \quad (5)$$

Since surface forces are negligible in the bulk phase,

$$d\hat{\mu}^b = d\mu^b. \quad (6)$$

The condition for distribution of solute between the two phases is

$$d\hat{\mu}^b = d\hat{\mu}^S, \quad (7)$$

from which we have

$$RT d \ln a^b = RT d \ln a^S - A d\gamma. \quad (8)$$

So far no approximations have been made in the derivation. Eq. 8 is valid for any solute distributed between any pair of bulk and surface phases regardless of the nature of intermolecular forces in these phases. To proceed further, we need to know how interfacial tension varies with composition. Prigogine and Defay (13) showed that surface tension (liquid-vapor interface) for a binary solution is accurately given by

$$\sigma_{12} = \sigma_1 X_1 + \sigma_2 X_2 - \beta X_1 X_2 \quad (9)$$

where the subscripts denote the two components, X , the mole fractions and β , a small constant. In order to avoid unnecessary confusion we shall denote surface tension by σ and interfacial tension by γ . The third term on the right hand side of Eq. 9 is usually small and may be safely ignored when one of the mole frac-

tions is small. Eq. 9 should also apply for interfacial tensions of binary solutions.

In order to be able to integrate Eq. 8 we have to follow a convention regarding standard states. Standard states based on Henry's Law are commonly used for studies of solute distribution between two phases. Integration of Eq. 8 with this convention gives,

$$\frac{1}{X_2^S} \ln \frac{X_2^S}{X_2^b} = \frac{A}{RT} (\gamma_2 - \gamma_1), \quad (10)$$

where Eq. 9 (with γ in place of σ) is used for the evaluation of the term involving interfacial tension. Subscripts 1 and 2 denote solvent and solute respectively. Note that we have substituted mole fractions for activities. Since

$$(1/X_2^S) \approx (1 - X_2^S) = \ln X_1^S \quad (11)$$

and X_1^S is very nearly equal to unity Eq. 10 takes the form:

$$\ln \frac{X_2^S}{X_2^b} = \ln K = \frac{A}{RT} (\gamma_2 - \gamma_1). \quad (12)$$

It should be noted that a simple expression for equilibrium constant, such as the one given in Eq. 12, does not follow from theory unless the solution is dilute.

DISCUSSION

Eqs. 8 and 12 relate equilibrium constant to other measurable quantities, A and γ . Reliable methods have been devised for estimation of solid-liquid and liquid-liquid interfacial tensions (14,15) since these quantities are significant in the studies of wetting, surface energies of solids and many industrial processes. Thus Eqs. 8 and 12 provide a bridge between liquid chromatography and interfacial studies.

We will now show that Eq. 12 is consistent with experimental observations. According to this equation, $\ln K$ for a series of compounds (solutes) should vary linearly with their interfacial tensions (γ_2) provided γ_1 and A remain constant (i.e., same solvent and column). Note that γ_2 refers to interfacial tension between the solute and the stationary phase and hence depends on both these phases. (Similarly, γ_1 depends on both the solvent and the stationary phase.) γ_2 values for systems involving the stationary phases of chromatography are not available at present. In order to demonstrate the quantitative validity of Eq. 12, we will use reasonable estimates for γ_2 . According to Fowkes (15) interfacial tension between two phases (say a and b) may be estimated from the surface tension of each phase against its own vapor. Fowkes theory has been remarkably successful in predicting interfacial tensions (16). For systems of interest in the present study, his equation has the form:

$$\gamma_2 = \sigma_2 + \sigma_s - 2\sqrt{\sigma_2\sigma_s} \quad , \quad (13)$$

where σ_2 and σ_s are the surface tensions of solute and stationary phases. Since the stationary phase is the same for all solutes in an experiment, we should expect interfacial tensions of solute-stationary phase systems to be proportional to the surface tensions of the solutes. Hence, $\ln K$ and $\ln k$, where k is the capacity factor, should increase with surface tension. Fig. 1 shows that this is indeed the case.

Experimental points (17) in Fig. 1 follow a straight line graph closely indicating that σ_s is relatively small. From the experimental values of capacity factors in Fig. 1, we conclude that $\gamma_2 > \gamma_1$. Even though Eq. 12 relates K , and not k , to interfacial tension, this statement is still correct since $k = K\phi$ where the constant ϕ is the volume ratio (stationary phase to mobile phase) which has been estimated to be less than unity (18). Small interfacial tension between the solvent and the stationary phase results if the stationary phase has solvent molecules incorporated into it. (The more the stationary phase approaches the solvent

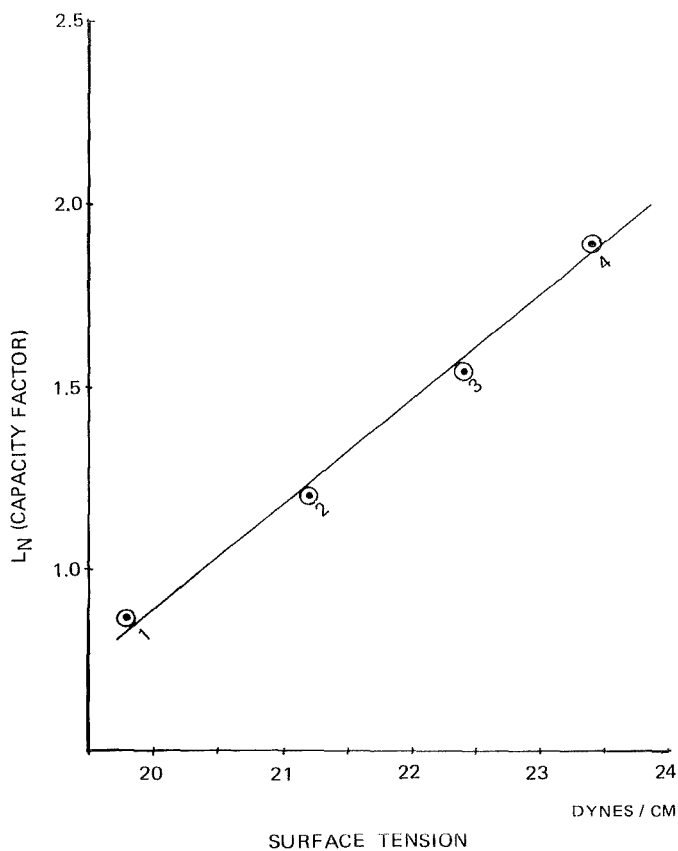


FIGURE 1:

Logarithm of capacity factors (k) as a function of surface tension of solutes. k values are taken from H. Colin and G. Guiochon (Reference 17) solutes 1: n-heptane; 2: n-octane; 3: n-nonane; 4: n-decane. Surface tensions are obtained from CRC Handbook of Physics and Chemistry, 1982.

phase in composition the less would be their interfacial tension.) This conclusion also agrees with the results of previous investigations (19).

It is known experimentally that retention and separation are influenced by chain length of the stationary phase. Practicing chromatographers use this phenomenon in designing appropriate columns for a given system. Attempts have been made to explain the variation of selectivity with chain length by such factors as the surface structure of the stationary phase or steric effects. It should be noted that the mechanisms suggested previously (3,5,6,7,8,9,10) do not explicitly consider the effect of chain length on separation. The theory developed here, however, gives a handle on the problem through the quantity A in Eq. 12.

Eq. 8 follows from first principles of equilibrium thermodynamics and Eq. 12 has no serious approximations. However, interfacial tensions for materials of chromatographic interest are not readily available. Otherwise application of Eq. 12 would be simple and straightforward. We have demonstrated here, with the aid of the available data, the validity of Eq. 12. Work in progress is aimed at (i) evaluation of interfacial tensions from experiment and theory and (ii) numerical estimation, with the aid of Eq. 12, of parameters such as the volume ratio and areas of stationary phases.

ACKNOWLEDGMENT

We wish to thank Professors Quintus Fernando and Michael F. Burke for their encouragement and critical comments. T.G. wishes to acknowledge Professor Henry Freiser for helpful discussions.

REFERENCES

1. Knox, J.H. High Performance Liquid Chromatography. Edinburgh University Press, Edinburgh, U.K. (1978).
2. Locke, D.C. In Advances in Chromatography. Giddings, J.C. and Keller, R.A., Eds., Marcel Dekker, pp. 47-89. New York, N.Y. (1969).
3. Martire, D.E. and Boehm, R.E. J. Liq. Chromatogr. 3:753 (1980).
4. Martire, D.E. and Boehm, R.E. J. Phys. Chem. 84:3620 (1980).

5. Horvath, C. and Melander, W.J. *J. Chromatogr. Sci.* 15:393 (1977).
6. Scott, R.P.W. *J. Chromatogr.* 122:35 (1976).
7. Snyder, L.R. and Poppe, H.J. *J. Chromatogr.* 189:363 (1980).
8. Tijssen, R., Billiet, H.A.H., and Schoenmakers, P.J. *J. Chromatogr.* 122:185 (1976).
9. Fon, C., Novosel, B. and Guiochon, G. *J. Chromatogr.* 83:77 (1973).
10. Horvath, C. Melander, W. and Molnar, I. *J. Chromatogr.* 125:129 (1976).
11. Aveyard, R. and Haydon, D.A. *An Introduction to Principles of Surface Chemistry.* University Press. pp. 9-15. Cambridge, U.K. (1973).
12. Andrews, F.C. *Thermodynamics: Principles and Applications.* Wiley-Interscience. pp. 267-272, New York, N.Y. (1971).
13. Prigogine, I. and Defay, R. *J. Chim. Phys.* 46:367 (1949).
14. Good, R.J. and Girifalco, L.A. *J. Phys. Chem.* 64:561 (1960).
15. Fowkes, F.M. In *Contact Angle, Wettability and Adhesion.* Gould, R.F., Ed., American Chemical Society. pp. 99-112. Washington, D.C. (1964).
16. Zettlemoyer, A.C. In *Hydrophobic Surfaces.* Fowkes, F.M., Ed., Academic Press, New York (1969).
17. Colin, H. and Guiochon, G.J. *J. Chromatogr. Sci.* 18:54 (1980).
18. Blevins, D.D. *The synthesis and characterization of bonded phase chromatographic adsorbents.* Dissertation. University of Arizona (1982).
19. Lochmuller, C.H. and Wilder, D.R. *J. Chromatogr. Sci.* 17:574 (1979).

LIQUID CHROMATOGRAPHIC BEHAVIOR OF BIOLOGICAL THIOLS AND
THE CORRESPONDING DISULFIDES

L.A. Allison, J. Keddington and R.E. Shoup*
Bioanalytical Systems Inc.
Research Laboratories
1205 Kent Avenue
West Lafayette, Indiana 47906

ABSTRACT

Reverse-phase, ion-exchange, and reverse-phase ion-pairing were evaluated as liquid chromatographic modes for the isocratic separation of cysteine, cystine, glutathione (reduced and oxidized), homocysteine, and penicillamine (reduced and oxidized). A series dual Hg/Au amperometric detector was used to detect both thiols and disulfides. Reverse-phase ion-pairing was determined to provide the most satisfactory performance for a liquid chromatographic separation of the compounds of interest.

INTRODUCTION

There are a number of thiol compounds which are of biological interest. In living systems, glutathione (GSH), cysteine (CSH), and the corresponding disulfides (GSSG and CSSC) are intricately involved in maintaining proper cellular function. The thiol moiety is also present in penicillamine (PSH), a therapeutic agent used as an anti-arthritic and in heavy metal poisoning. One pathway for penicillamine metabolism involves formation of

disulfides by reaction with another penicillamine molecule or other physiological thiols.

Determination of thiol compounds by liquid chromatography has recently received considerable attention, utilizing various detection schemes. The most common approach for cysteine (1, 2, 6, 8-10), glutathione (1, 2, 7-10), and penicillamine (1-3) has employed strong cation-exchange chromatography with mobile phases of acidic pH. Reverse-phase chromatography with heptane sulfonic acid as an ion-pairing agent has also been used in the separation of cysteine, homocysteine (HSH), and penicillamine (4), and a strong anion-exchange separation has been reported for several thiols, including glutathione and cysteine (9).

Often, measurement of both the thiols and disulfides in a given biological or chemical matrix is desirable, to provide a complete profile of the system. Due to the scarcity of suitable detectors for disulfides, there have been few reports on chromatographic characteristics of underivatized disulfides. Egli and Asper (6) used strong cation-exchange for a mixture containing cystine (CSSC), cysteine and penicillamine, as did another report on glutathione, cystine, cysteine, and methionine (10). Strong anion exchange with a mobile phase of pH 8.4 was used for GSSG and cystine (5), although the resolution and peak shapes were rather unsatisfactory.

A series dual Hg/Au electrochemical detector has recently been developed in our laboratory for the detection of both thiols and disulfides in liquid chromatographic eluents (11). Briefly, the detector reduces disulfides at an upstream electrode and detects the resultant thiols and any naturally present thiols at the downstream electrode. Using this detector, we now report on the liquid chromatographic behavior of mixtures of selected thiols and disulfides. Strong cation-exchange, reverse-phase, and reverse phase ion-pairing were evaluated as separation schemes for cysteine, cystine, glutathione, homocysteine, penicillamine, glutathione disulfide and penicillamine disulfide.

MATERIALS

Chemicals

L-cysteine, L-cystine, glutathione (reduced), glutathione (oxidized), and D-penicillamine were purchased from Sigma Chemical Co. (St. Louis, MO). D-penicillamine disulfide was obtained from Aldrich Chemical Co. (Milwaukee, WI) and DL-homocysteine was purchased from ICN Pharmaceuticals, Inc. (Cleveland, OH). Sodium octyl sulfate and ethylene diamine tetraacetic acid were obtained from Eastman Kodak Co. (Rochester, NY). All other reagents, including buffer salts, acids, and methanol, were reagent grade.

Apparatus

A Bioanalytical Systems LC-154 liquid chromatograph with dual mercury/gold detector was used. All teflon tubing was replaced with stainless steel to exclude oxygen. The system has been described in detail elsewhere (11). Columns used were BAS Biophase ODS 5 μ , 4.6 x 250 mm, and DuPont Zorbax 300 SCX, 4.6 x 250 mm. Detector output was integrated using either an LDC-308 Integrator or Hewlett Packard 3390A Reporting Integrator. Mobile phase flow rates were either 1.5 mL/min or 1.0 mL/min.

Methods

All mobile phases were prepared using deionized distilled water and filtered with 0.2 μ Nylon 66 membranes (Rainin Instrument Co., Inc., Woburn, MA). Mobile phases were refluxed at slightly above room temperature and continually purged with nitrogen to remove dissolved oxygen.

Stock standard solutions of individual compounds were prepared to a concentration of 1 mM in deionized, distilled water containing 1 g/L Na₂EDTA. The cystine stock solution was prepared in dilute NaOH at a concentration of 0.1 mM. All stock solutions were stored at 4°C and prepared weekly. Dilutions and

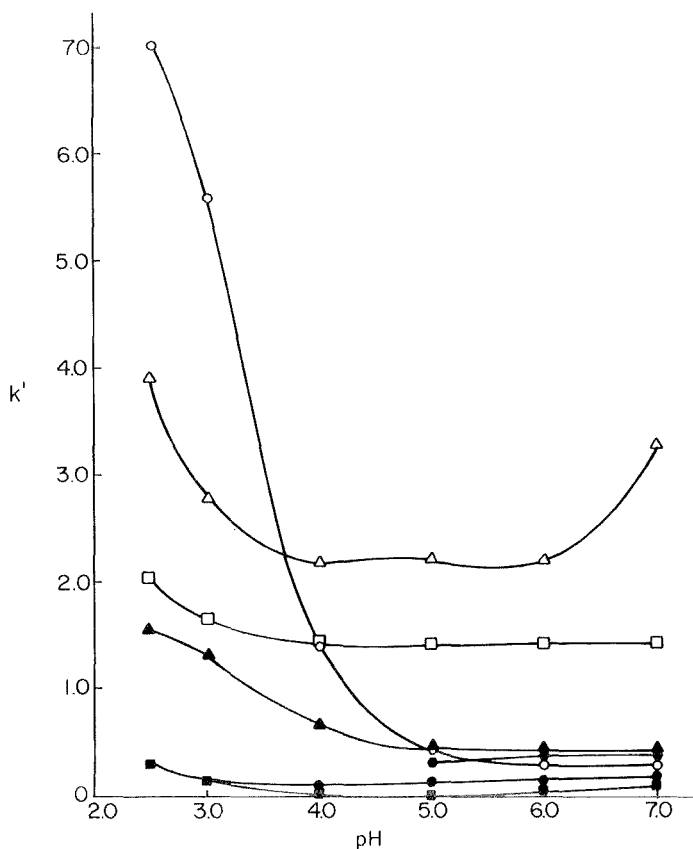


FIGURE 1. Capacity factors (k') of thiols and disulfides as a function of mobile phase pH. Mobile phase consisted of 0.1M phosphate buffer adjusted to the desired pH. A Biophase ODS 5 μ column was used with a flow rate of 1.5 mL/min. Curves represent cysteine (\bullet), cystine (\blacksquare), reduced glutathione (\blacktriangle), homocysteine (\bullet), oxidized glutathione (\circ), reduced penicillamine (\square), and oxidized penicillamine (\triangle).

mixtures of standard solutions were prepared every two or three days from the stock solutions. Cystine solutions were acidified using dilute HClO_4 prior to injection. Injections were made by overloading a 20 μL or 100 μL loop with deoxygenated standard solution.

The dual Hg/Au electrodes were prepared as described elsewhere (11). The flow channel was defined with the two electrodes in the series arrangement. The upstream electrode was held at -1.0V and the downstream electrode was monitored to obtain the chromatographic tracing.

RESULTS AND DISCUSSION

Reverse-Phase Chromatography

The behavior of the thiols and disulfides of interest was first investigated by using a reverse-phase column (Biophase ODS, 5 μ) and varying the pH of the 0.1 M phosphate mobile phase over the range from 2.5 to 7.0. Figure 1 illustrates the measured capacity factors (k') versus mobile phase pH. At acidic pH values, reasonable retention is obtained for GSH, GSSG, PSH and PSSP, but they are observed to elute earlier with increasing pH. This is as expected from the ionizable functional groups in the molecules, which include carboxylic acids ($\text{pK}_a \approx 2$), amines ($\text{pK}_a \approx 8-9$) and thiols ($\text{pK}_a \approx 9-11$). In regions of intermediate pH (4-7), the majority of these compounds exist as zwitterions, with little or no retention on the hydrophobic column. As the pH decreases, the carboxylic acid groups are becoming increasingly protonated, with a concomitant increase in retention. The maximum capacity factor for the longest retained compound, however, is only 7.0, demonstrating that these small, relatively polar molecules are not retained to any great extent, and limiting the flexibility of the separation. Cystine and cysteine are not retained or resolved at any available pH on an ODS column.

It is interesting to note that penicillamine disulfide does not reduce as readily as the other disulfides at the upstream

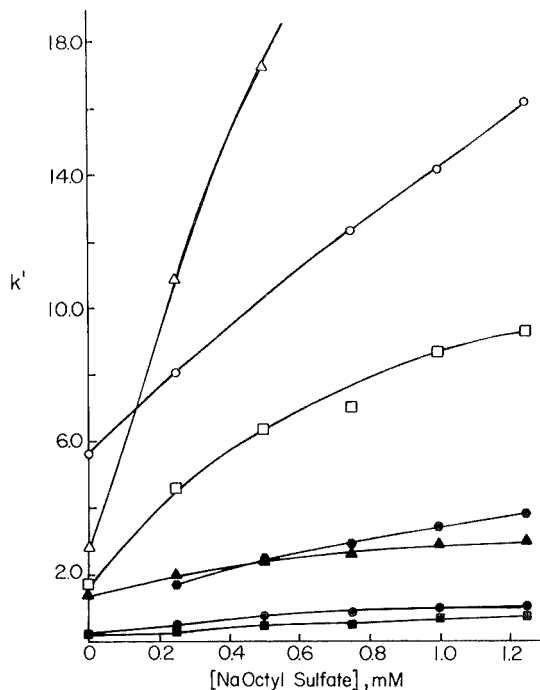


FIGURE 2. Capacity factors (k') of thiols and disulfides as a function of concentration of sodium octyl sulfate. A Biophase ODS 5 μ column was used with 0.1 M monochloroacetate buffer, pH 3.0, flow rate 1.5 mL/min. Curves labeled as in Figure 1.

electrode. Response for PSSP as measured at the downstream electrode is approximately one-hundred fold less than that for cystine and glutathione disulfide, except at pH 5.0, where the response for PSSP is comparable to other disulfides.

Reverse-Phase Ion-Pair Chromatography

A more useful set of mobile phase conditions for the thiols and disulfides was that using sodium octyl sulfate as an ion-pairing reagent with a C18 column. The mobile phase consisted of 0.1 M monochloroacetate (MCAA) buffer, adjusted to pH 3.0 to

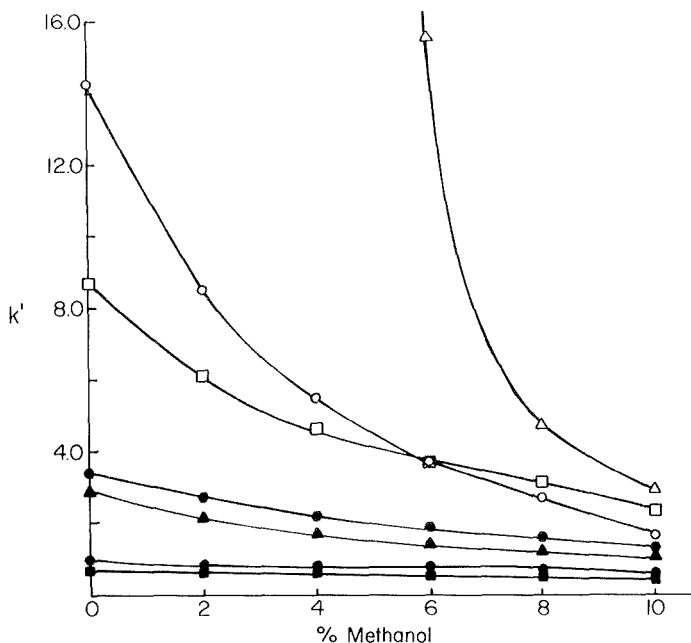


FIGURE 3. Capacity factors (k') of thiols and disulfides as a function of concentration of methanol in mobile phase. Sodium octyl sulfate concentration was fixed at 1.0 mM in 0.1M monochloroacetate buffer, pH 3.0, with a Biophase ODS column. Curves labeled as in Figure 1.

ensure that the compounds carried a net positive charge. In Figure 2, k' is plotted versus concentration of sodium octyl sulfate, demonstrating the large increase in retention which can be effected using this approach. Each of the compounds underwent similar shifts in retention, although penicillamine disulfide was changed to a markedly greater extent than the others. The ion-pairing was successful in resolving cysteine and cystine from one another.

Figure 3 shows the effect on k' of increasing percentages of methanol in the mobile phase. In this manner, the ion-pairing was utilized to increase retention and resolution of cysteine and

cystine, and methanol was added to speed elution of longer-retained compounds. Cysteine and cystine were not significantly affected by addition of methanol, while PSSP, GSSG, and penicillamine were moved in to more reasonable retention times. The chromatogram in Figure 4 illustrates the separation obtained using 1.0 mM sodium octyl sulfate with 4% methanol and a flow rate of 1.5 mL/min. Excluding PSSP, the chromatogram was complete in thirteen minutes and the peak shapes were quite satisfactory.

A third variable which was manipulated in ion-pairing chromatography was the ionic strength of the mobile phase buffer. By changing the molarity of monochloroacetate, the retention times could be correspondingly changed. The effects obtained with ionic strength variations were of less magnitude than those observed when changing sodium octyl sulfate or methanol concentration. Ionic strength, then, can be used to "fine-tune" the reverse-phase ion-pairing separation to achieve the desired chromatographic characteristics. Figure 5 shows a chromatogram of the selected compounds using 0.25 M monochloroacetate buffer, with 1.0 mM sodium octyl sulfate and 6% methanol, flow rate 1.0 mL/min. The chromatogram was complete within 10 minutes, although cysteine and cystine were closer to the void volume response than with 0.1M MCAA, which could pose a problem with real samples.

Based on the described studies, the chromatographic conditions that were adopted for future studies utilized the Biophase ODS 5 μ column with a mobile phase containing 0.1 M MCAA buffer, pH 3.0, 1.0 mM sodium octyl sulfate, with 4% methanol.

Ion-Exchange Chromatography

As the majority of literature work on these compounds has been performed using cation exchange, a column of this type was also investigated. The initial conditions consisted of the Zorbax SCX column with a mobile phase of 18.4 mM ammonium citrate and 60.7 mM phosphoric acid (final pH 2.49), producing the separa-

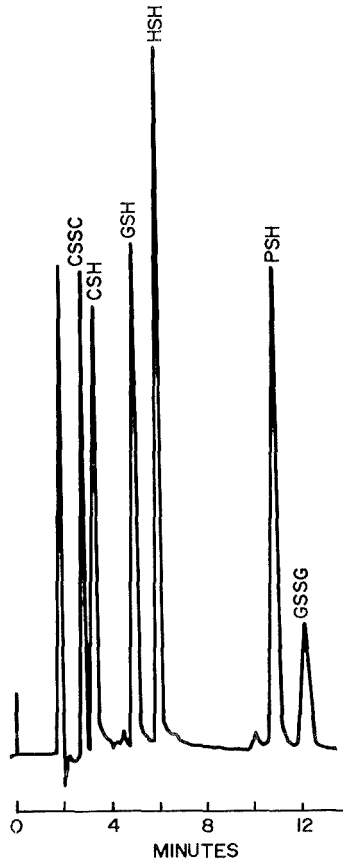


FIGURE 4. Reverse-phase ion-pair separation of thiols and disulfides. Column: Biophase ODS 5 μ ; mobile phase: 0.1M monochloroacetate buffer, pH 3.0, 1.0 mM sodium octyl sulfate, 4% methanol.

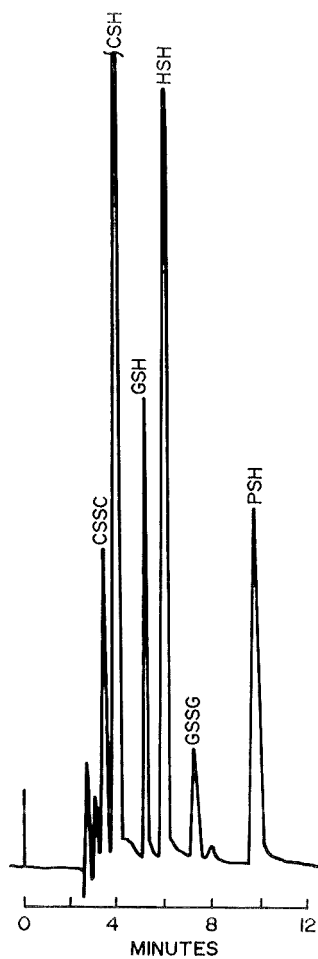


FIGURE 5. Effect of ionic strength on reverse-phase ion-pair separation of thiols and disulfides. Chromatographic conditions as in Figure 4, except monochloroacetate buffer was 0.25M.

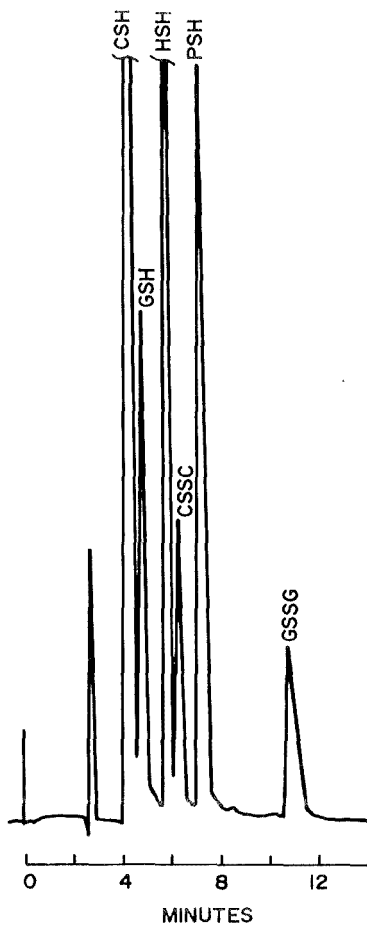


FIGURE 6. Strong cation-exchange separation of thiols and disulfides. A Zorbax SCX column was used, with a mobile phase containing 18.4 mM ammonium citrate and 60.7 mM phosphoric acid, flow rate 1.0 mL/min.

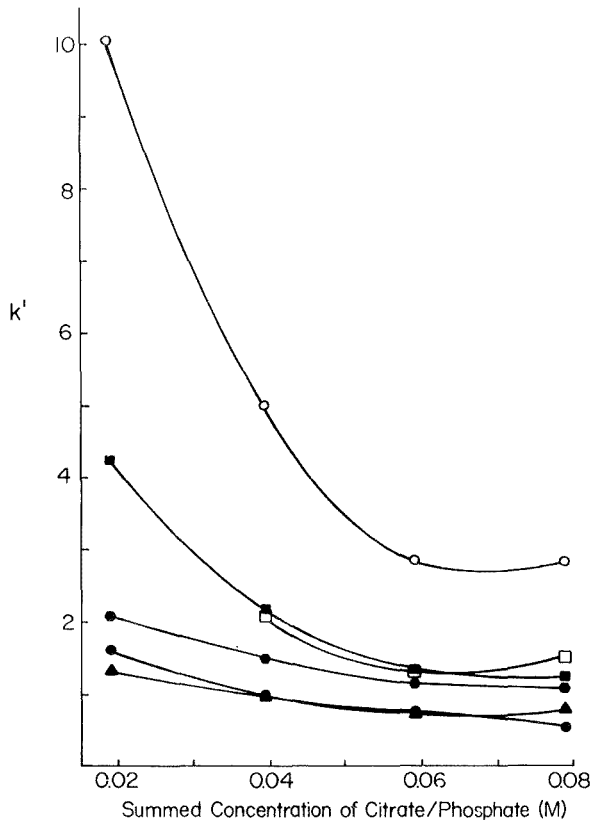


FIGURE 7. Capacity factors (k') of thiols and disulfides as a function of mobile phase buffer concentration. Mobile phase was phosphate/citrate buffer at a flow rate of 1.0 mL/min. with a Zorbax SCX column. Curves labeled as in Figure 1.

tion shown in Figure 6. This separation was considered to be less than optimum, as cysteine/glutathione and homocysteine/cystine were not completely resolved. Increasing the mobile phase to pH 3.5 moved all peaks into the void volume.

The ionic strength was decreased in order to modify the separation; Figure 7 details the effects of ionic strength on k' . When the molarities were 75 and 50% of initial values, several

compounds coeluted, as shown. Peak shapes began to rapidly deteriorate after a k' value of about 5, with broadening and severe tailing.

Cation-exchange chromatography was found in these experiments to be inferior to reverse-phase ion-pair chromatography for applications requiring resolution of all of the thiols and disulfides in our mixture. It could, however, be optimized to provide satisfactory performance for one or two selected compounds.

CONCLUSIONS

In summary, three types of liquid chromatographic separations were evaluated for the LCEC determination of cysteine, cystine, homocysteine, glutathione (reduced and oxidized), and penicillamine (reduced and oxidized): reverse-phase, reverse-phase ion-pairing and strong cation-exchange. Conditions were found which produced satisfactory performance with both reverse-phase ion-pairing and ion-exchange. The reverse-phase ion-pairing mode was determined to be preferable, based on better peak shapes and the high degree of flexibility possible by varying methanol content, ion-pairing reagent concentration, and ionic strength.

REFERENCES

1. Zygmunt, B., Hanekamp, H.B., Bos, P. and Frei, R.W., *Fresenius Z. Anal. Chem.*, 311, 197 (1982).
2. Kreuzig, F. and Frank, J., *J. Chromatogr.*, 218, 615 (1981).
3. Bergstrom, R.F., Kay, D.R. and Wagner, J.G., *J. Chromatogr., Biomed. Appl.*, 222, 445 (1981).
4. Beales, D., Finch, R., McLean, A.E.M., Smith, M., and Wilson, I.D., *J. Chromatogr., Biomed. Appl.*, 226, 498 (1981).
5. Studebaker, J.F., Slocum, S.A. and Lewis, E.L., *Anal. Chem.*, 50, 1501 (1978).
6. Eggli, R. and Asper, R., *Analytica Chimica Acta*, 101, 253 (1978).
7. Rabenstein, D.L. and Saetre, R., *Clin. Chem.*, 24, 1140 (1978).

8. Saetre, R. and Rabenstein, D.L., *J. Agric. Food Chem.*, 26, 982 (1978).
9. Nakamura, H. and Z. Tamura, *Anal. Chem.*, 53, 2190 (1981).
10. Werkhoven-Goewie, C.E., Niessen, W.M.A., Brinkman, U.A.Th. and Frei, R.W., *J. Chromatogr.*, 203, 165 (1981).
11. Allison, L.A. and Shoup, R.E., *Anal. Chem.*, accepted for publication, January, 1983.

SIMULTANEOUS DETERMINATION OF CADMIUM, COBALT, COPPER,
LEAD, MERCURY AND NICKEL IN ZINC SULFATE PLANT ELECTROLYTE
USING LIQUID CHROMATOGRAPHY WITH ELECTROCHEMICAL
AND SPECTROPHOTOMETRIC DETECTION

A.M. Bond* and G.G. Wallace
Division of Chemical and Physical Sciences,
Deakin University,
Waurin Ponds, Victoria 3217, Australia

ABSTRACT

The current efficiency (cost) of electrolytic production of high purity metallic zinc from zinc sulfate plant electrolyte is critically dependent on the concentration of a number of trace elements. The matrix, containing a very large concentration excess of zinc sulfate in concentrated sulfuric acid presents difficulties for determining low concentrations of other metals with many analytical methods. In this work it is shown that Cd, Co, Cu, Pb, Hg and Ni impurities may be simultaneously determined at concentrations less than or equal to 1 ppm using a combination of solvent extraction, high performance liquid chromatography and electrochemical or spectrophotometric detection. Solvent extraction utilizes the formation of pyrrolidine dithiocarbamate complexes, which after removal of zinc complexes and excess ligand on an anion exchange column can be separated on a C-18 reverse phase chromatographic column and detected by UV/Visible spectrophotometric or electrochemical detection. Other combinations of chromatographic and detection procedures were thwarted by the very large concentration excess of zinc and other problems.

INTRODUCTION

The determination of trace elements in the presence of a very large excess of another element is a problem frequently encountered by the analytical chemist (1). Even so called specific methods, can exhibit interference effects when confronted with a matrix of this type (2-4).

In the mining industry, the industrial process to produce high purity metals frequently requires the preliminary production of a concentrate where obviously the concentration of the element to be refined is very high. Nevertheless, in many metal refining processes it is extremely important to monitor the concentration of trace impurities present at various stages of the refining. The overall efficiency of the process may be severely decreased in the presence of certain metals, even at trace levels. A number of methods have been reported for the determination of specific elements in various concentrates (5-11). Commonly, electrochemical techniques or atomic absorption spectrometry have been used. These methods become time consuming if a number of elements need to be determined. For example, Beyer and Bond (10) have determined both the major and some minor elements (Cd, Cu, Pb and Zn) simultaneously in lead and zinc concentrates by polarographic techniques. However, in this procedure the number of elements which can be determined simultaneously is limited, which is typically true in problems of this kind.

The electrolytic production of high purity metallic zinc uses a plant electrolyte which is essentially a very concentrated solution

of zinc sulfate (100-108 g/L) in sulfuric acid (up to 110 g/L). The current efficiency for zinc production decreases substantially in the presence of trace impurities; i.e. cost of production is increased. Consequently, the zinc sulfate electrolyte has to be monitored very closely during the production process. Unfortunately this is not a matrix conducive to the atomic absorption method and many problems exist in the analytical work (11). In these laboratories, a method has been developed for trace metal analysis using liquid chromatography (LC) with electrochemical (LCEC) and/or UV-Visible spectrophotometric (LCUV) detection (12,13), which can be automated (14) with microprocessor based instrumentation. In the present report, the application to multi-element determination in the presence of a huge excess of zinc is examined on samples of zinc sulfate.

The method is based on formation of dithiocarbamate complexes followed by separation and subsequent electrochemical or spectrophotometric detection. Two modes of operation are available:

- (i) The metal-dithiocarbamate complex can be formed external to the chromatographic system and prior to injection onto the separating column. Complex formation may be undertaken in a solvent identical to that for chromatographic separation or in aqueous solution followed by extraction into a suitable organic solvent (15).
- (ii) If the kinetics of dithiocarbamate complex formation is sufficiently rapid, the complex can be formed 'in situ' by including the ligand in the chromatographic solvent. This is the method amenable to complete automation (14). With this method, Ni and Cu (14)

as well as Pb, Co, Hg and Cd (15) can be determined in a single injection within ten minutes.

Other elements (e.g., Cr, As, Sb and Se) cannot be determined in this mode for various reasons (13,15), and recourse to the first mentioned method with external complex formation may need to be considered.

In the present work both modes of operation were considered for the simultaneous determination of Ni, Cu, Co, Pb, Hg and Cd in zinc concentrates.

It might be anticipated that the very large concentration of zinc would mitigate against successful development of a chromatographic method based on electrochemical and/or spectrophotometric detection. In principle, the chromatography might be expected to be inadequate to achieve the required separation which must be high with either spectrophotometric or electrochemical detection since zinc dithiocarbamate gives a response with both detectors. However, two major factors influence the possibility of success applying our new method for metal analysis to zinc plant electrolyte: (i) The stability constant of the zinc dithiocarbamate is small compared with most other metal-dithiocarbamates (16-18), (ii) Evidence for the formation of anionic zinc dithiocarbamate complexes has been reported (19-21). In previous work (14) an anion exchange guard column was designed to trap excess negatively charged dithiocarbamate ligand. The same guard column may therefore at least partially remove the zinc dithiocarbamate complex.

EXPERIMENTALReagents and Standard Solutions

All chemicals used were of analytical grade purity unless otherwise stated. Commercially available diethyl and pyrrolidine dithiocarbamate salts were recrystallized from ethanol prior to use.

Standard solutions of the metals concerned were prepared by dissolving copper nitrate, nickel chloride, cobalt nitrate, lead nitrate, mercuric nitrate, cadmium chloride and selenium dioxide in distilled deionized water. Standard solutions were also prepared in a 'zinc sulfate-sulfuric acid' matrix corresponding to "pure" plant electrolyte. These standards were always used in analytical determinations.

Acetate buffer was prepared using the method described by Vogel (22).

Liquid chromatographic grade (LC) grade acetonitrile, methanol, dichloromethane and chloroform were used throughout this work.

Zinc sulfate electrolyte samples were provided by the Electrolytic Zinc Company, Risdon, Tasmania, Australia.

Instrumentation

Instrumental details concerning the chromatographic and electrochemical instrumentation have been described previously (12-14). Chromatography equipment and spectrophotometric detection were based on Waters equipment whilst electrochemical instrumentation was either from Princeton Applied Research (PAR) Corporation, Bioanalytical Systems (BAS), or home built. In this work the electrochemical detector was a Bioanalytical Systems (BAS)

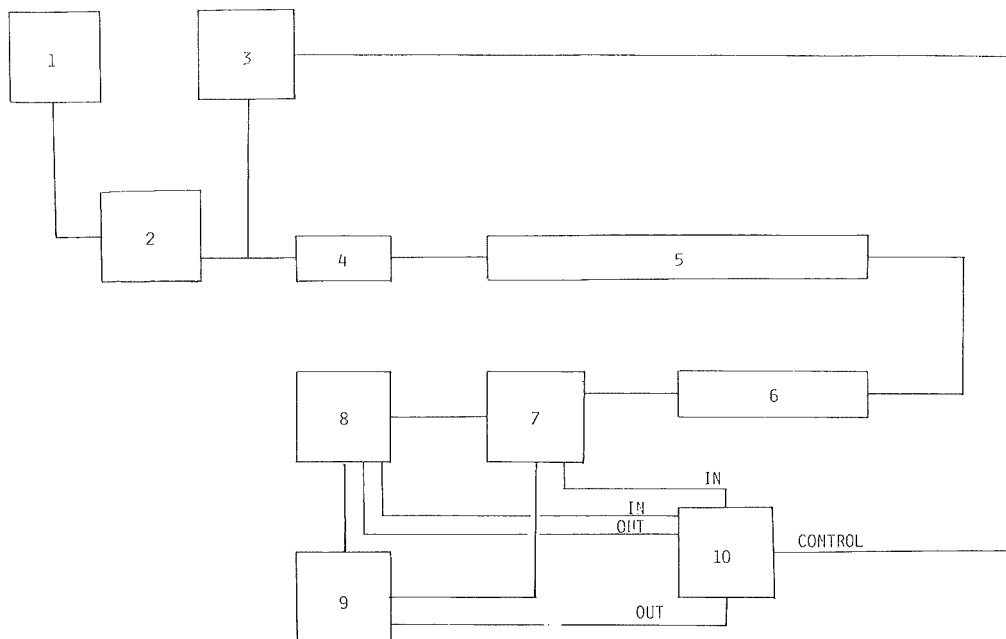


Figure 1

Flow Diagram of Instrumentation.

1. Chromatographic solvent: e.g. External mode : 70% acetonitrile : 30% acetate buffer, pH = 6 (.02 M), .01 M NaNO₃. In situ mode : as above but add 10⁻⁴ M NH₄pydtc.
2. Solvent Delivery System : Typical flow rate = 1-3 mL/min.
3. Injection System : can be either manual or automatic. Typical injection is 10-100 μ L.
4. Guard column : containing (i) separator resin to protect separator column, e.g. C-18 resin and (ii) ion exchange resin to trap excess dithiocarbamate (external mode), e.g. Amberlite CG-400.
5. Separator column : e.g. C-18 reverse phase from Waters Assoc. Length = 30 cm; i.d. = 3.9 mm.
6. Suppressor column : to remove excess dithiocarbamate (in situ mode), packed with ion exchange resin as in guard column. Length = 20 cm; i.d. = 3.9 mm.

TL5 cell with glassy carbon working electrode, and an aqueous Ag/AgCl (3M KCl) reference electrode. Columns were basically as described in reference 14. A typical experimental arrangement is shown schematically in Figure 1.

Electrochemical experiments in a conventional cell were performed using glassy carbon working and auxiliary electrodes and a Ag/AgCl (satd. LiCl : methanol or dichloromethane) reference electrode.

Unless otherwise stated all data were obtained at $(22 \pm 1)^{\circ}\text{C}$ and all solutions were degassed with nitrogen.

RESULTS AND DISCUSSION

The two methods of dithiocarbamate complex formation described in the introduction were examined to ascertain the effect of the large zinc concentration present in zinc sulfate electrolyte.

(i) External Dithiocarbamate Complex Formation

In this mode, diethyl or pyrrolidine dithiocarbamate complexes need to be formed in a buffered aqueous sample of zinc sulfate electrolyte by addition of an aqueous solution of diethyl or pyrrolidine dithiocarbamate salt. The metal complexes are then extracted into an organic phase (dichloromethane or chloroform were found to be suitable) prior to injection onto the column. The

-
7. Spectrophotometric detector.
 8. Electrochemical detector.
 9. Readout device.
 10. Microprocessor.

buffer solution was made 1% (w/v) in NaNO_3 to enhance the extraction efficiency (23). Injection of very pure zinc sulfate electrolyte without any guard column gives an extremely large zinc dithiocarbamate response using spectrophotometric detection ($\lambda = 254 \text{ nm}$) or electrochemical detection (DC potential = 0.80 V) as shown in Figure 2(a,c). However, insertion of an anion exchange guard column is very efficient in removing this response, as shown in Figure 2 (b,d). This method can therefore be used for trace metal determination in zinc sulfate electrolyte with considerable advantage since Cd, Co, Cu, Pb, Hg and Ni may be determined simultaneously if no interference effects are in operation.

Initial studies to examine the extraction behaviour of the various metals in the presence and absence of zinc sulfate were undertaken with differential pulse voltammetry at a glassy carbon working electrode. Each of the dithiocarbamate complexes gives very well defined oxidation responses in organic solvents (19,24). The metal complexes were extracted into dichloromethane, and the electrochemistry then investigated in this solvent after addition of $0.1 \text{ M Bu}_4\text{NClO}_4$ as a suitable supporting electrolyte.

The extraction efficiency and stability of the metal complexes in the presence and absence of zinc sulfate electrolyte could be investigated conveniently in this manner. For those metal complexes which could be measured directly by voltammetry in a conventional electrochemical cell in the presence of a large excess of zinc, data agreed well with that found in liquid chromatographic work after chromatographic removal of zinc. In all cases it was found that the

TABLE 1

Extraction of Metal Pyrrolidine Dithiocarbamate Complexes in Presence and Absence of Zinc Sulfate Electrolyte^{a,b}.

Metal	Percentage of metal dithiocarbamate signal obtained for extraction in presence and absence of zinc sulfate electrolyte.	Percentage of original metal dithiocarbamate signal remaining after two hours.	
		Without Zn	With Zn
Ni	18%	95%	100%
Co	15%	100%	100%
Pb	75%	100%	100%
Hg	85%	100%	100%
Cd	10%	100%	100%
Cu	100%	100%	100%

(a) Percentages quoted typically have a mean deviation of $\pm 3\%$.

(b) Extractions were performed with dichloromethane as in text (see later). Results are average values obtained by two methods.

(i) Differential pulse voltammetry (conventional cell). Scan rate = 5 mV/sec. Duration between pulses = 0.5 sec. Modulation amplitude = 50 mV.

(ii) Extractions were performed and samples injected into the LCEC/UV system described in Fig. 1. Injection volume = 10 μ l. Flow rate = 2 mL/min. UV detection λ = 254 nm. Electrochemical detection DC (+ 1.20 V) vs Ag/AgCl (3 M KCl).

stability of the metal dithiocarbamates was increased in the presence of zinc dithiocarbamate as has been reported by other workers (25,26). Results are summarized in Table 1.

The ligand chosen for extraction in all quantitative studies was pyrrolidine dithiocarbamate (pydtc⁻) rather than diethyldithiocarbamate, (dedtc⁻) for a number of reasons. Firstly, pydtc⁻ has been shown to exchange more readily than

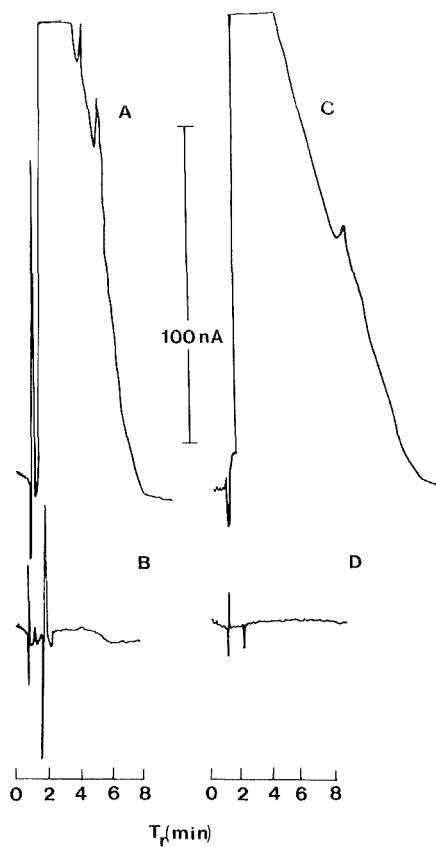


Figure 2

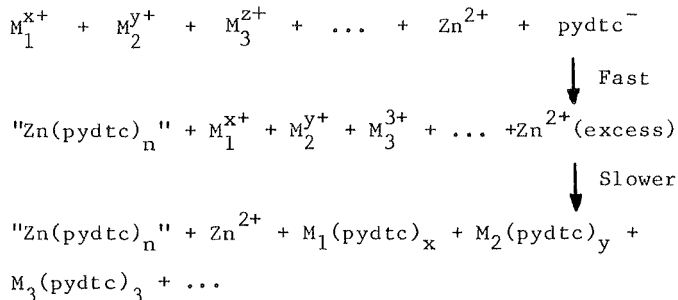
Injection ($10 \mu\text{L}$) of a ZnSO_4 solution (108 g Zn/L) in distilled H_2O . Chromatographic system as described in Fig. 1. Solvent flow rate = 3 mL/min .

- (a) spectrophotometric detection ($\lambda = 254 \text{ nm}$).
- (b) as for (a) but insert ion exchange guard column.
- (c) electrochemical detection DC (potential = $+ 1.20 \text{ V}$).
- (d) as for (c) but insert ion exchange guard column.

dedtc⁻ (18). Secondly, pydtc⁻ is more stable than the dedtc⁻ ligand in acidic solutions, such as encountered with zinc sulfate electrolyte. Finally, a significant response attributable to Zn(dedtc)₂ is observed when the dedtc⁻ ligand is used. This complex has a retention volume similar to Cu(dedtc)₂ and causes interference.

Acetate buffer (pH = 4) was found suitable for extraction of all metals considered.

The basis of the extraction is shown in the reaction scheme below.



"Zn(pydtc)_n" is then trapped on anion exchange guard column and M₁(pydtc)_x + M₂(pydtc)_y + M₃(pydtc)₃ + ... are separated on a reverse phase C-18 chromatographic column and detected. Zn²⁺ does not respond at either detector operating under appropriate conditions.

In this reaction scheme, "Zn(pydtc)_n" is probably a mixture of neutral and anionic complexes. Upon injection some of these complexes break down to give free (pydtc)⁻ (15) which is trapped on the guard column.

M₁^{x+}, M₂^{y+}, M₃^{z+} ... are trace metals and Zn²⁺ is

in a very large concentration excess over other metal ions being detected.

In such an extraction it would be ideal to use as much ligand as possible in order to increase the rate of formation of the metal dithiocarbamate complexes. However, if more than 5 mL of 1% (w/v) pydtc⁻ is used with 1 mL of zinc sulfate electrolyte and 10 mL of extracting solvent, "Zn(pydtc)_n" begins to precipitate at the organic/aqueous interface.

For the determination of low concentrations of metals it is also obviously desirable to use as much zinc electrolyte (sample) as possible. However, use of too much electrolyte introduces too much zinc and therefore decreases the signals (extraction efficiency) of most of the other metals. Variation of zinc concentration at the \pm 10% level was found experimentally to produce a constant trace metal signal (\pm 3%). There are obviously a number of constraints on the extraction procedure that can be used prior to chromatography and detection. In summary, the recommended analytical method is as follows:

- (i) Add 10 mL 1 M acetate buffer (pH = 4.2) containing 1% NaNO₃ (w/v) to 1 mL of zinc plant electrolyte.
- (ii) Add 5 mL of 1% aqueous pydtc⁻ (w/v). Shake mechanically for ten minutes.
- (iii) Add 10 mL extracting solvent (dichloromethane, or chloroform).
- (iv) Shake for a further ten minutes.
- (v) Leave to separate for five minutes.

- (vi) Draw off sample from organic layer and inject a 10 μ L sample into the chromatographic system consisting of 70% acetonitrile/30% buffer etc. as the running solvent, a guard column to remove excess pydtc⁻ and "zinc dithiocarbamate" and a reverse phase C-18 separating column (see Figure 1).
- (vii) Detect the metal with electrochemical or spectrophotometric detection after chromatographic separation.

With the above procedure, calibration curves were constructed for the metals concerned. All were linear for concentrations from the detection limit to at least 20 ppm. Fig. 3 shows a typical chromatogram. Chromatographic resolution between the Cu and Hg responses can be achieved by replacing 70% acetonitrile with (50% acetonitrile + 20% methanol) in the chromatographic solvent.

The only chemical interference observed with other elements known to be present was when mercury was monitored in the presence of selenium. In this situation, complex behaviour was observed in that the mercury response was split into two peaks (Fig. 4), implying that mercury selenium complexes are being formed via exchange reactions. (Results are similar with or without ZnSO₄ present).

Detection limits for both electrochemical and spectrophotometric detection are listed in Table II. Note that in previous work (13-14) the electrochemical detector has proved superior with respect to sensitivity. However in this work, even though the guard column does trap most of the pydtc⁻ and "Zn(pydtc)_n" some

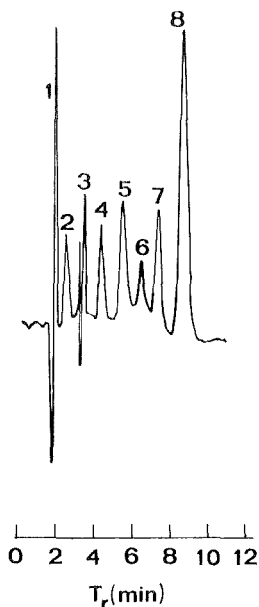


Figure 3

Determination of cadmium (2 ppm), lead (5 ppm) [peak 5], nickel (5 ppm) [peak 6], cobalt (5 ppm) [peak 7], mercury (5 ppm) and copper (5 ppm) [peak 8] in $ZnSO_4$ (108 g Zn/L). Peak 4 is due to thiuramdisulfide.

Extraction performed as in text using dichloromethane as extracting solvent. Peaks (1), (2) and (3) in blank. Chromatographic system as in Fig. 1. Injection volume = 10 μ L, flow rate = 2 mL/min. Spectrophotometric detection ($\lambda = 254$ nm).

material(s) inhibiting the electrochemical response must be entering the detector since the current per unit concentration is less than that obtained in the absence of zinc when relatively positive DC potentials are used for detection.

Examination of plant electrolyte zinc samples was successfully carried out (see Fig. 5). Data obtained using the method of



Figure 4

Injection of mercury (peak 2) in the presence of selenium (peak 1) results in another discrete response (peak 3). System as in Fig. 1. Flow rate = 3 mL/min. Injection volume = 10 μ L.

(A) 10 ppm selenium. Peak 1 may be the thiuram disulfide dimer rather than selenium.

(B) 10 ppm mercury.

(C) 10 ppm selenium + 10 ppm mercury.

Extraction performed as outlined in text using dichloromethane as extracting solvent (no $ZnSO_4$ present). Spectrophotometric

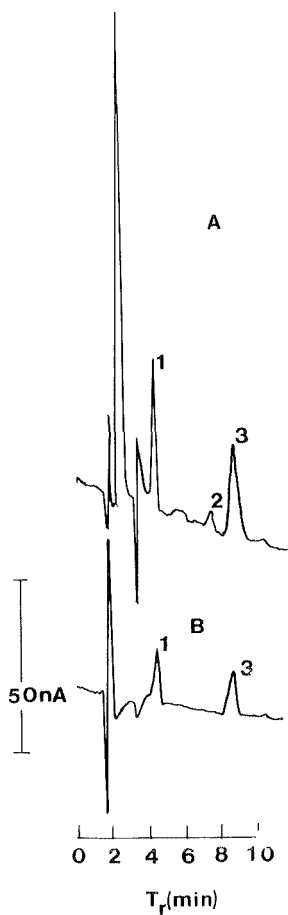


Figure 5

Injection (10 μ L) of a zinc plant electrolyte. Determination of 13 ppm cadmium (peak 1), 2 ppm cobalt (peak 2) and 7 ppm Cu (peak 3). Chromatographic system as in Fig. 1. Flow rate = 3 mL/min. Injection volume = 10 μ L. Extraction as outlined in text using dichloromethane as extracting solvent.

(A) spectrophotometric detection ($\lambda = 254$ nm).

(B) electrochemical detection. DC (potential = +1.20 V).

standard additions were in excellent agreement with those obtained by conventional techniques based on individual determinations by atomic absorption spectrometry (100 fold dilution) or polarography (11), implying that the method is relatively interference free. No problems from other major constituents in the electrolyte (e.g. Mn, 12 g/L) were observed. Direct rather than standard addition methods of calibration was also satisfactory, except for the mercury-selenium combination noted above. This again is indicative that interferences are generally minimal.

(ii) 'In situ' Dithiocarbamate Complex Formation

Several problems arise with this mode of operation.

The highly ionic zinc concentrate (~ 100 g/L Zn) needs to be miscible with a suitable chromatographic solvent. Both acetonitrile-water and methanol-water chromatographic solvents previously employed (14) were investigated with respect to miscibility. The zinc electrolyte was found to be immiscible with 70% acetonitrile solution, although this problem can be eliminated by a preliminary twenty-fold dilution and a corresponding loss in sensitivity. Although the zinc concentrate is in fact miscible with 70% methanol, zinc dithiocarbamate is not as soluble in methanol and precipitation may occur in the chromatographic system which is undesirable. If the UV-visible spectrophotometric detector is set at 254 nm or the electrochemical detector operated at potentials more positive than +0.80 V a very large zinc dithiocarbamate response is observed as shown in Fig. 6. Tuning of the spectrophotometric detector to $\lambda = 400$ nm or electrochemical detector to +0.60 V alleviates this problem significantly. However,

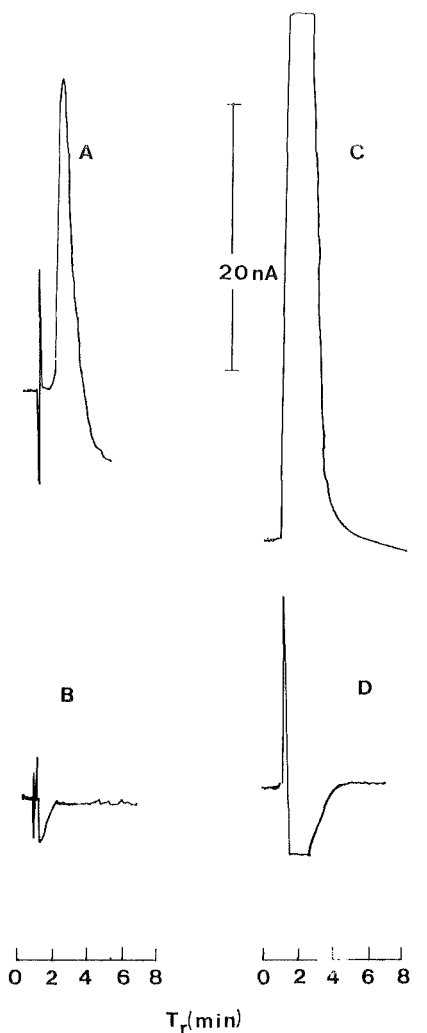


Figure 6

Blank (10 μ L injection of ZnSO_4 electrolyte (108 g Zn/L) diluted twenty fold) determinations under various conditions.

- (A) spectrophotometric detection ($\lambda = 254$ nm).
- (B) spectrophotometric detection ($\lambda = 350$ nm).
- (C) electrochemical detection DC (potential = +0.80 V).
- (D) electrochemical detection DC (potential = + 0.60 V).

Chromatographic system as in Fig. 1 (in situ mode). Flow rate = 3 mL/min.

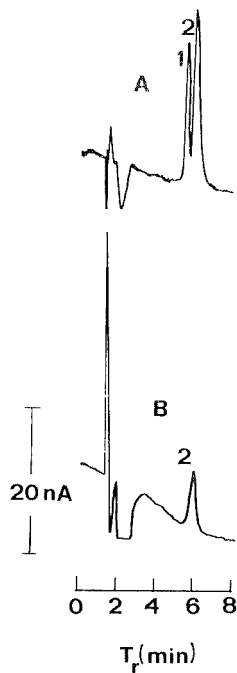


Figure 7

Determination of cobalt (20 ppm) [peak 1] and copper (260 ppm) [peak 2] in a zinc plant electrolyte (2 g/L H_2SO_4) sample after a twenty fold dilution.

(A) spectrophotometric detection ($\lambda = 350$ nm).

(B) electrochemical detection. DC (potential = + 0.60 V).

Chromatographic system as in Fig. 1 (in situ mode). Flow rate = 3 mL/min. Injection volume = 10 μ L.

under these conditions, detection is limited to Ni, Cu and Co (spectrophotometric detection) and Ni and Cu (electrochemical detection). Data obtained in the presence and absence of zinc electrolyte show that the trace metal response is not the same as that observed when no zinc is present for metals other than Cu. The ratio of signal observed in the presence and absence of zinc is 100% for copper, 65% for nickel and 48% for cobalt. Thus, whilst copper determinations retain their sensitivity, the sensitivity for nickel and cobalt are decreased. Fig. 7 shows an example of an injection of a zinc plant electrolyte sample which demonstrates that the method does work. Data are presented in Table 2.

However, a further problem which mitigates against the long term use of the 'in situ' complex formation method was observed with long term monitoring under automated conditions. Repeated injections of the zinc electrolyte lead to relatively rapid deterioration in the performance of the separating column and column regeneration is required at more frequent intervals than required on zinc free samples. In an endeavour to provide improved performance, the 'in situ' complex formation mode was examined with a suppressor column in the system prior to the detectors in order to trap the excess ligand as well as the zinc dithiocarbamate complex. However under the conditions of ligand being included in the running solvent, this can only work for a few injections until the suppressor column is overloaded and fails to work.

In summary, for the particular example of trace metal determination in zinc plant electrolyte, the external dithiocarbamate complex formation method is considerably superior

TABLE 2

Limits of detection^a in presence of zinc sulfate electrolyte.

Metal	Detection Limits			
	External Mode ^{b,c}		'In situ' mode ^{d,e}	
	spectrophotometric detection	electrochemical injection	spectrophotometric detection	electrochemical detection
	(ppm)	(ppm)	(ppm)	(ppm)
Cu	0.1	0.1	0.1	0.1
Ni	0.5	2	0.5	0.5
Co	0.2	2	0.2	
Pb	0.1	1		
Hg	1	1		
Cd	0.5	0.5		

(a) For signal to noise ratio of 2, using a 10 μ L injection.

(b) Using recommended extraction procedure (see text) with dichloromethane.

(c) External mode: $\lambda = 254$ nm - DC (+ 1.20V) linear to 20 ppm.

(d) Direct injection.

(e) 'In situ' mode: $\lambda = 400$ nm - DC potential = + 0.60 V.

Results obtained on chromatographic system as outlined in Fig. 1.

and must be recommended, even though it requires more time consuming procedures.

ACKNOWLEDGEMENT

Extensive and invaluable discussions with M. Newman of the Electrolytic Zinc Company, Risdon, Tasmania, Australia were held through the duration of this project. The assistance of these discussions is gratefully acknowledged. The work described in this

paper was partially funded by a Research Grant from the Electrolytic Zinc Company, Risdon, Tasmania, Australia. Financial assistance for equipment was also received from the Australian Research Grants Scheme and the Ordnance Factory, Maribyrnong, Victoria, Australia.

REFERENCES

1. Smith, R.G. and Windom, H.L., A solvent extraction technique for determining nanogram per litre concentrations of cadmium, copper, nickel and zinc in seawater, *Anal. Chim. Acta.*, 113, 39, 1980.
2. Durst, R.A., Ion Selective Electrodes, Nat. Bur. Stand. (U.S.) Spec. Publ. 314, Washington, 1969.
3. Pinta, M., Modern Methods for Trace Element Analysis, Ann Arbor Science, Mich., 1978.
4. Bond, A.M., Modern Polarographic Methods in Analytical Chemistry, Marcel Dekker, New York, 1980.
5. Donaldson, E.M., Spectrophotometric determination of selenium in concentrates and high-purity copper metal with 3,3'-Diaminobenzidine after separation by xanthate extraction, *Talanta*, 24, 441, 1977.
6. Donaldson, E.M., Spectrophotometric determination of bismuth in concentrates and non-ferrous alloys by the iodide method after separations by diethyldithiocarbamate and xanthate extraction, *Talanta*, 25, 131, 1978.
7. Donaldson, E.M., Determination of antimony in concentrates, ores and non-ferrous materials by atomic-absorption spectrophotometry after iron-lanthanum collection or by the iodide method after further xanthate extraction, *Talanta*, 26, 999, 1979.
8. Donaldson, E.M., Determination of bismuth in ores, concentrates and non-ferrous alloys by atomic-absorption spectrophotometry after separation by diethyldithiocarbamate extraction or iron collection, *Talanta*, 26, 1119, 1979.
9. Gallego, M., Garcio-Vargas, M. and Valcarcel, M., Pyridine-2-carbaldehyde 2-Hydroxybenzoylhydrazine as a selective reagent for the extraction and spectrophotometric determination of Iron(II), *Analyst*, 104, 613, 1979.
10. Beyer, M.E. and Bond, A.M., Simultaneous determination of cadmium, copper, lead and zinc in lead and zinc concentrates by

- AC polarographic methods - comparison with atomic absorption spectrometry, *Anal. Chim. Acta.*, 75, 409, 1975.
11. Pilkington, E.S., Weeks, C.E., Bond, A.M., Determination of zinc plant electrolyte by differential pulse polarography and anodic stripping voltammetry, *Anal. Chem.*, 48, 1665, 1976.
 12. Bond, A.M. and Wallace, G.G., Determination of copper as a dithiocarbamate complex by reverse-phase liquid chromatography with electrochemical detection, *Anal. Chem.* 53, 1209, 1981.
 13. Bond, A.M. and Wallace, G.G., Simultaneous determination of copper, nickel, cobalt, chromium(VI) and chromium(III) by liquid chromatography with electrochemical detection, *Anal. Chem.* 54, 1706, 1982.
 14. Bond, A.M. and Wallace, G.G., Automated monitoring of nickel and copper by high performance liquid chromatography with electrochemical and spectrophotometric detection, *Anal. Chem.* (In Press).
 15. Bond, A.M. and Wallace, G.G., Simultaneous determination of copper, nickel, cobalt, chromium(VI), chromium(III), lead, mercury, cadmium and selenium as dithiocarbamate complexes using liquid chromatography with electrochemical and/or spectrophotometric detection. Unpublished work, Deakin University, 1983.
 16. Hulanick, A., Complexation reactions of dithiocarbamates, *Talanta*, 14, 1371, 1967.
 17. Бусев, А.И., Быр'ко, В.М., Yen, H.K. and Kvesivadze A.G., Translated from *Zhurnal Analiticheskoi Khimii*, Vol. 26, No. 11, pp. 2069 - 2074. November 1971 : page 1849.
 18. Sachinials, J. and Grant, M.W., Metal exchange reactions between divalent metal ions and their dithiocarbamate complexes in dimethyl sulfoxide : a kinetic and mechanistic study, *Aust. J. Chem.* 34, 2195, 1981 and references cited therein.
 19. Coucouvanis, D., The Chemistry of dithioacid and 1,1 dithiolate complexes, 1968-1977, *Progr. Inorg. Chem.* 26, 301, 1979 and references cited therein.
 20. McCleverty, J.A. and Morrison, N.J., Metal dithiocarbamates and related species. Part 2, *J. Chem. Soc. Dalton*, 2169, 1976.
 21. Nieuwpoort, A., Dix, A.H., Porskamp, P.A.T.W. and van der Linden, J.G.M., Preparation and electrochemical behaviour of tris dithiocarbamate complexes $[Bu_4N] M - (Et_2dth)_3$, with M = Ba, Zn, Cd and Hg, *Inorg. Chim. Acta.*, 35, 221, 1979.

22. Vogel, A., A Textbook of Quantitative Inorganic Analysis, Longmans, London, 1968.
23. Morrison, G.H. and Freiser, H., Solvent Extraction in Analytical Chemistry, John Wiley & Sons, New York, 1957.
24. Bond, A.M., Hendrickson, A.R. and Martin, R.L., Redox behaviour of 1,1 dithio and related chelates of transition metals (In Press) 1983.
25. Taddia, M., Atomic absorption spectrometry of cadmium after solvent extraction with zinc dibenzldithiocarbamate, Microchem. J. 26, 340, 1981.
26. Bajo, S. and Wyttenbach, A., Lead, cadmium and zinc bis(diethyldithiocarbamate) and diethyldithiocarbamic acid as reagents for liquid-liquid extraction, Anal. Chem. 51, 376, 1979.

**ELECTROKINETIC DETECTION IN REVERSED PHASE HIGH
PERFORMANCE LIQUID CHROMATOGRAPHY
PART I. VOLATILE FATTY ACIDS**

Wiktor Kemula, Bronisław K. Głód and Włodzimierz Kutner
Institute of Physical Chemistry
Polish Academy of Sciences
Kasprzaka 44/52
01-224 Warszawa
Poland

ABSTRACT

Conditions of electrokinetic detection are elaborated for volatile fatty acids (acetic, propionic, isobutyric and valeric) in reversed phase high performance liquid chromatography, HPLC. A simple, open tube capillary electrokinetic detector was constructed. The working unit of the detector was a capillary made of polytetrafluoroethylene, PTFE, or stainless-steel. The output signal of the detector was the streaming potential of the capillary which was measured against earth. When chromatograms were developed in non-buffered polar solution of mobile phase, the retention volume, V_R , of acids increased with the increase of concentration of acids in the sample. The detectability of the detector with PTFE capillary used as a working unit was of the order of 10^{-12} mole for a 5 μ l injected sample and the reproducibility was 5% (relative standard deviation, R.S.D., for ten consecutive injections). The linear dynamic range was close to two orders of magnitude of the concentrations of acids.

INTRODUCTION

In the search for a new reliable universal detector for liquid chromatography, electrochemical detectors based on the measurement of streaming current and streaming potential have been recently tested and applied [1-3]. In 1964 a patent was drawn for the first electrokinetic detector for liquid chromatography by A n d o *et al.* [4]. The working unit of that detector is an open tube dielectric capillary or

packed with a dielectric support. At both ends of that capillary there are Pt or Au electrodes between which the streaming potential is measured. The detector has been used for reversed phase liquid chromatography. In further models of electrokinetic detectors the streaming current was measured. The latter devices were applied both for normal and reversed phase liquid chromatography, LC. The streaming current and streaming potential encountered under conditions of reversed phase LC [4, 5] are described by the S m o l u c h o w s k i equation [3, 6–9], and for flow conditions relevant to normal phase LC [10–15] the streaming current is described by the G a v i s and K o s z m a n theory [16–20]. It was also shown that the electrokinetic detection signal could be measured directly at a chromatographic column [12–14]. This is advantageous especially for capillary liquid chromatography where extra-column effects of chromatographic band broadening are crucial [12–14]. Only an electrokinetic detector makes it possible to measure the exclusion volume directly during chromatographic elution [11]. Moreover, the electrokinetic detector is useful for studying the so-called "vacant" peaks [11]. The spray impact detector operates on a similar principle as the electrokinetic one [21]. The spray impact detector is based on the L e n a r d effect discovered in 1892 where the electric charge is non-uniformly distributed when liquid droplets are sprayed onto the conducting target.

In the present paper the results are given obtained with the use of our simple electrokinetic detector as applied to the detection of volatile fatty acids in the effluent of the reversed phase chromatographic column. In the detector the streaming potential was measured at the working unit which consisted of an open dielectric or metal tube capillary.

Volatile fatty acids play an important role in food industry when manufacturing wine, cheese or processed fruit as flavour ingredients. Also their determination in blood plasma and lymph may make it possible to follow the mammals metabolism paths [22]. So there is a need for the determination of these acids both in trace amounts and in a wide range of concentrations. Volatile fatty acids were determined chromatographically many times before especially by gas [23–28] and thin layer chromatographies [29, 30]. Classical and high performance LC were also used for the purpose [31–36]. However, serious detection problems were encountered for acids with short aliphatic chains, which led to the need of applying complex detection methods or on or off line derivatization of substances in the sample. B u s h *et al.* [22] succeeded to separate volatile fatty acids, i.e. acetic, propionic, butyric, valeric and isovaleric ones, by reversed phase HPLC with UV (210 nm) detection on the C₁₈ μ BONDPAK column in less than 20 minutes. The quoted authors used MeOH + 0.1 M NaH₂PO₄, pH 3.5 (10 + 90) v/v as the mobile phase. It seemed interesting to repeat their measurements with another type of detection for comparison, since the UV (210 nm) detector is sensitive to even trace amounts of contaminations. Volatile fatty acids C₄ – C₂₂ were also recently separated by the reversed phase HPLC on a Nukleosil 7 C₁₈ column using electrokinetic detection in which the

streaming current was measured [5]. The disadvantage encountered was, however, the strong dependence of the baseline current on the flow rate, J , of the mobile phase. With the increase of J by 0.1 ml min^{-1} the baseline current increased by 1.8×10^{-8} A, while the heights of the chromatographic peaks were only of the order of 10^{-9} – 10^{-8} A. Thus a minor instability in J already deteriorated markedly the reproducibility. Besides, the size of the sample used was as large as 2 cm^3 and was comparable to the dead volume of the column. Such a large sample size is considered disadvantageous in HPLC because of the disturbance to the column it causes during sample injection.

EXPERIMENTAL

The design and electronic diagram of the electrokinetic detector is shown in Fig. 1. The eluate from the chromatographic column (1) is pumped through a 50–60% porous filter (2), and next through a stainless-steel junction ($16 \times 1 \text{ mm I.D.}$) (4) to the working capillary (3). A PTFE or stainless-steel 1H18N9T open tube capillary of 0.4 or 0.2 mm I.D., respectively, and 20 mm long was used as the working unit of the detector. The stainless-steel capillary was insulated from the rest of the system by a PTFE tightening ferrule (5). The eluate was drained off to waste by the stainless-steel capillary (6) of 1 mm I.D. which was insulated from the earthed screen (7) by a PTFE connector (8). The chromatographic column and its pumping system, joint and the screen were earthed. The streaming potential, $\Delta\varphi$, as measured as the potential of the capillary (6) against earth using an electronic circuit with an operational RCA-715 amplifier of $10^{11} \Omega$ input resistance (9). The potential $\Delta\varphi$ was recorded with a Mera-Tronik V-543 (Warszawa, Poland) multimeter and Radelkis OH-814/1 (Budapest, Hungary) potentiometric recorder. The operational amplifier was fed from a stabilized Unitra-Unima ZT-980-2 (Warszawa, Poland) electric feeder. The Institute of Physical Chemistry, Polish Academy of Sciences (Warszawa, Poland) chromatograph HPLC type 302 was used. The pump of the chromatograph was a syringe type pump with mobile phase flow rate adjusted in the range from 0.06 to 6.0 ml min^{-1} . It was equipped with a $5 \mu\text{l}$ high pressure injection valve. The column used was a stainless-steel 1H18N9T column $150 \times 4 \text{ mm I.D.}$ slurry packed by a modified viscous method [37] with LiChrosorb RP-18, $10 \mu\text{m}$ (E. Merck, Darmstadt, FRG) in a mixture of dioxane + tetrachloromethane (50 + 50) v/v at 42 MPa, or packed with glass beads 80 mesh (B.D.H., Poole, England) by a dry method. A mobile phase solution was prepared using redistilled water and analytical grade methanol (E. Merck, Darmstadt, FRG). Other chemicals were of analytical grade (P.O.Ch., Gliwice, Poland). The mobile phase was degassed for two hours prior to chromatographic measurements in an ultrasonic bath under a water aspirator.

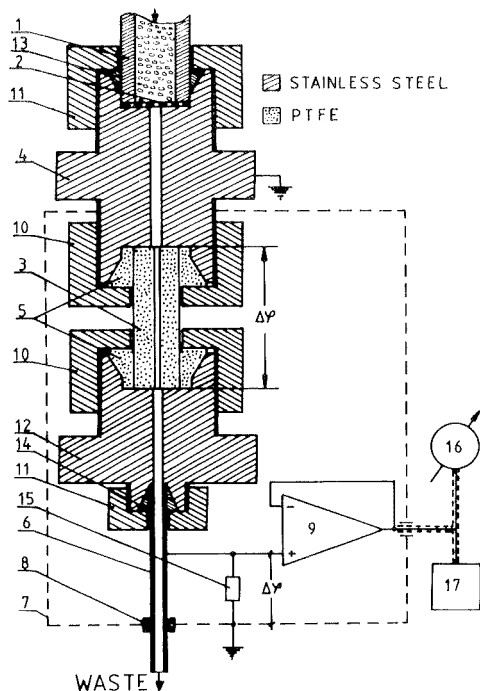


FIGURE 1. Diagram of the electrokinetic detector and its electronic set-up for the measurement of streaming potential.

1 — HPLC column packed with LiChrosorb RP-18, 10 μm ,
 2 — porous filter, 3 — working PTFE capillary, 4 — stainless-steel M12/M12 joint,
 5 — PTFE tightening ferrule, 6 — stainless-steel draining capillary, 7 — earthed shield,
 8 — PTFE connector, 9 — operational amplifier RCA-715, 10 — M12 nut,
 11 — M6 nut, 12 — stainless-steel M12/M6 joint, 13 — stainless-steel 5/10 ferrule,
 14 — stainless-steel 4/3.5 ferrule, 15 — 10^{11} Ohm resistor, 16 — digital voltmeter,
 17 — X-t recorder.

RESULTS AND DISCUSSION

Elektrokinetic measurements were carried out using a PTFE (20 x 0.4 mm I.D.) or stainless-steel (20 x 0.2 mm I.D.) capillary. The results, if not stated otherwise, refer to the PTFE capillary.

Preliminary experiments performed without the chromatographic column showed (Fig. 2) that peak heights, $\Delta(\Delta\varphi)$, decrease with the increase of the flow rate of the mobile phase of the composition MeOH + H₂O (10 + 90) v/v which is further

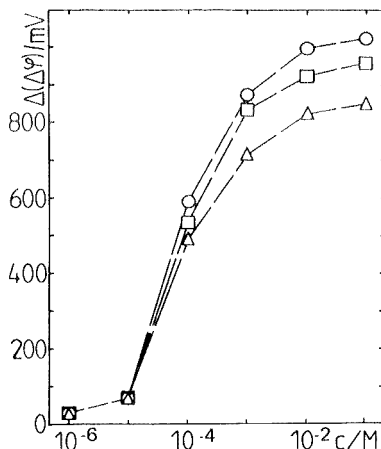


FIGURE 2. Dependence of the streaming potential changes (heights of chromatographic peaks), $\Delta(\Delta\varphi)$, on the concentration of propionic acid obtained using the electrokinetic detector with PTFE capillary (20 x 0.4 mm I.D.) without chromatographic column. Mobile phase: MeOH + H₂O (10 + 90) v/v, sample size — 5 μ l. Flow rate: 0.6 (O), 1.8 (□), 3.0 (Δ) ml min⁻¹.

used, from 0.3 to 3.0 ml min⁻¹. The value of $\Delta(\Delta\varphi)$ was measured as the difference between the streaming potential value at a peak maximum and the background potential, $\Delta\varphi_b$. The detection limit of acids per 5 μ l injection size was close to 10⁻¹² mole (10⁻⁶ M) for the PTFE capillary and 10⁻¹⁰ mole (10⁻⁴ M) for the stainless-steel capillary. A similar dependence of peak heights on the flow rate and concentration has been observed for other studied substances [38]. It was found that the detectability of the detector is nearly by two orders of magnitude higher for ionic compounds (e.g. aliphatic or aromatic carboxylic acids or inorganic salts) than for nonionic ones (e.g. ketones).

Fig. 3 shows the HPLC reversed phase chromatograms of mixtures containing 10⁻⁴ M and 10⁻³ M of each of the acids: acetic, propionic, isobutyric and valeric in Figs. 3 a and 3 b, c, respectively. The mobile phase used was of the composition indicated earlier and the flow rate was 1.2 (Fig. 3 a, b) and 4.2 ml min⁻¹ (Fig. 3 c). As it is shown in Figs. 3 b and 3 c, $\Delta(\Delta\varphi)$ changes its sign from positive to negative when the flow rate increases above a certain value, J_0 . At the same time $\Delta\varphi_b$ increases. Sample injection is accompanied by two spikes, the first being negative and the second one positive (in Fig. 3 they are not separated and are indicated by a vertical segment because of the recorder delay). These spikes are caused by the flow rate disturbance which accompanies sample injection. The first negative spike which

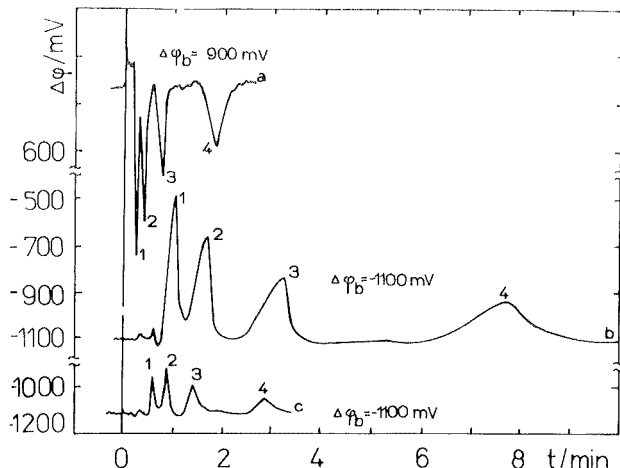


FIGURE 3. HPLC chromatograms of volatile fatty acids recorded with the use of the electrokinetic detector with PTFE capillary (20 x 0.4 mm I.D.), separated on stainless-steel column 150 x 4 mm I. D., packed with LiChrosorb RP-18, 10 μ m. Mobile phase: MeOH + H₂O (10 + 90) v/v, sample size — 5 μ l. Concentration of acids, in *M*, and flow rate, in ml min⁻¹: a — 10⁻³, 4.2; b — 10⁻³, 1.2; c — 10⁻⁴, 1.2. The peaks: acetic (1), propionic (2), isobutyric (3), and valeric (4) acid.

appears is attributed to the decrease of the flow rate, and the following positive one is due to the increase of flow rate caused by the instantaneous increase of pressure. Heights of both spikes increase with the increase of the mobile phase flow rate. Fig. 4 shows the $\Delta(\Delta\varphi)$ vs J plot for all 10⁻³ *M* acids. It is seen that for the smallest available flow rate, i.e. for $J = 0.06$ ml min⁻¹ the sign of $\Delta(\Delta\varphi)$ is positive, and it decreases with the increase of flow rate. With the increase of J , $\Delta\varphi_b$ always increases. For J close to 2.7 ml min⁻¹ all peaks disappear in the chromatogram, and for $J > 2.7$ ml min⁻¹ the peak changes its sign. With the further increase of J the absolute value of $\Delta(\Delta\varphi)$ also increases. This is presumably due to some constant potentials, e.g. potential from the electrochemical cell or changes of the potential during sample injection (as a result of changes of capacity) interfering with the streaming potential. When the flow rate exceeds 5.4 ml min⁻¹ a decrease in the absolute value of $\Delta(\Delta\varphi)$ is observed. Fig. 5 shows the dependence of the height (Fig. 5 a) and surface area (Fig. 5 b) of peaks on the logarithm of concentration of acids. The detectability for the detector with the PTFE capillary (20 x 0.4 mm I.D.) at the signal to noise ratio of two and J in the range from 0.6 to 1.2 ml min⁻¹ was close to 10⁻¹² mole. The peak to peak reproducibility of signals calculated as a relative standard deviation (R.S.D.) of separate measurements of the peak height in ten consecutive

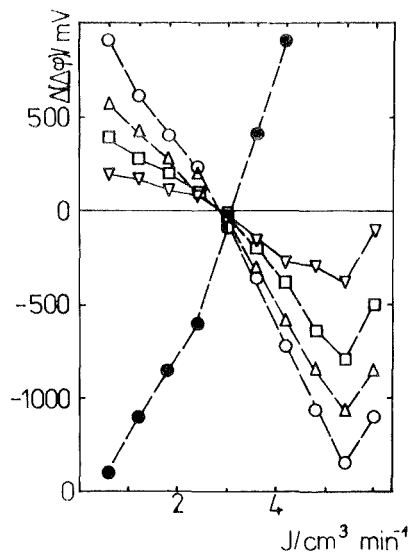


FIGURE 4. Plot of chromatographic peak height, $\Delta(\Delta\phi)$, vs. mobile phase flow rate, J , of $5\ \mu\text{l}$ sample of mixture of $1\ \text{mM}$ acetic (O), propionic (Δ), isobutyric (\square), and valeric (∇) acid. Other conditions as in Fig. 3.

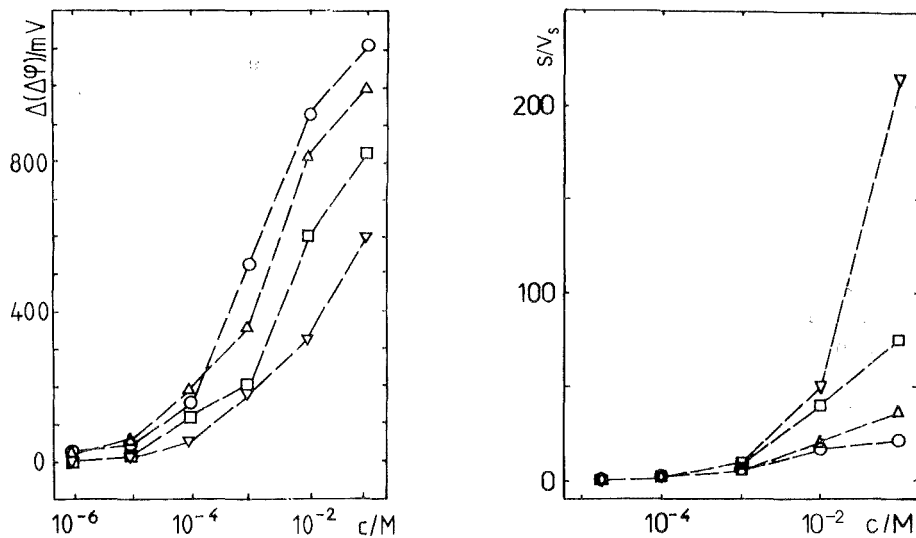


FIGURE 5. Dependence of height (a) and area (b) of the chromatographic peaks on the logarithm of concentration of volatile fatty acids: acetic (O), propionic (Δ), isobutyric (\square), valeric (∇). Flow rate $1.2\ \text{ml}\ \text{min}^{-1}$. Other conditions as in Fig. 3.

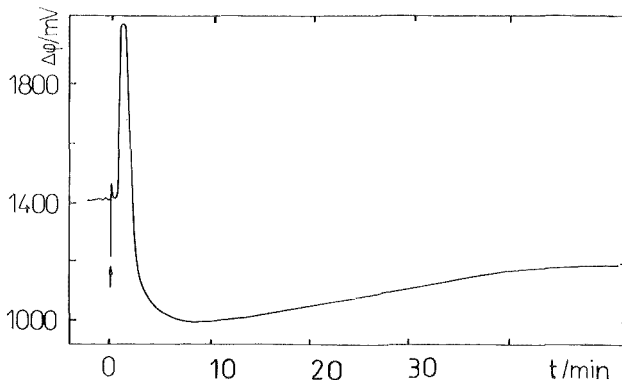


FIGURE 6. HPLC chromatogram of 1 *M* propionic acid, flow rate — 1.2 ml min⁻¹, column 150 × 4 mm I.D., packed with glass beads *ca.* 80 mesh. Other conditions as in Fig. 3.

injections each containing 1 *mM* of every acid was better than 5%, and for lower and higher concentrations was somewhat poorer and varied in the range from 5 to 15%. For smaller concentrations it was limited by the noise level of $\Delta\varphi_b$ and for higher concentrations it resulted most probably from the irreversible adsorption of acids on the surface of the capillary inner wall. Day to day reproducibility was not as good as that mentioned above. However, it could be improved by repeated sample injecting. Adsorption equilibria are then probably attained. The first peak in a series is usually lower than the subsequent ones. The value of $\Delta\varphi_b$ does not assume its original value when acids of concentration higher than 10^{-3} *M* are injected but remains at lower level. This creates some difficulties in peak height or surface area determinations. The original value of $\Delta\varphi_b$ is reached after several up to several dozen minutes. This is probably the result of the irreversible adsorption of acids. Such a behaviour was exemplified in Fig. 6 for 1 *M* propionic acid at $J = 1.2$ ml min⁻¹, (150 × 4 mm I.D.) column packed with glass beads. The largest peak surface area was obtained for valeric acid (Fig. 5 b) to which corresponds the broadest band in the chromatogram (Fig. 3). The reproducibility of the peak surface area was poorer than the corresponding peak height and was approximately equal to 10% (R.S.D. for ten consecutive injections) for 1 *mM* propionic acid at $J = 1.2$ ml min⁻¹. The linear dynamic range was close to two orders of magnitude of the acid concentration.

The heights of the chromatographic peaks obtained using the detector with the stainless-steel capillary (20 × 0.2 mm I.D.) were about three times smaller than those obtained using a PTFE capillary. The stainless-steel capillary revealed also worse detectability, equal to *ca.* 5×10^{-5} *M*, and reproducibility which was better than 30% (R.S.D. for ten consecutive injections).

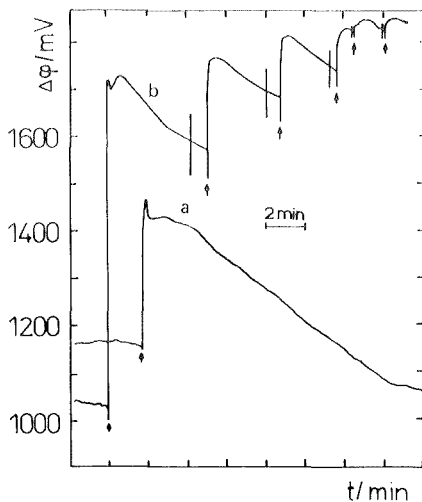


FIGURE 7. Changes of the streaming potential in time for consecutive injections of *ca.* $1\ M$ $\text{TEA}^+ \text{C}_6\text{H}_5\text{COO}^-$ ion-pair without a column. Flow rate- $0.6\ \text{ml/min}$, sample size - $5\ \mu\text{l}$, mobile phase: isopropanol + methylene chloride + hexane (20 + 60 + 20) v/v/v the detector working unit - stainless-steel capillary $100 \times 0.2\ \text{mm I.D.}$

The measurements presented above were performed using a nonbuffered mobile phase. Addition of any electrolyte e.g. buffer to the mobile phase causes a decrease of the heights of chromatographic peaks due to the increase of conductivity which results in the so-called "short circuit effect". This leads to the decrease of reproducibility and detectability. But in the absence of a buffer in the mobile phase the retention volume, V_R , was highly dependent on the concentration of acids in the sample (cf. Figs. 3 b and 3 c) which would be inconvenient for analytical purposes. This effect resulted from retaining of mainly non-dissociated substances by the reversed phase, RP, support. The degree of dissociation of acids and their pH increase with dilution, and the dissociated acids are eluted in shorter time [39]. The most pronounced changes in the V_R were observed for high concentrations of the acid. For concentrations smaller than $10^{-5}\ M$ these changes were practically independent of the concentration of acid. We tried to eliminate dependence of V_R on acids concentration by:

(i) Applying dilute buffer solutions. However, phosphate or citrate buffers diluted as much as $10^{-4}\ M$ proved useless, since their buffer capacities are insufficient to prevent V_R of acids from being independent of their concentration. When more concentrated buffers were used, $\Delta(\Delta\phi)$ decreased drastically due to the "short circle effect".

(ii) Applying the mobile phase of high content of organic solvent MeOH or AcCN in order to decrease the degree of dissociation of acids and to eliminate the necessity of buffering the solution. This resulted in the increase of height of peaks but at the same time the retention volume of all acids decreased so much that they were eluted all together.

(iii) Separating acids using ion-pair normal phase chromatography with a buffer and tetraalkylammonium ions as the stationary phase on the LiChrosorb Si 100, 10 μm support (as it was proposed in [40,41]). However, it appeared that ion-pairs formed of acid anions (injected to the column) and tetrabutylammonium cations, TBA^+ , (present in the stationary phase) were irreversibly adsorbed on the inner **surface of the capillary wall, what is exemplified in a model experiment in the absence of a column shown in Fig. 7.** After the injection of benzoic acid $\Delta\varphi$ returned to the value characteristic for the baseline potential after a long time (curve a). In the successive injections smaller peaks were obtained (curve b).

(iv) Separating acids using ion-pair reversed phase chromatography. The addition of the tetraethylammonium cation, TEA^+ , to the mobile phase resulted in the decrease of peaks and also of the detectability as well as of reproducibility as a result of the irreversible adsorption of TEA^+ on the inner surface of the capillary wall. We made therefore an attempt to separate acids in very dilute solutions of TEAClO_4 without buffers what will be described in part 2 of this work [42].

ACKNOWLEDGMENT

The work was carried out within the frames of the research project 03.10 of the Polish Academy of Sciences.

REFERENCES

1. Štulík, K., Pacáková, V., *Elektrochemické Detektory v Kapalinové Chromatografii*, Chem. Listy, **73**, 795, 1979.
2. Meirs, R. B., *Developments in Chromatography—2*, Knapman, C. E. H., eds., Applied Sci. Publ. LTD, London, 1980, pp. 1–32.
3. Głód, B. K., *Mechanizmy Powstawania Potencjału i Prądu Przepływu oraz Ich Zastosowania*, Wiad. Chem., Submitted.
4. Ando, N., Tanizaki, Y., Hasegawa, F., *Liquid Chromatography and Chromatographs*, U.S. Pat., 3,352,643, 1967.
5. Terabe, S., Yamamoto, K., Ando, T., *Streaming Current Detector for Reversed-Phase Liquid Chromatography*, Can. J. Chem., **59**, 1531, 1981.

6. Smoluchowski, M., *Krak. Anz.*, 192, 1908.
7. *Elektricheskie Svoistva Kapilarnykh Sistem*, Zhukov, I. I., ed., A.N. USSR, Moskva-Leningrad, 1956.
8. Rutgers, A. J., De Smet, M., *Electrosmosis, Streaming Potential and Surface Conductance*, *Trans. Farady Soc.*, **40**, 102, 1947.
9. Rutgers, A. J., De Smet, M., *Researches on Electro-Endosmosis*, *Trans. Farady Soc.*, **41**, 758, 1948.
10. Šlais, K., Krejčí, M., *Generation of Electricity in Low-Conductivity Liquids as a Detection Principle in Liquid Chromatography*, *J. Chromatogr.*, **148**, 99, 1978.
11. Krejčí, M., Kouřilova, D., Vespalec, R., Šlais, K., *Measurement of Exclusion Volumes of Packed Columns by Means of Electrokinetic Detection*, *J. Chromatogr.*, **191**, 3, 1980.
12. Krejčí, M., Šlais, K., Tesařík, K., *Electrokinetic Detection in Liquid Chromatography. Measurement of the Streaming Current Generated on Analytical and Capillary Column*, *J. Chromatogr.*, **149**, 654, 1978.
13. Vespalec, R., *Effect of the Components of the Chromatographic System on the Electrokinetic Streaming Current Generated in Liquid Chromatography Columns*, *J. Chromatogr.*, **210**, 11, 1981.
14. Krejčí, M., Kouřilova, D., Vespalec, R., *Electrokinetic Detection at Different Points in a Narrow Bore Glass Column in Liquid Chromatography*, *J. Chromatogr.*, **219**, 61, 1981.
15. Krejčí, M., Šlais, K., *Detekční Zařízení pro Kapalinovou Chromatografii*, *Czech. Pat.*, 184,097, 1975.
16. Koszman, I., Gavis, J., *Development of Charge in Low-Conductivity Liquids Flowing Past Surfaces. Engineering Predictions From the Theory Developed for Tube Flow*, *Chem. Eng. Sci.*, **17**, 1013, 1962.
17. Koszman, I., Gavis, J., *Development of Charge in Low-Conductivity Liquids Flowing Past Surfaces. Experimental Verification and Application of the Theory Developed for Tube Flow*, *Chem. Eng. Sci.*, **17**, 1023, 1962.
18. Gavis, J., *Non-Linear Equation for Transport of Electric Charge in Low Dielectric Constant Fluids*, *Chem. Eng. Sci.*, **22**, 359, 1967.
19. Gavis, J., *Charge Generation in Low Dielectric Constant Liquids Flowing Past Surfaces: Non-Linear Theory for Turbulent Flow in Tubes*, *Chem. Eng. Sci.*, **22**, 365, 1967.
20. Gavis, J., Wagner, J. P., *Electric Charge Generation During Flow of Hydrocarbons Through Microporous Media*, *Chem. Eng. Sci.*, **23**, 381, 1968.

21. Mowery, R. A., Juvet, R. S., A New, Sensitive Detector for Liquid Chromatography: The Spray Impact Detector, *J. Chromatogr. Sci.*, **12**, 687, 1974.
22. Bush, K. J., Russell, R. W., Young, J. W., Quantitative Separation of Volatile Fatty Acids by High-Pressure Liquid Chromatography, *J. Liq. Chromatogr.*, **2**, 1367, 1979.
23. Ettre, L. S., Purcell, J. E., *Advances in Chromatography*, vol. 10, Giddings, J. C., Keller, R. A., eds., Marcel Dekker Inc., New York, 1974, pp. 75–78, 81–82.
24. Nonaka, A., *Advances in Chromatography*, vol. 12, Giddings, J. C., Keller, R. A., eds., Marcel Dekker Inc., New York, 1975, pp. 241–248.
25. Averill, W., Support-Coated Open Tubular Columns. Present State of the Art, *Chromatogr. Newslett.*, **1**, 27, 1972.
26. Andrews, J. F., Thomas, J. F., Oearson, E. A., Determination of Volatile Acids by Gas Chromatography, *Water Sewage Works*, **111**, 206, 1964.
27. Brooks, J. B., Liddle, J. A., Alley, C. C., Electron Capture Gas Chromatography and Mass Spectral Studies of Iodomethyltetramethylmethyldisiloxane Esters and Iodomethyldimethylsilyl Ether of Some Short-Chain Acids, Hydroxy Acids, and Alcohols, *Anal. Chem.*, **47**, 1960, 1975.
28. Alley, C. C., Brooks, J. B., Chondhary, G., Electron Capture Gas-Liquid-Chromatography of Short-Chain Acids as Their 2,2,2-Trichloroethyl Esters, *Anal. Chem.*, **48**, 387, 1976.
29. Wang, K.-T., Lin, Y.-T., Wang, I. S., Y., *Advances in Chromatography*, vol. 11, Giddings, J. C., Keller, R. A., eds., Marcel Dekker Inc., New York, 1975, pp. 95–97.
30. Thomson, A. C., Medin, P. A., Separation of Organic Acids by Thin-Layer Chromatography of Their 2,4-Dinitrophenylhydrazide Derivatives and Their Analytical Determination, *J. Chromatogr.*, **21**, 13, 1966.
31. Ramsey, H. A., Separation of Organic Acids in Blood by Partition Chromatography, *J. Dairy Sci.*, **46**, 480, 1963.
32. Stahl, K. W., Schafer, G., Lamprecht, W., Design of a High Efficiency Liquid Chromatograph Using Specific Detection and its Evaluation for Analysis of Tricarboxylic Acid Cycle (TCA) Intermediates and Related Compounds on a Nano-Equivalent Scale, *J. Chromatogr. Sci.*, **10**, 95, 1972.
33. Takayama, K., Jordi, H.C., Benson, F., Separation of Fatty Acids as Their p-Bromophenacyl Esters on a C₃₀-Bonded Silica Column by High-Performance Liquid Chromatography, *J. Liq. Chromatogr.* **21**, 13, 1966.
34. Guebitz, G., Derivatization of Fatty Acids with 1-Chlormethylisatin for High-Performance Liquid Chromatography, *J. Chromatogr.*, **187**, 208, 1980.

35. Jordi, H. C., Separation of Long and Short-Chain Fatty Acids as Naphthacyl and Substituted Phenacyl Esters by High-Pressure Liquid Chromatography, *J. Liq. Chromatogr.*, **1**, 215, 1978.
36. Miller, R. A., Bussell, N. E., Ricketts, C., Quantitation of Long Chain Fatty Acids as the Methoxyphenacyl Esters, *J. Liq. Chromatogr.*, **1**, 291, 1978.
37. Daniewski, W., Bylina, A., Fiutkowski, A., Krupka, A., The Method of Column Packing for High Performance Liquid Chromatography, *Polish Pat.*, 112,126, 1977.
38. Głód, B. K., Kutner, W. and Kemula, W., Unpublished Results.
39. Tilly-Melin, A., Askemark, Y., Wahlund, K.-G., Schill, G., Retention Behavior of Carboxylic Acids and Their Quaternary Ammonium Ion Pairs in Reversed Phase Chromatography with Acetonitrile as Organic Modifier in the Mobile Phase, *Anal. Chem.*, **51**, 976, 1979.
40. Karger, B. L., Su, S. C., High Performance Ion Pair Partition Chromatography: The Separation of Thyroid Hormones and Sulfa Drugs, *J. Chromatogr. Sci.*, **12**, 678, 1974.
41. Persson, B.-A., Karger, B. L., High Performance Ion Pair Partition Chromatography: The Separation of Biogenic Amines and Their Metabolites, *J. Chromatogr. Sci.*, **12**, 521, 1974.
42. Kemula, W., Głód, B. K., Kutner, W., Electrokinetic Detection in Reversed Phase High Performance Liquid Chromatography. Part 2. Quaternary Ammonium Ion-Pairs of Some Volatile Fatty Acids, *J. Liq. Chromatogr.*, This Issue.

**ELECTROKINETIC DETECTION IN REVERSED PHASE HIGH
PERFORMANCE LIQUID CHROMATOGRAPHY
PART II. QUATERNARY AMMONIUM ION-PAIRS
OF SOME VOLATILE FATTY ACIDS**

Wiktor Kemula, Bronisław K. Głód and Włodzimierz Kutner
Institute of Physical Chemistry
Polish Academy of Sciences
Kasprzaka 44/52
01-224 Warszawa
Poland

ABSTRACT

The conditions of electrokinetic detection were elaborated for tetraethylammonium, TEA^+ , ion-pairs of volatile fatty acids (acetic, propionic, isobutyric and valeric) in reversed phase high performance liquid chromatography, HPLC. To eliminate the dependence of the retention volume V_R , on the concentration of acids found in the first part of this work, TEA^+ was added to the non-buffered mobile phase. In the presence of pairing TEA^+ ions, V_R appeared to be invariant with the concentration of acids in the sample in a definite concentration range. The detectability of the detector, with a polytetrafluoroethylene, PTFE, capillary as its working unit, was of the order of 10^{-10} mole and the reproducibility was 5% (relative standard deviation, R.S.D., for ten consecutive injections). The linear dynamic range extended over two orders of magnitude of the acid concentrations.

EXPERIMENTAL

The detector and chromatograph construction as well as the chromatographic procedure have been described in part 1 of the present work [1]. As working units of the detector PTFE, borosilicate glass (Jena, GDR) or 1H18N9T stainless-steel open tube capillaries of different diameter and length were used.

The mobile phase solution was prepared using redistilled water and analytical grade methanol (E. Merck, Darmstadt, FRG). Tetraethylammonium perchlorate, TEAClO₄, was prepared according to [2] by precipitation of the water insoluble TEAClO₄ from the aqueous solution of analytical grade tetraethylammonium bromide, TEABr, (Reahim, USSR) and HClO₄ of the same grade (VEB Laborchemie—Apolda, GDR) at 60°C.

RESULTS AND DISCUSSION

In part 1 of the present work [1] the HPLC separation and electrokinetic detection conditions of volatile fatty acids (acetic, propionic, isobutyric and valeric) were elaborated. The retention volumes of acids appeared, however to be strongly dependent on their concentrations. That is why in the present paper attempts are made to eliminate this effect by separating the acids in the ion-pair reversed phase HPLC mode.

The electrokinetic measurements were carried out with dielectric, i.e. PTFE, borosilicate glass or metal, i.e. stainless-steel, capillaries of different dimensions as **working units of the detector. The results, if not stated otherwise, have been obtained with the PTFE capillary (20 x 0.4 mm I.D.).**

The retention volumes of the studied acids in ion-pair reversed phase chromatography appeared to be independent of the concentration of acids in the injected sample in a definite range of concentrations, depending on the concentration of TEA⁺ in the mobile phase. Thus, the chromatogram obtained under these conditions (Fig. 1) does not differ much from that obtained for acids in the absence of TEA⁺ (cf. Fig. 1 [1]). Also the dependence of changes of the streaming potential, $\Delta(\Delta\varphi)$, on the mobile phase flow rate, J , was analogous to that presented in Fig. 4 of ref. [1]. The change of the sign of chromatographic peak heights (Figs. 1 a and 1 b) is observed as previously for flow rates higher than some critical value, J^0 . When the mobile phase of the same composition as previously (MeOH + H₂O (10 + 90) v/v) contained additionally 10⁻⁴ M TEAClO₄ (this mobile phase was used in further experiments), the retention volume is independent of concentration of acids in the injected sample in the acid concentration range 10⁻⁵–10⁻³ M (Fig. 2). Practically up to the acid concentration of 5x10⁻³ M the changes of the retention volume are so small that a change of the sequence of chromatographic peaks is not likely. In Fig. 2 the dependence of the retention volume on concentration of acids is shown as determined directly (dashed line) and by the ion-pair method (solid line) at 10⁻⁴ M TEAClO₄. That figure shows that after addition of TEAClO₄ to the mobile phase at a concentration not exceeding 10⁻⁴ M (without a buffer) the retention volume of the studied acids is independent of the acid concentration in a wider range of their concentrations than in the absence of the pairing counter ion (cf. Figs. 1 b, c and 3 b, c in [1]). In Table 1 the influence is presented of TEA⁺ concentration on the

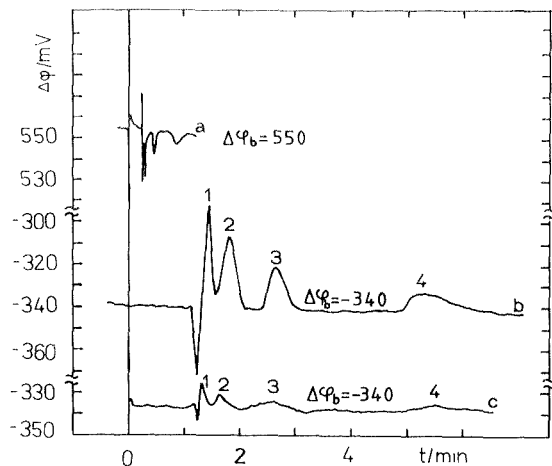


FIGURE 1. HPLC chromatogram of volatile fatty acids separated as ion-pairs on stainless-steel column 150 x 4 mm I.D., LiChrosorb RP-18, 10 μ m, recorded using the electrokinetic detector with PTFE capillary (20 x 0.4 mm I. D.), sample size 5 μ l; mobile phase 10⁻⁴ M TEAClO₄ in MeOH + H₂O (10 + 90) v/v; acids concentrations in M, and flow rates in ml min⁻¹: a - 10⁻³, 4.2; b - 10⁻³, 0.6; c - 10⁻⁴, 0.6. The peaks: 1 - acetic, 2 - propionic, 3 - isobutyric, and 4 - valeric acid.

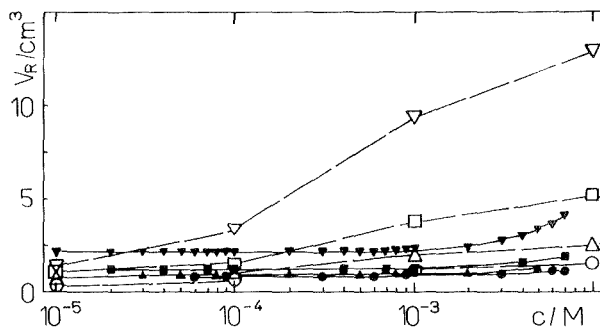


FIGURE 2. Dependence of retention volume on concentration of volatile fatty acids (dashed lines): acetic (O), propionic (Δ), isobutyric (\square), and valeric (∇) and of their ion-pairs (solid lines). Flow rate 0.6 ml min⁻¹, other conditions as in Fig. 1.

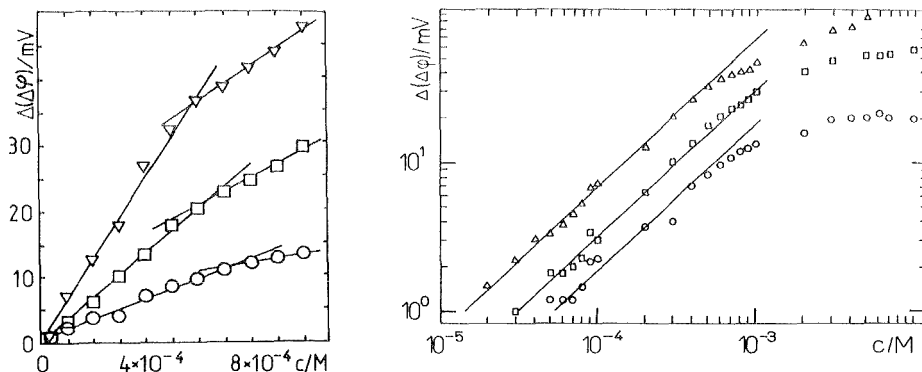


FIGURE 3. Dependence of height (a) and logarithm of height (b) of HPLC chromatographic peaks recorded using the electrokinetic detector with PTFE capillary (20×0.4 mm I. D.) on concentration (a) and logarithm of concentration (b) of propionic (Δ), isobutyric (\square), and valeric (\circ), acids separated as ion-pairs in reversed phase HPLC; other conditions as in Fig. 2.

acids detectability, W , and on the maximum concentration of acids, c^{\max} , at which the changes of V_R are so small that a change in the elution sequence of acids could not occur. As it is seen, the increase of TEA^+ concentration in the mobile phase causes a decrease of detectability but also a shift of the acid concentration range, in which V_R is independent of the concentration of acids, towards higher concentrations. When the concentration of TEA^+ increases by one order of magnitude, the peak heights decrease several times. At the concentration of TEA^+ equal to 10^{-4} M the peak heights are about ten times smaller than in the absence of TEA^+ . Fig. 3 shows the dependence of the peak heights (3 a) and the logarithm of the peak heights (3 b) on concentration (3 a) and the logarithm of concentration of acids (3 b) determined as ion-pairs. From this figure it is seen that the linear dynamic range extends to at least one order of magnitude, i.e. $2 \times 10^{-5} - 7 \times 10^{-4}$ M or $2 \times 10^{-5} - 1 \times 10^{-3}$ M for the cases presented in Fig. 3 a and 3 b, respectively. The slope of all curves in Fig. 3 b, $d \log[\Delta(\Delta\varphi)]/d \log c$, is the same and equal to about unity. Within the linear sections of the calibration curves the response of the detector may be described by the known formula

$$\Delta(\Delta\varphi) = \Delta(\Delta\varphi)^0 + k c^n,$$

where: $\Delta(\Delta\varphi)^0$ is the residual signal of the changes of streaming potential, k the sensitivity and n the detector response index.

Then for $\Delta(\Delta\varphi) \gg \Delta(\Delta\varphi)^0$ we have

$$\log \Delta(\Delta\varphi) = \log k + n \log c.$$

TABLE 1

Dependence of the Detectability of Propionic Acid, $W_{C_2H_5COOH}$, and Its Maximum Concentration $c_{C_2H_5COOH}^{\max}$, at which the Changes of V_R are so Small That the Change in the Sequence of Peaks Could not Occur, on TEA^+ Concentration.

c_{TEAClO_4} [M]	$W_{C_2H_5COOH}$ [M]	$c_{C_2H_5COOH}^{\max}$ [M]
0	5×10^{-7}	5×10^{-5}
10^{-6}	$(2-5) \times 10^{-7}$	8×10^{-5}
10^{-5}	$(2-5) \times 10^{-6}$	5×10^{-4}
10^{-4}	$(2-5) \times 10^{-5}$	5×10^{-3}
10^{-3}	5×10^{-4}	—
10^{-2}	5×10^{-4}	—

For the studied acids in the range of almost two orders of magnitudes of concentration $n = 1$, and the sensitivity of the detector for all acids is in the limits of $(2-8) \times 10^{-4}$ for concentrations of acids smaller than 7×10^{-4} M, and for higher concentration it is about half that value. In ion-pair HPLC of acids the reproducibility is better than 5% (R.S.D. for ten consecutive injections), like in direct HPLC determination of acids. With the increase of flow rate in the ion-pair chromatography method for $J < 3.4$ ml min⁻¹ a decrease of the peak heights was observed. For $J = 3.4$ ml min⁻¹ the peaks disappear altogether in the chromatogram. For $J > 3.4$ ml min⁻¹ the peaks change their sign to negative and their absolute value increase.

In Fig. 4 the dependence of HPLC chromatographic peak heights of propionic acid of different concentration (1×10^{-4} , 5×10^{-4} , 10×10^{-4} M) on the flow rate is presented. Analogous curves were obtained for other acids. As it is seen, the value of the flow rate at which the relationship $\Delta(\Delta\phi) = f(J)$ passes the zero point, J^0 , is independent of the acid concentration. For the PTFE capillary (20 x 0.35 mm I.D.) this value is 1.65 ml min⁻¹. It should be noted that at higher flow rates, in this case higher than 4.8 ml min⁻¹, we observe like in the direct method a decrease of the absolute value of peak heights (i.e. at $J = 4.8$ ml min⁻¹ the relationship $\Delta(\Delta\phi) = f(J)$ has a minimum).

With the increase of the PTFE capillary diameter, of 15 mm length, the peak heights decrease (Fig. 5). At the same time the stability of the baseline potential is improved. Changes in the capillary diameter do not influence the relative reproducibility of the detector. However, for capillaries of smaller diameters longer time was required for the baseline potential to stabilize. With the increase of the capillary length (Fig.

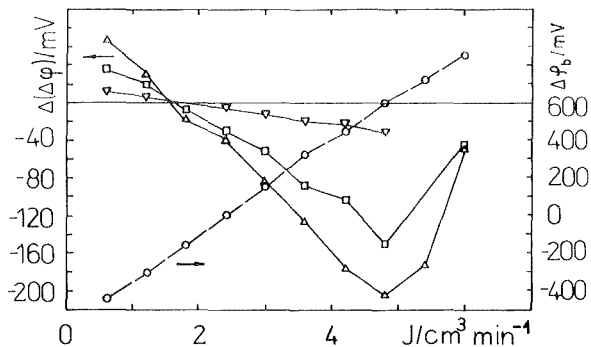


FIGURE 4. Plot of chromatographic peak height, $\Delta(\Delta\varphi)$, against flow rate, J , for 0.1 (∇), 0.5 (\square), and 1 mM (Δ) propionic acid, dashed line—the baseline potential; other conditions as in Fig. 2.

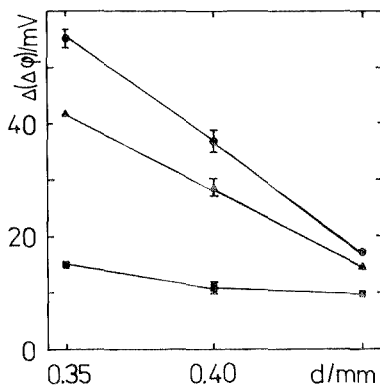


FIGURE 5. Plot of chromatographic peak height, $\Delta(\Delta\varphi)$, vs inner diameter, d , of PTFE capillary 15 mm long for 1 mM propionic (O), isobutric (Δ), valeric (\square) acids; other conditions as in Fig. 2.

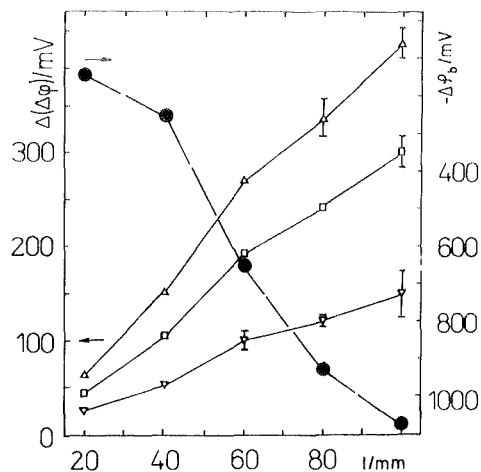


FIGURE 6. Plot of chromatographic peak height, $\Delta(\Delta\phi)$, vs length, l , of PTFE capillary (0.2 mm I.D.) for 1 mM propionic (Δ), isobutyric (\square), valeric (∇) acids; dashed line—the baseline potential; other conditions as in Fig. 2.

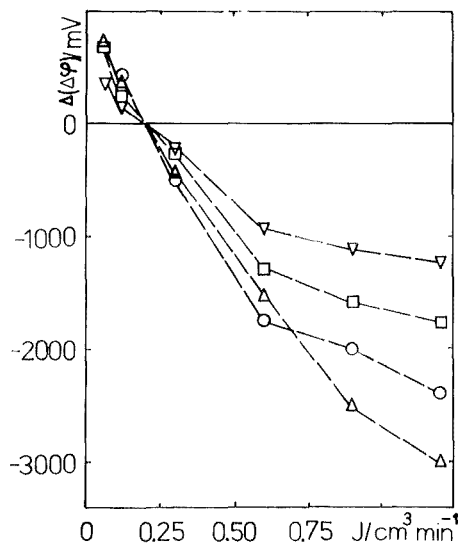


FIGURE 7. Dependence of height of HPLC chromatographic peak, $\Delta(\Delta\phi)$, on flow rate, J , for 1 mM acetic (O), propionic (Δ), isobutyric (\square), valeric (∇) acids. The detector working unit—borosilicate glass capillary (20 x 0.13 mm I.D.) other conditions as in Fig. 2.

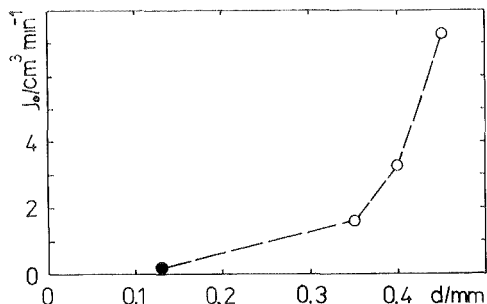


FIGURE 8. Dependence of flow rate, J^0 , corresponding to the zero point of the relationship $\Delta(\Delta\varphi)$ on J , on diameter, d , of dielectric capillary 20 mm long; PTFE (●), borosilicate glass (○); other conditions as in Fig. 2.

6) the peaks heights increased as well but at the same time the baseline potential became less stable and shifted towards more negative values.

Substitution of the PTFE capillary (20 x 0.4 mm I.D.) for the borosilicate glass one (20 x 0.13 mm I.D.) led to a fortyfold increase of the peak heights (Fig. 7). However, the baseline potential was less stable, what was the reason why the relative reproducibility was only about 5% (R.S.D. for ten consecutive injections). Hence, the general conclusion can be made that the application of a capillary of a smaller inner diameter leads to the increase of the absolute value of the baseline potential (this was why the use of the borosilicate glass capillary at $J > 1.2$ ml min⁻¹ was impossible) and of the peak heights, and also makes $\Delta(\nabla\delta)$ more sensitive to changes of J . For the glass capillary $J^0 = 0.21$ ml min⁻¹. Fig. 8 shows the dependence of J^0 on the diameter of the capillary made of a dielectric. As it is seen, J^0 increases with the increase of the capillary diameter.

The chromatographic peaks obtained using a stainless-steel capillary (40 x 0.2 mm I.D.) were about twice smaller than these obtained when using the PTFE one (20 x 0.4 mm I.D.); when a stainless-steel capillary (20 x 0.2 mm I.D.) was used the peaks were hardly distinguishable from noise. The reproducibility for the stainless-steel capillary (40 x 0.2 mm I.D.) was better than 30% (R.S.D. for ten consecutive injections). The nature of the recorded chromatograms was unaffected irrespective of whether streaming potential was measured against earth at the working (3) or at draining (6) capillary (see Fig. 1 in [1]). No change of sign was observed at the dependence of peak heights on the flow rate in the accessible range of J , i.e. from 0.06 to 6.0 ml min⁻¹ for the stainless-steel capillary (40 x 0.2 mm I.D.). Moreover, in contrast to the working capillary made of a dielectric, only a minor increase of heights of the chromatographic peaks with the increase of flow rate was observed. This is why the stainless-steel capillary seems to be more useful for analytical purposes.

GENERAL DISCUSSION AND CONCLUSIONS

The electrokinetic detector is specific for ionic and universal for nonionic substances [3]. This may be explained by the Smoluchowski equation [4–6], which may be expressed in following forms

$$\Delta\varphi = q \delta \Delta p / \eta \kappa = \epsilon \epsilon_0 \Delta p / 4 \pi \eta \kappa = \epsilon \epsilon_0 \zeta |v| / 2 \pi \kappa \delta,$$

were:

- q — surface density of charge, $C\ m^{-2}$,
- δ — thickness of the mobile part of the electric double layer, m ,
- Δp — pressure difference at capillary ends, Pa ,
- η — dynamic viscosity coefficient, P ,
- κ — specific conductivity, $\Omega^{-1}\ m^{-1}$,
- ϵ — dielectric constant, n. dim.,
- ϵ_0 — dielectric constant of vacuum, $8.9 \times 10^{-12}\ F\ m^{-1}$,
- ζ — electrokinetic potential, V ,
- v — flow velocity of fluid, $m\ s^{-1}$,
- r — radius of capillary, m .

After sample injection the value of ϵ , κ , ζ , and η of the mobile phase change. In dilute solutions the change of ϵ and η are very small. If, in injected sample solution, an ionic substance is present, κ and ζ also change markedly, due to the change of the thickness of the electric double layer. For instance, for water of very high purity at $20^\circ C$ $\eta = 1.002\ cP$ and $\kappa = 10^{-8} - 10^{-7}\ \Omega^{-1}\ cm^{-1}$, whereas for 20% acetic acid at the same temperature $\eta = 1.41\ cP$ and $\kappa = 1.61\ \Omega^{-1}\ cm^{-1}$ [7].

The electrokinetic detector appeared to be very sensitive even to minor contaminations of the surface of the inner capillary wall. If the surface was "poisoned" with irreversibly adsorbed substances (e.g. quaternary ammonium ions, or higher fatty acids of high concentration) two or even three peaks were observed. To avoid this effect the detector had to be washed with 20 or even 200 cm^3 of the mobile phase which was pumped through it [8].

In the presented detector design the working capillary was connected directly to the chromatographic column. Because of the very small dead volume of the detector of ca. 2 μl the detector seems to be particularly suited for liquid capillary chromatography [9, 10].

The detector model described here was used for measuring the potential. Therefore it is particularly useful for reversed phase liquid chromatography in which the electrokinetic conductivity of the mobile phase is usually higher than $10^{-7} - 10^{-6}\ \Omega^{-1}\ cm^{-1}$.

The construction of the presented model of the electrokinetic detector is very simple. The detector may be made from materials available in any laboratory. The peak heights measured are almost invariant with temperature. The detector is cheap and easy to handle. However, its reproducibility might be the object of improvement. The detector can be used only to the limited number of separated systems. It is less sensitive to non-polar substances and it is difficult to use when the mobile phase contains buffers or substances which adsorb specifically on the inner surface of the capillary wall. It cannot be used in LC with gradient elution or flow rate. **The mobile phase must be degassed before use because any bubble of gas when entering the detector cuts the electric circuit and as a result a peak is formed on a chromatogram.**

As it was shown, better detectability and reproducibility were obtained with the dielectric capillary than with the metallic one. The detectability for acids determined with the use of the PTFE capillary (20 x 0.4 mm I.D.) was of the order of 10^{-12} mole, and for non-ionic substances (e.g. ketones) of the order of 10^{-10} mole [11]. The reproducibility for this capillary was better than 5% (R.S.D. for ten consecutive injections). The linear dynamic range of the detector extended to more than one order of magnitude of concentration. Nearly the same linear dynamic range of fatty acids was reported for the electrokinetic detector in which the streaming current was measured [3] and for the UV (210 nm) detector [12]. But the detectability of the former one was only $5 \times 10^{-9} - 1 \times 10^{-8}$ g [3], and the lower limit of the linear dynamic range of the latter was 2.5×10^{-7} mole [12].

The presented detector model reveals a much smaller dependence of its baseline on the flow rate as compared with the detector with which streaming current was measured [3]. With the increase of J by 0.1 ml min^{-1} in the range of $0.6 - 1.8 \text{ ml min}^{-1}$, the baseline potential increased by only 35 mV for the mobile phase of the composition MeOH + H₂O (10 + 90) v/v or of 2.5 mV for $10^{-4} \text{ M TEAClO}_4$ in MeOH + H₂O (10 + 90) v/v, respectively.

It has been shown that even at concentrations of the quaternary ammonium cations without buffers as small as $10^{-5} - 10^{-4} \text{ M}$ the determination of volatile fatty acids was possible in the ion-pair chromatography system. The addition of quaternary ammonium pairing cations to the mobile phase made the retention volume independent of acid concentration in the injected sample in a definite range of concentrations. However, in this case the reproducibility of the detector was poorer (e.g. 10^{-10} mole for $c_{\text{TEA}^+} = 10^{-4} \text{ M}$).

For capillaries made of a dielectric a pronounced dependence was observed of chromatographic peak heights on the flow rate. The value of J^0 was independent of the concentrations of acids, but it was the higher the greater was the diameter of the capillary used. The longer was the capillary or the smaller was its diameter the higher were the peaks observed, but the relative reproducibility for all of them was unaffected.

The reproducibility and detectability of the detector equipped with the stainless-steel capillary was in fact poorer than that of the detector with the PTFE ca-

pillary and equaled about 30% and $2.5 \times 10^{-10} M$, respectively; however, the heights of peaks in the former were less dependent on the flow rate, what might be advantageous in analytical practice.

ACKNOWLEDGMENTS

The authors wish to thank Dr D. Sybilska for her precious suggestions. The work was carried out within the frames of the research project 03.10. of the Polish Academy of Sciences.

REFERENCES

1. Kemula, W., Głód, B. K., Kutner, W., Electrokinetic Detection in Reversed Phase High Performance Liquid Chromatography. Part 1. Volatile Fatty Acids, *J. Liq. Chromatogr.*, This Issue.
2. Kolthoff, I. M., Coetzee, J. F., Polarography in Acetonitrile. I. Metal Ions Which Have Comparable Polarographic Properties in Acetonitrile and in Water, *J. Am. Chem. Soc.*, **79**, 870, 1957.
3. Terabe, S., Yamamoto, K., Ando, T., Streaming Current Detector for Reversed-Phase Liquid Chromatography, *Can. J. Chem.*, **59**, 1531, 1981.
4. Smoluchowski, M., *Krak. Anz.*, 192, 1908.
5. Głód, B. K., Mechanizmy Powstawania Potencjału i Prądu Przepływu oraz Ich Zastosowania, *Wiad. Chem.*, Submitted.
6. Elektricheskie Svoistva Kapilarnykh Sistem, Zhukov, I. I., ed., A. N. USSR, Moskva—Leningrad, 1956.
7. Spravochnik po Elektrokhimii, Suchotin, A. M., ed., Khimiya, Leningrad, 1981, pp. 51 — 94.
8. Vespalec, R., Effect of the Components of the Chromatographic System on the Electrokinetic Streaming Current Generated in Liquid Chromatography Columns, *J. Chromatogr.*, **210**, 1, 1981.
9. Krejčí, M., Šlais, K., Tesařík, K., Electrokinetic Detection in Liquid Chromatography. Measurement of the Streaming Current Generated on Analytical and Capillary Column, *J. Chromatogr.*, **149**, 645, 1978.
10. Krejčí, M., Kouřilova, D., Vespalec, R., Electrokinetic Detection at Different Points in a Narrow Bore Glass Column in Liquid Chromatography, *J. Chromatogr.*, **219**, 61, 1981.
11. Głód, B. K., Kutner, W., Kemula, W., Unpublished Results.

12. Bush, K. J., Russell, R. W., Young, J. W., Quantitative Separation of Volatile Fatty Acids by High-Pressure Liquid Chromatography, *J. Liq. Chromatogr.*, **2**, 1367, 1979.

**FABRICATION AND CHARACTERISATION OF LEAK-TIGHT GLASSY CARBON ELECTRODES,
SEALED IN GLASS EMPLOYING SILICON COATING, FOR USE IN ELECTROCHEMICAL
DETECTION**

J.C. Hoogvliet*, J.A.G. van Bezooyen, A.C.J. Hermans-Lokkerbol,
C.J. van der Poel and W.P. van Bennekom

Department of Pharmaceutical Analysis and Analytical Chemistry, Gorlaeus
Laboratories, Subfaculty of Pharmacy, State University, Wassenaarseweg 76,
2333 AL Leiden, The Netherlands

SUMMARY

Glassy carbon discs have been coated with silicon in a chemical vapour deposition process to obtain leak-tight electrodes, sealed in glass. Electrodes with coatings thicker than 5 μm prove to be leak-tight in contrast with uncoated ones. Silicon-coated electrodes show faster decay of charging current, less noise and decreased background current. Leak-tightness and electron microscope information correlate well with the electrochemical data. All results can be ascribed to the absence of a void between glassy carbon and glass at Si-coated electrodes. By silicon coating, signal-to-noise ratios are improved with a factor of about 5, as is demonstrated for catecholamines and metabolites in liquid chromatography with electrochemical detection.

INTRODUCTION

Electrochemical flow-through detectors are widely used for low-level, selective and inexpensive analysis of a large variety of substances. Nowadays those which employ some form of carbon as working electrode constitute the majority, being used for mainly oxidative detection in liquid chromatography.

From experience it is known that new electrodes behave differently from repolished ones. This (long-term!) deterioration, being reflected in more noise and a higher background current, is known as "aging" and is of extreme importance for lowest-level determinations. Since it was believed that electrode fabrication plays an important role in aging, this aspect of electrochemical detection has been studied in detail.

There are several ways to fabricate glassy carbon (GC) electrodes for detectors. Electrodes can be press-fitted or sealed in Kel-F, Teflon, plexiglas or glass. In the PB-2 confined wall-jet flow-through detector [1], the GC working and auxiliary electrodes (WE resp. AE) are sealed in holders of borosilicate glass (Fig. 1). The coefficient of thermal expansion of the glass matches that of the used GC within a narrow range (resp. 32 and $35 \times 10^{-7}/^{\circ}\text{C}$).

With these electrodes used directly after fabrication, very low detection limits can be obtained [1]. In the time, however, electrochemical behaviour gradually deteriorates. We have observed even faster deterioration in organic solvents like acetonitrile and methanol, eventually leading to cracking of the glass holder. Mostly, the initial electrode characteristics can not be recovered by repolishing. It appears that solvents can penetrate in a thin void between the GC and glass in spite of the matched expansion coefficients. Similar aging behaviour has been observed by us with GC electrodes, press-fitted or glued in Kel-F.

According to Levy and Farina [2], leak-tight electrodes can be obtained by coating the GC with silicon (Si). For the same purpose SiO and SiO_2 coating techniques have been described [3,4]. These GC electrodes, sealed in glass, have been developed for and only applied (as far as we know) in high temperature electrochemical studies (ca. 500°C). It seemed likely to us that Si-coated electrodes would offer comparable advantages in aqueous and organic solvents at room temperature.

In the present work Si-coated GC electrodes, sealed in glass, are manufactured and compared with conventional ones. The influence of the thickness of the coating on charging and background currents, noise and long-term stability is studied in batch and flow experiments. The electrochemical results are correlated with leak-tightness and electron microscope (EM) information.

EXPERIMENTAL.**Electrode fabrication**

Circular GC discs (V10, Le Carbone Lorraine, Paris, France) with a diameter of 10 mm, all made from a single plate, were ground with 40 μm carborundum powder and cleaned ultrasonically in methanol before coating.

The discs were placed in a cold wall chemical vapour deposition reactor, operating at atmospheric pressure with hydrogen as carrier gas, and brought to 1250 °C by an inductively heated graphite susceptor. Polycrystalline Si coatings were deposited by thermal decomposition of trichlorosilane (2% by volume). The growth rate of the Si layers amounted to 3 $\mu\text{m}/\text{min}$. Si coatings of 5, 15 and 40 μm were prepared. The thermal expansion coefficient of Si is $30 \times 10^{-7}/^\circ\text{C}$.

Next, the discs were sealed in tubes of borosilicate glass (Duran 8330, Jena Glaswerk, Mainz, GFR). Si was removed from the frontside by grinding. The surface was polished to a mirrorlike finish with 6 and finally with 1 μm diamond spray (Engis Ltd., Maidstone, U.K.). Electrical contact (shielded cable) was established with silver paint (Elecolit 325, 3M, Leiden, The Netherlands). The connection was mechanically fixed with a non-conductive resin (Araldite, AW 136/HY 994, Ciba Geigy, Arnhem, The Netherlands). Electrodes without Si coating were prepared in an identical manner. For EM studies, unpolished dummy electrodes were made by cutting off the glass holder just above the GC.

Electrode characterisation

All electrodes have been checked for leak-tightness with a helium leak detector (Leybold-Heraeus, Köln, GFR). With an EM (Cambridge S180) secondary electron image (SEI) and backscattered electron image (BSEI) pictures of the dummy electrodes were made for surface and material contrast information respectively. A thin layer of gold has been sputtered onto the samples to prevent charging of the glass.

Electrochemical measurements were performed with a Bruker E310 modular research polarograph (Bruker, Brussels, Belgium). The currents in the chronoamperometric experiments were sampled and digitized by a MINC-11/03 microcomputer (Digital Equipment Corporation, MA, USA). Data-acquisition and -processing was controlled by a Fortran program and curves were plotted with a HP 7220C plotter (Hewlett Packard Company, San Diego, CA, USA).

The GC AE (diameter 10 mm and coated with 40 μm Si), the SCE reference electrode (home made) and one of the WE's were placed in the PB-2 detector

(Fig. 1). In the batch experiments a 0.05 M phosphate buffer of pH 3.5 containing 0.1 M NaClO_4 , and methanol with 0.1 M NaClO_4 as supporting electrolyte, acidified to "pH" 1.5 with HClO_4 were used. The distance between WE and AE was about 1 cm.

Chromatography

Polygosil 50-5C8 (5 μm , Machery-Nagel & Co., Düren, GFR) was packed in a stainless steel Valco column (100x3.0 mm i.d.) and coated in situ with tri-n-butyl-phosphate (TBP). The eluent, saturated with TBP and thermostatted at 25 °C, was an aqueous 0.05 M phosphate/0.1 M HClO_4 solution, adjusted to pH 3.5 with NaOH [6]. About 10 mg of EDTA per litre eluent was added in order to decrease the (steady-state) background current.

An Orlita 1515 reciprocating pump (Giessen, GFR) and an injection valve with fixed loop (Rheodyne 7010, Berkeley, CA, USA) were used. In the chromatographic experiments, the distance between WE and AE was 50 μm , adjusted with a PVC spacer.

Mixtures of noradrenaline HCl (Sigma), adrenaline bitartrate (Boehringer-Ingelheim), bis(4-hydroxy-3-methoxy)phenylglycol piperazine salt (Sigma) and 3-hydroxytyramine HCl (Aldrich) were prepared in 1 M NaClO_4 aqueous solutions, acidified to pH 3.0 with HClO_4 .

The chromatographic conditions of the recordings of brain tissue (Fig. 7) are described by Van Valkenburg et al. [7].

All chemicals were reagent grade and used as received. Demineralized water was additionally purified by a Milli-Q Water Purification System (Millipore, Bedford, MA, USA).

RESULTS AND DISCUSSION

Leak-tightness of the electrodes

The influence of the thickness of the Si coatings on the leak-tightness was investigated by a helium leak test and EM. Both methods reveal that 5 μm of Si is not sufficient to obtain leak-tight seals. From the EM results it

seen that the carbon surface at the side is not entirely covered with Si. Polishing and a better controlled coating procedure would probably give better results. Electrodes with 15 and 40 μm Si coatings were leak-tight in all cases.

The uncoated electrode leaked; on the EM picture (Fig. 3), it can be seen that a void of about 1 μm is present between GC and

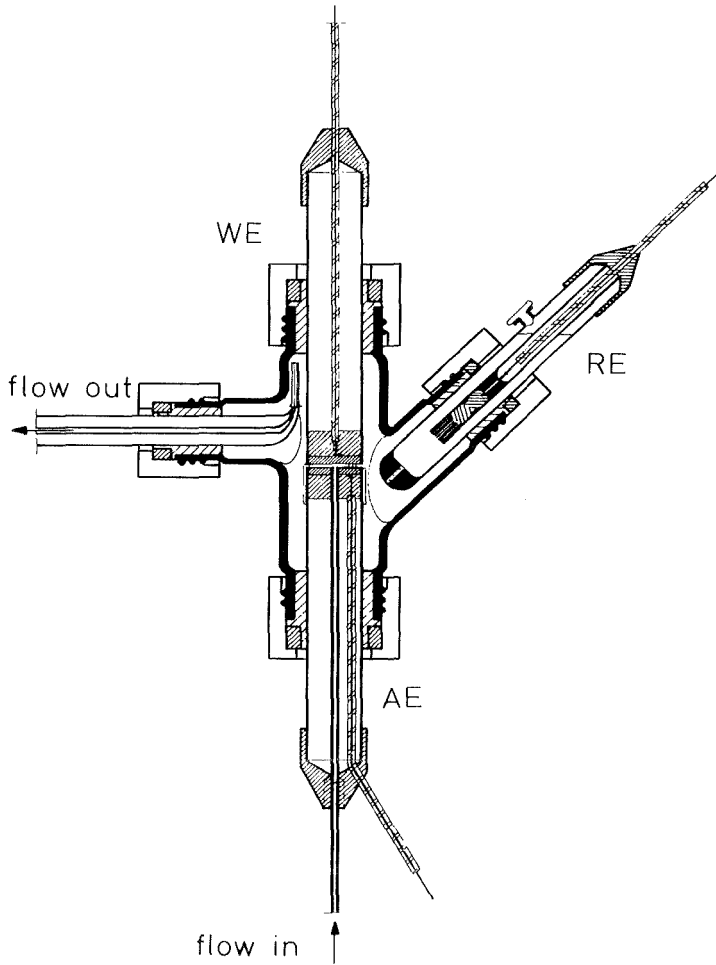


Fig. 1. The PB-2 confined wall-jet detector.

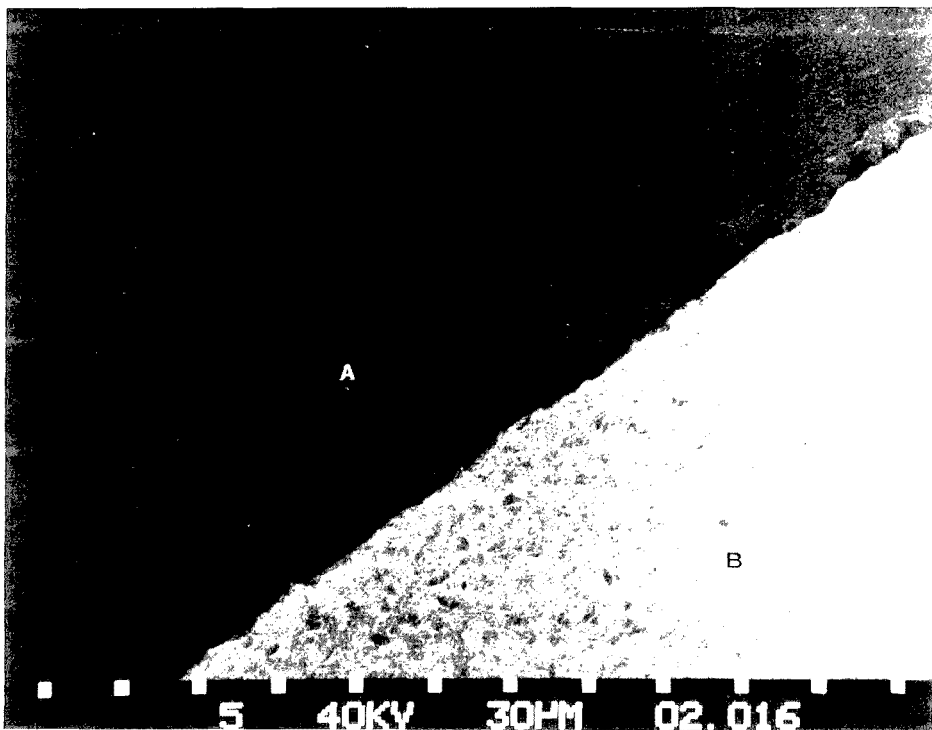
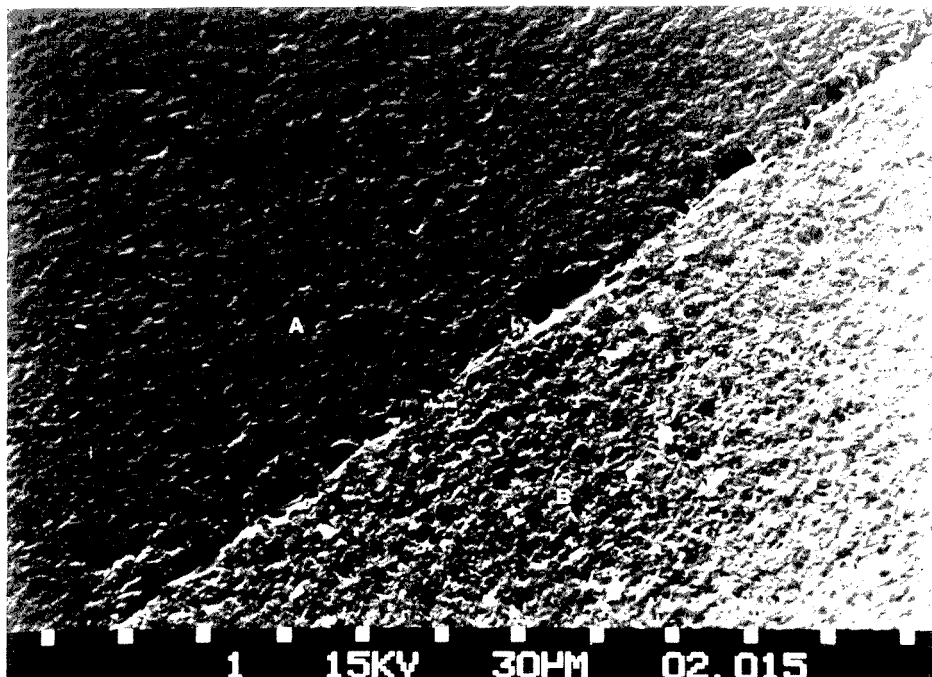


Fig. 2. EM photographs of an uncoated electrode. SEI (upper) and BSEI (lower) pictures of the interface between GC (A) and glass (B). The surface is not polished.

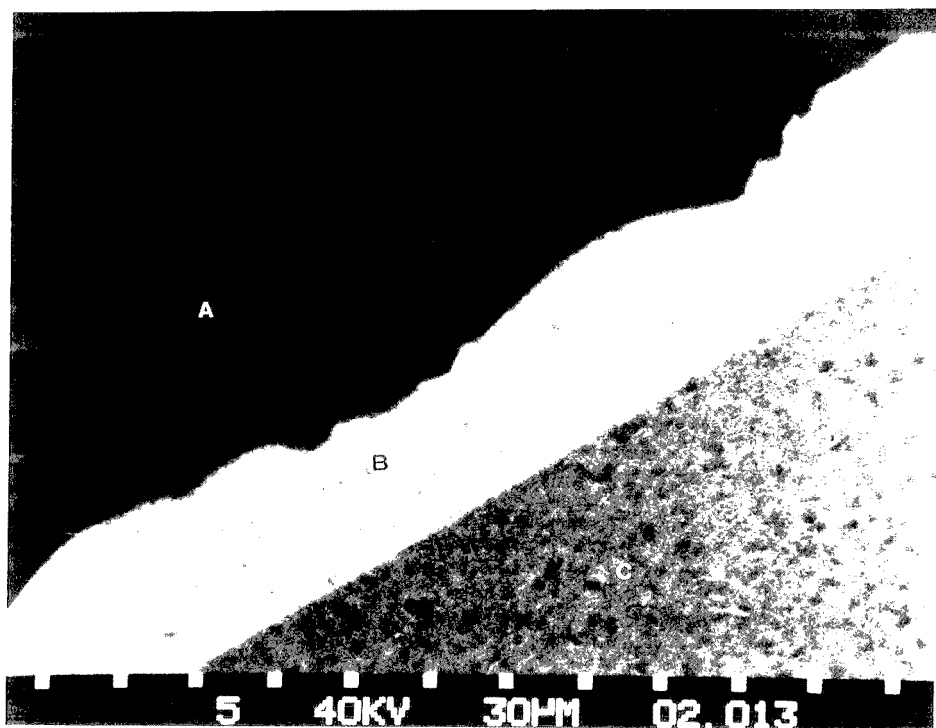
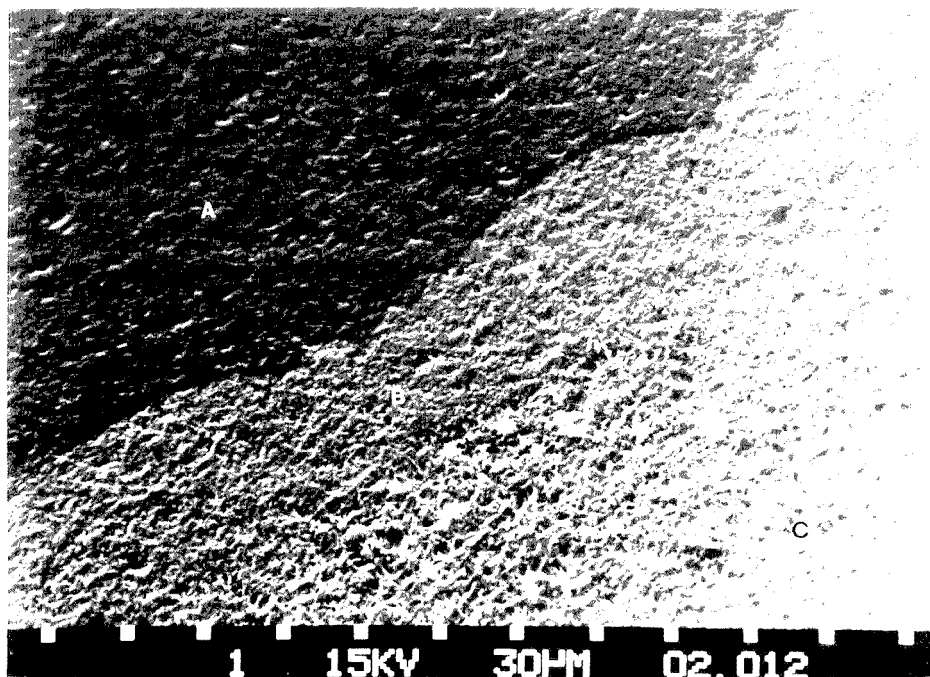


Fig. 3. EM photographs of a 40 μm Si-coated electrode. SEI (upper) and BSEI (lower) pictures of the interface between GC (A), Si (B) and glass (C). The surface is not polished.

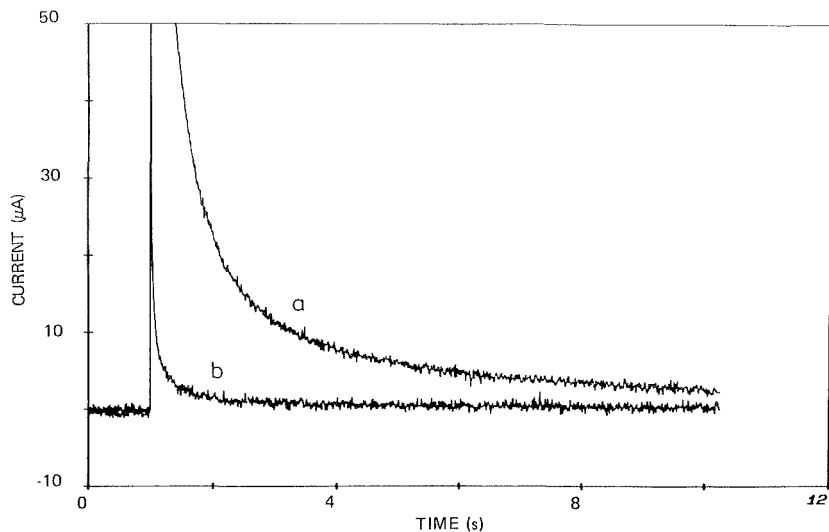


Fig. 4. Current-time plots after application of a potential step from 0 to + 0.5 V vs. SCE for an uncoated (a) and 40 μm Si-coated (b) electrode, directly after fabrication, both recorded in phosphate buffer. Sampling frequency: 100 Hz. Data have not been averaged.

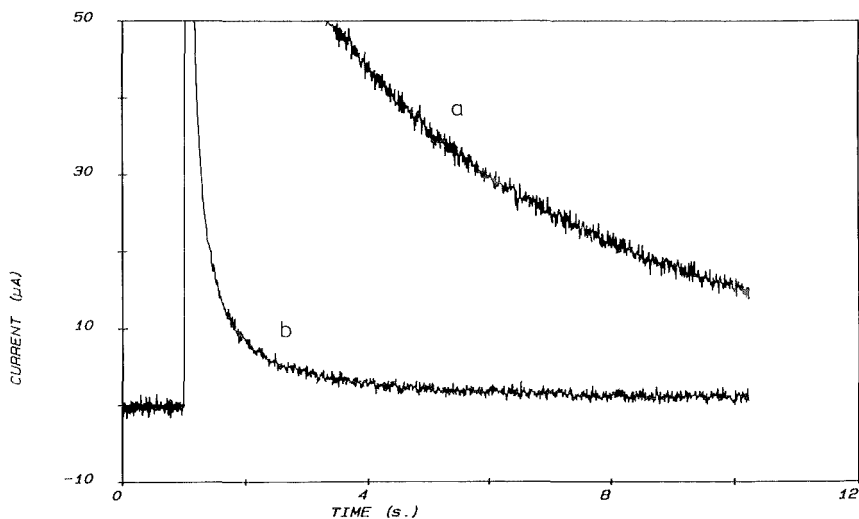


Fig. 5. Current-time plots for the uncoated (a) and 40 μm Si-coated (b) electrode, recorded after been in use for 100 h at + 0.8 V vs. SCE. Experimental conditions as in Fig. 4.

glass. In electrochemical experiments leakage of methanol was observed.

In Figure 3, the 40 μm Si-coated electrode is shown. The EM pictures indicate that the seals between GC and Si and between Si and glass are very good. The good seal between Si and GC can be ascribed to the formation of a thin layer of silicon carbide (SiC) during the coating process. The sealing between Si and glass is ascribed to the fact that Si is well wetted by glass, due to formation of SiO_2 at the surface in contact with air.

The long-term stability of the electrodes ($>5\mu\text{m}$ Si) proved to be good. In the period between fabrication and this moment (8 months), none of the Si-coated electrodes broke down and all are still leak-tight.

Influence of Si coating on the charging current

The influence of the thickness of the Si coating on the magnitude and decay of the charging current in the phosphate buffer and the methanolic solution was investigated by chronoamperometry. A potential step from 0 to + 0.5 V vs. SCE was applied. The resulting currents are entirely due to recharging of the electrical double layer and to formation/oxidation of surface groups of the electrode material itself [5].

In Fig. 4, the results in the phosphate buffer for uncoated and 40 μm Si-coated electrodes (new ones) are shown. No significant differences between the current-time curves recorded in methanol and phosphate buffer were observed. The curves for 5 and 15 μm Si-coated electrodes very much resemble the one with 40 μm Si. The experiments were repeated with the uncoated and 40 μm Si-coated electrode after both had been in use for about 100 h at + 0.8 V vs. SCE (Fig. 5). The conclusion is that there are important differences in decay between uncoated and Si-coated electrodes. This difference is already significant directly after fabrication, but becomes more pronounced when the electrodes have been in use for some time.

Comparable differences in charging current were observed in cyclic voltammetry and in differential pulse amperometry (DPA). In DPA, e.g., the recorded background current of a 40 μm Si-coated electrode is 4 times smaller than of an uncoated one. These differences in behaviour are explained by the absence of the extra impedance due to the void between GC and glass. Accumulation of impurities and electrolyte in the void may also contribute to the observed deterioration. Nevertheless, some residual current persists at GC electrodes, even in absence of a void, because of micropores in the material and of formation/oxidation of surface groups [5].

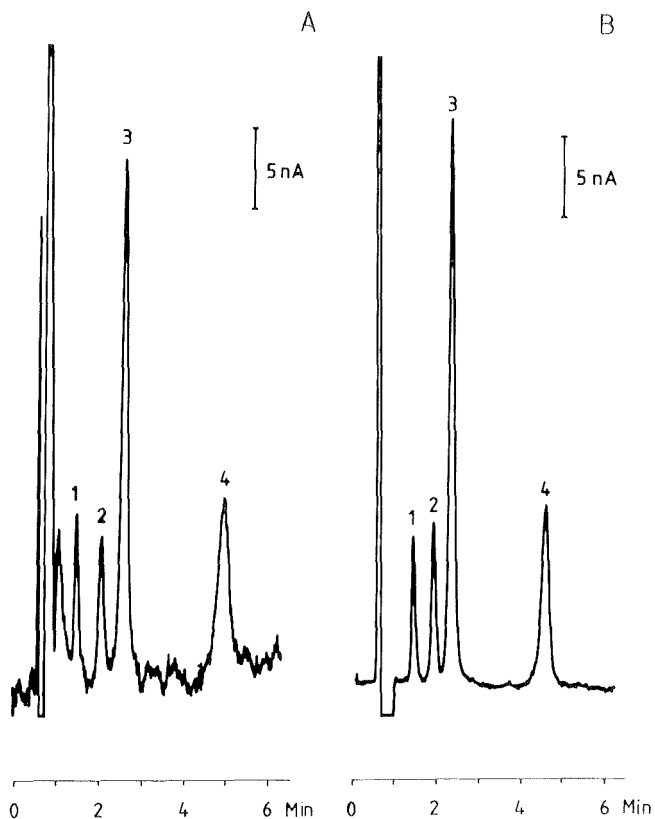


Fig. 6. Chromatograms of a mixture of 1.6 ng 3-methoxy-4-hydroxyphenylethyleneglycol (1), 1.0 ng adrenaline (2), 2.8 ng noradrenaline (3) and 1.1 ng dopamine (4) at the uncoated (A) and 40 μm Si-coated electrode (B). The flowrate was 0.7 mL/min and the used time constant was 1.0 s. The peak-to-peak noise levels are about 2.0 (A) and 0.4 nA (B). ($E = +0.8$ V vs. SCE, 20- μL loop).

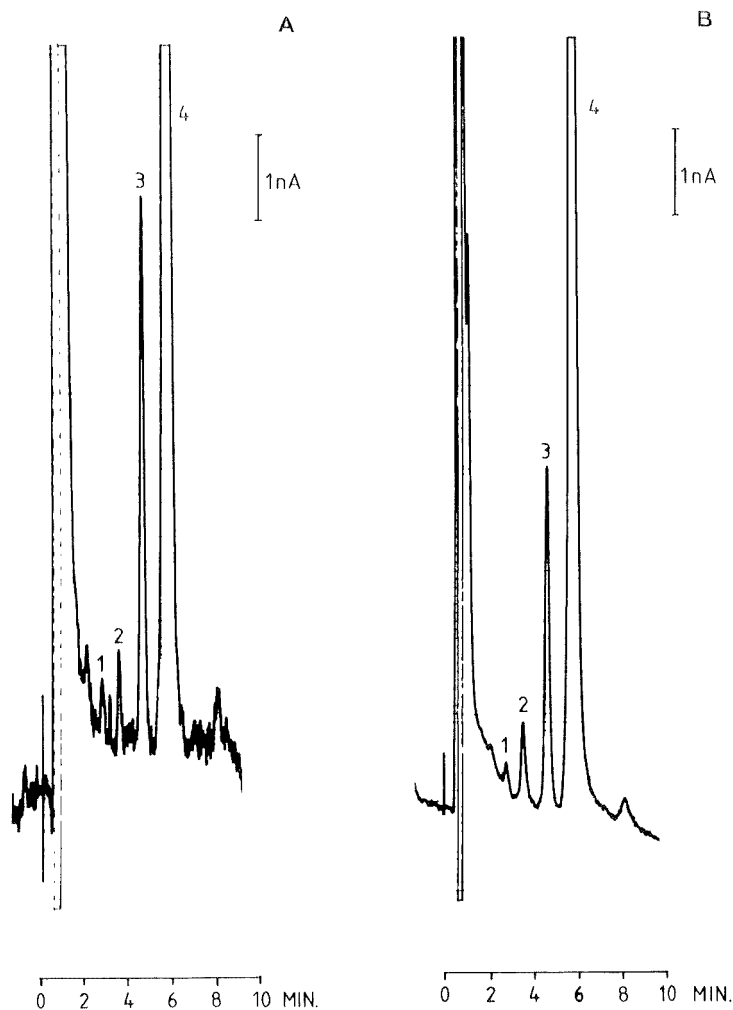


Fig. 7. Chromatograms of a sample obtained from rat tuberculum olfactorium at the uncoated (A) and 40 μm Si-coated electrode (B). The supernatant derived from about 0.5 mg tissue was dissolved in 0.1 M HClO_4 and injected. Peaks: noradrenaline (1), homovanillic acid (2), dihydroxyphenylacetic acid (3) and dopamine (4). The flow rate was 0.8 mL/min and the used time constant was 2.2 s. The peak-to-peak noise levels are about 0.5 (A) and 0.1 nA (B). ($E = +0.8$ V vs. SCE, 100- μL loop).

Application of the electrodes in electrochemical detection

Si coatings have also a pronounced effect on the noise and S/N ratio. The improvement is illustrated by chromatograms, recorded with an uncoated and 40 μm Si-coated electrode. Both electrodes were repolished after about 200 h of use. Since repolishing, the electrodes had been used for about 50 h at + 0.8 V vs. SCE before the chromatograms were recorded (Fig. 6). Because both electrodes, with equal geometric area, were not pretreated electrochemically, the I/E relationships of the detected compounds may be different, being reflected in differences in sensitivity (Figs. 6 and 7).

Because of the influence of Si coating on the decay of the charging current, the background current at the Si-coated electrode reached a steady state (35 nA) within 30 min, while about 2 h were needed for the uncoated one (55 nA). The electrodes were also compared in the determination of dopamine and its acidic metabolites in rat brain tissue [7]. Both were repolished and the chromatograms were recorded after a 24 h equilibration at + 0.8 V vs. SCE (Fig. 7). The recorded background currents were 95 and 55 nA at the uncoated and coated electrode respectively.

The S/N ratios in both determinations are improved with a factor of about 5 by Si coating.

Preliminary experiments indicate that the electrochemical phenomena, observed at uncoated GC electrodes, sealed in glass, are also more or less present at electrodes, press-fitted or sealed in Kel-F, Teflon and plexiglas. Work on further characterisation of these Si-coated GC electrodes is in progress.

CONCLUSIONS

It is concluded that the noise, background current and decay of charging current, are partly determined by a void between GC and glass, in which electrolyte can penetrate. This void is not present at electrodes coated with 15 μm or more Si, resulting in improved electrode performance. Thus, because of faster decay of charging current, decreased noise and lower background current, Si coating of GC is advantageous in those fields of electrochemistry where low detection limits and/or low charging currents are required, notably, in liquid chromatography with electrochemical detection.

ACKNOWLEDGEMENTS

The authors are grateful to Dr. Ir. J. Bezemer of the Laboratory for Experimental Physics in Utrecht for coating the glassy carbon samples with silicon, to Mrs Ing. C.J.G. van Hoek and Mr. M.J. van Noord of the Laboratory for Electron Microscopy of the State University in Leiden for making the EM photographs, and to dr. C.F.M. van Valkenburg for recording the chromatograms of rat brain tissue samples.

REFERENCES

- 1 W.P. van Bennekom, Ph.D. Thesis, State University, Leiden, The Netherlands, 1981
- 2 S.C. Levy and P.R. Farina, *Anal. Chem.*, 47 (1975) 604
- 3 H.A. Laitinen, Y. Yamamura and I. Uchida, *J. Electrochem. Soc.*, 125 (1978) 1450
- 4 I. Uchida, H. Urushibata and S. Toshima, *J. Appl. Electrochem.*, 12 (1982) 115
- 5 W.E. van der Linden and J.W. Dieker, *Anal. Chim. Acta*, 119 (1980) 1
- 6 H.J.L. Janssen, U.R. Tjaden, H.J. de Jong and K.-G. Wahlund, *J. Chromatogr.*, 202 (1980) 223
- 7 C.F.M. van Valkenburg, U.R. Tjaden, J. van der Krogt and B. van der Leden, *J. Neurochem.*, 39 (1982) 990

DETERMINATION OF THE OXIDIZED AND REDUCED FORMS OF BIOPTERIN
IN TISSUE SAMPLES

C. E. Lunte and P. T. Kissinger

Department of Chemistry
Purdue University
West Lafayette, Indiana 47907

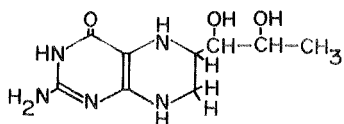
ABSTRACT

Biopterin, in its reduced form, is a cofactor to the enzymes catalyzing the rate-limiting reactions in the synthesis of both the catecholamines and serotonin. It has been suggested that it may serve a role in the regulation of these neurotransmitters. Altered biopterin concentrations have also been reported in various neural disorders. In this report, we describe a method using liquid chromatography/electrochemistry to quantitate both the oxidized and reduced forms of biopterin in mouse tissue samples. This method employs a dual-electrode amperometric detector in the parallel-adjacent configuration. Subpicomole detection limits were achieved for all oxidation states.

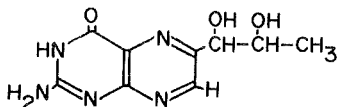
INTRODUCTION

L-*erythro*-tetrahydrobiopterin (Figure 1) has been shown to be a cofactor in several hydroxylation reactions. These include the hydroxylation of phenylalanine (1), tryptophan (2) and tyrosine (3). Recently, there has been speculation that the concentration of tetrahydrobiopterin may serve a function in the regulation of these reactions (4). In order to elucidate the role of tetrahydrobiopterin and to study the mechanism of its function, a method is needed to quantitate it at the picomole level in various tissue samples.

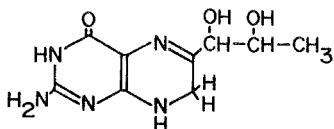
Several methods of determining biopterin concentrations are available: a bioassay using *Crithidia fascioulata* (5), a radioenzymatic assay (6),



5,6,7,8-TETRAHYDROBIOPTERIN



BIOPTERIN



7,8-DIHYDROBIOPTERIN

Figure 1. Structures of the oxidized and reduced forms of biopterin.

an immunoassay (7), and liquid chromatography with fluorescence detection (8,9). None of these methods can directly detect all of the oxidation states of biopterin. We have recently reported a method employing liquid chromatography/electrochemistry (LCEC) for the determination of a variety of pterin species and oxidation states in urine (10). Bräutigam and Dreesen have also described the detection of tetrahydrobiopterin by LCEC (11). In this report, a method using LCEC with a dual-electrode detector is described for the determination of the stable oxidation states of biopterin in tissue samples.

EXPERIMENTAL

Chemicals. All chemicals were reagent grade or better. Biopterin was purchased from Calbiochem-Behring (La Jolla, CA). Octyl sodium sulfate was obtained from Eastman Kodak Co. (Rochester, NY). Tetrahydrobiopterin was a gift of Dr. A. Niederweiser (Zürich, Switzerland). Tetrahydrobiopterin and 7,8-dihydrobiopterin were prepared as described previously (10).

Apparatus. The chromatography system employed consisted of an Altex 110 pump and dual LC-4B amperometric detectors (Bioanalytical Systems, West Lafayette,

IN). Chromatography was performed on a Biophase ODS 5 μ column (25 cm x 4.6 mm). The column was thermostated at 30°C by an LC-23 column heater and an LC-22 temperature controller (BAS). A 20 μ L injection loop was employed.

Liquid Chromatography. An "ion-pair" reverse-phase chromatographic system was used to achieve separation. The mobile phase was 3 mM octyl sodium sulfate in a 0.1 M sodium phosphate buffer, pH 2.5, with 15% methanol. A standard separation is shown in Figure 2. The mobile phase was prepared from distilled, deionized water and filtered through a 0.22 μ m filter (Millipore, Milford, MA). Oxygen was removed by continuous purging of the mobile phase with nitrogen and maintaining the mobile phase reservoir at a temperature of 40°C. A flow rate of 1.0 mL/min was used for all experiments.

Sample Preparation. Mice were sacrificed by decapitation. The organ of interest was removed, weighed wet, and homogenized in 0.1 M phosphoric acid containing 2 mM ascorbic acid. Approximately 1 mL of acid solution per gram of tissue was used. The sample was centrifuged at 15,000 x g for 15 minutes. The supernatant was saved and the pellet resuspended in a second volume of the acid solution. This was recentrifuged and the two supernatants combined. The combined supernatants were then filtered through a 0.22 μ m filter. The filtrate was injected onto the analytical column.

RESULTS AND DISCUSSION

Voltammetry of Biopterin

Hydrodynamic voltammograms (HDV's) of the oxidation states of biopterin are shown in Figure 3. It can be seen that a potential of only +300 mV versus Ag/AgCl is necessary for the detection of tetrahydrobiopterin while a potential of +600 mV is required if 7,8-dihydrobiopterin is to be detected. For the determination of oxidized biopterin a potential of -700 mV versus the Ag/AgCl electrode is needed for reduction.

Dual-Electrode Detection

The dual-electrode amperometric detector can be used to advantage in two modes for the detection of biopterin in tissues. Both techniques employ the

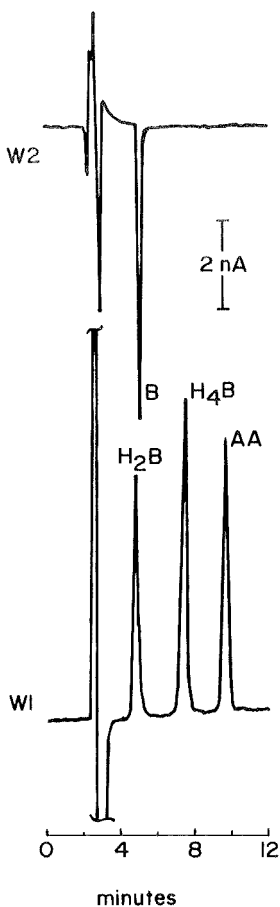


Figure 2. Standard separation of the oxidation states of biopterin. Chromatographic conditions: 3 mM octyl sodium sulfate in 0.1 M sodium phosphate buffer, pH 2.5, 15% MeOH. W1 = +600 mV, W2 = -700 mV. Peak identities: B, biopterin; H₂B, 7,8-dihydrobiopterin; H₄B, 5,6,7,8-tetrahydrobiopterin; AA, ascorbic acid.

electrodes in a parallel configuration with the electrodes adjacent to each other and normal to the direction of flow. If it is necessary to detect all oxidation states of biopterin, one electrode is poised at +600 mV to detect both reduced forms and the other electrode is poised at -700 mV to detect oxidized biopterin. However, if it is desired to detect tetrahydrobiopterin with greater selectivity and/or lower detection limits, one electrode can be operated at +300 mV to

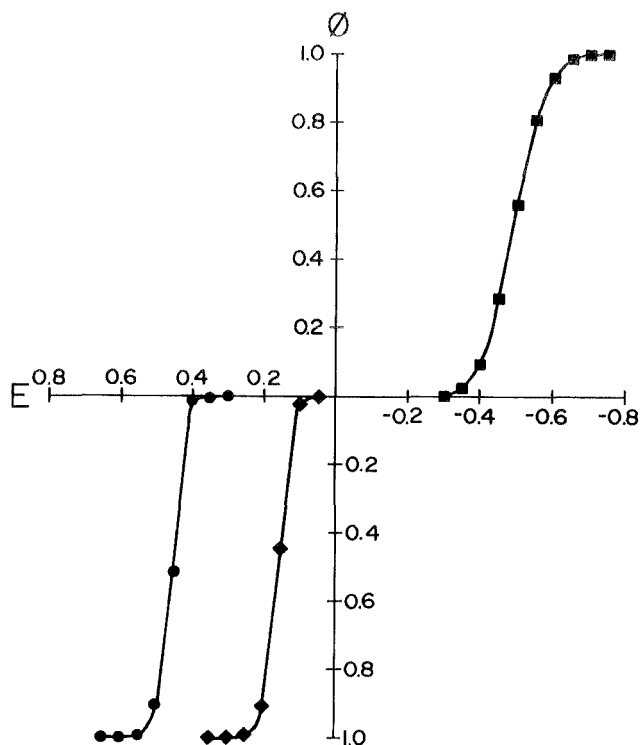


Figure 3. Hydrodynamic voltammograms of biopterin oxidation states. \blacksquare —oxidized biopterin, \blacklozenge —tetrahydrobiopterin, \bullet —dihydrobiopterin.

detect tetrahydrobiopterin and the other electrode at +700 mV to detect both tetrahydrobiopterin and 7,8-dihydrobiopterin. Figure 4 shows typical chromatograms obtained for both mouse brain and liver samples using potentials of +600 mV (lower trace) and -700 mV (upper trace). Figure 5 shows chromatograms obtained for the same samples with the electrodes operated at +600 mV (lower trace) and +300 mV (upper trace).

Linearity and Detection Limits

Response was linear over several orders of magnitude, from nanomoles to femtomoles injected, for all biopterin oxidation states. The limit-of-detection

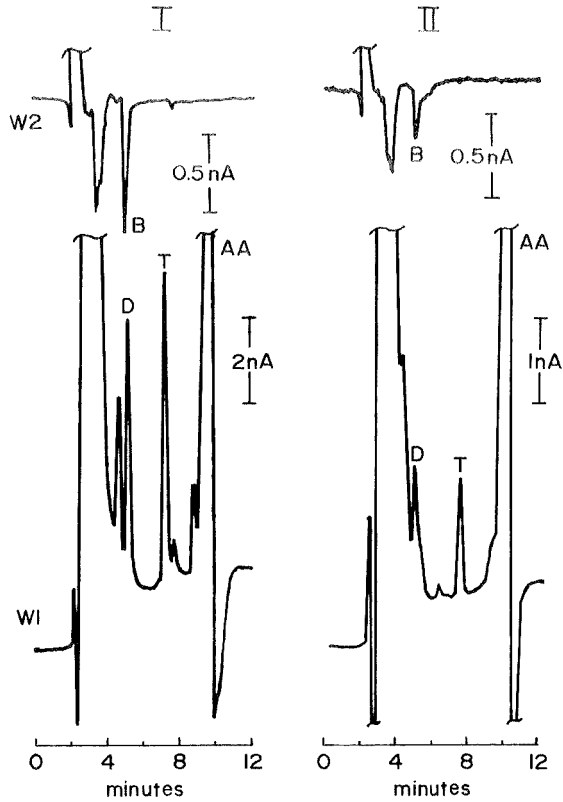


Figure 4. Detection of the oxidized and reduced forms of biopterin in mouse tissue samples. I = Liver, II = Brain. Conditions and peak identities as in Figure 2.

($S/N = 3$) was 0.53 picomoles for oxidized biopterin and 0.66 picomoles for 7,8-dihydrobiopterin. The detection limit for tetrahydrobiopterin depended upon the detector potential used; at +600 mV a limit of 0.69 picomoles was found while at a potential of +300 mV a limit-of-detection of 0.53 picomoles was achieved.

Peak Identification

Peaks in the sample chromatogram were identified in two ways. First, the retention time of the sample peak was compared with the retention time of the

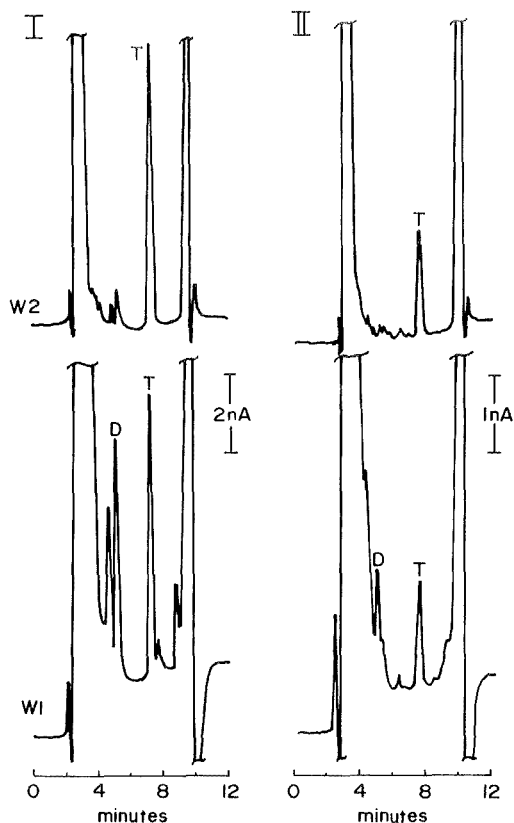


Figure 5. Selective detection of tetrahydrobiopterin in mouse tissue samples. I = Liver, II = Brain. W1 = +600 mV, W2 = +300 mV. Conditions and peak identities as in Figure 2.

authentic compound. Peaks were secondly identified by the voltammetric characterization procedure as described previously (10). Table 1 shows the voltammetric characterization data for all the oxidation states of biopterin. These two peak identification procedures allow structures to be assigned with a high degree of certainty.

Biopterin Concentrations in Mouse Tissues

As seen from Figure 4, little oxidized biopterin was detected in either the liver or brain samples. Both tetrahydrobiopterin and 7,8-dihydrobiopterin

TABLE 1

Voltammetric Characterization of Tissue Samples

DIHYDROBIOPTERIN

E (mV)	Std. ^a	Liver	Brain
+550	0.98	0.98	0.97
+500	0.68	0.68	0.66
+450	0.32	0.32	0.31
+400	0.07	0.07	0.06

TETRAHYDROBIOPTERIN

E (mV)	Std. ^b	Liver	Brain
+250	0.95	0.95	0.94
+200	0.78	0.77	0.78
+150	0.28	0.23	0.26
+100	0.06	0.07	0.06

BIOPTERIN

E (mV)	Std. ^c	Liver	Brain
-650	0.97	0.95	0.95
-600	0.91	0.89	0.88
-550	0.75	0.73	0.76
-500	0.51	0.49	0.49

^aCurrent normalized to that observed at +600 mV.

^bCurrent normalized to that observed at +300 mV.

^cCurrent normalized to that observed at -700 mV.

TABLE 2

Biopterin Concentrations (ug/g) in Mouse Tissues

(n = 9)	H ₄ BIOPTERIN	H ₂ BIOPTERIN	BIOPTERIN
Liver	1.96	0.189	0.071
Std. Dev.	0.28	0.087	0.028
Brain	0.189	0.079	0.053
Std. Dev.	0.034	0.056	0.027

were detected in both tissues, but the prevalent form was tetrahydrobiopterin in both cases. The 7,8-dihydrobiopterin is likely derived from quinonoid dihydrobiopterin, which has been reported to be the immediate oxidation product of tetrahydrobiopterin (12). The reported half-life for the tautomerization of quinonoid dihydrobiopterin to 7,8-dihydrobiopterin being about 5 minutes (13), the detection of quinonoid dihydrobiopterin would not be expected considering the time for sample preparation. The concentrations of biopterin found in mouse tissues are listed in Table 2.

As has been shown, LCEC with dual-electrode detection offers a powerful method for the detection of the various oxidation states of biopterin in tissue samples. The ability to directly detect both the oxidized and reduced forms of biopterin is an advantage over previous methods. Dual potential monitoring also allows more selective detection of the easily oxidized tetrahydrobiopterin while still detecting the more difficult to oxidize dihydrobiopterin.

ACKNOWLEDGEMENTS

The authors thank Dr. A. Niederweiser for the gift of tetrahydrobiopterin. We also thank G. Barone III for assistance in preparation of the tissue samples.

REFERENCES

1. S. Kaufman, *Biochim. Biophys. Acta*, 27(1958) 428.
2. T. Nagatsu, M. Levitt and S. Udenfriend, *J. Biol. Chem.*, 239(1964) 2910.
3. E. Jequir, D. Robinson, W. Lovenberg and A. Sjoerdsma, *Biochem. Pharmacol.*, 18(1969) 1071.
4. T. Nagatsu, *Trends in Biol. Sci.*, (1981) 276.
5. H. Baker, O. Frank, A. Shapiro and S. Hutner, *Methods Enzymol.*, 66(1980) 490.
6. G. Guroff, C. Rhoads and A. Abramowitz, *Anal. Biochem.*, 21(1967) 273.
7. T. Nagatsu, T. Yamaguchi, T. Kato, T. Sugimoto, S. Matsuura, M. Akino, S. Tsushima, N. Nakazawa and H. Ogawa, *Anal. Biochem.*, 110(1981) 182.
8. T. Fukushima and J. Nixon, *Anal. Biochem.*, 102(1980) 176.
9. B. Stea, R. Halpern, B. Halpern and R. Smith, *J. Chromatogr.*, 188(1980) 363.
10. P.T. Kissinger and C. Lunte, *Anal. Chem.*, in press.
11. M. Bräutigam and R. Dreesen, *Hoppe-Seyler's Z. Physiol. Chem.*, 363(1982) 341.
12. S. Kaufman, *J. Biol. Chem.*, 239(1964) 332.
13. J. Haavik and T. Fiatmark, *J. Chromatogr.*, 257(1983) 361.

INTERPRETATIONS OF VOLTAMMETRY IN THE STRIATUM
BASED ON CHROMATOGRAPHY OF STRIATAL DIALYSATE

Joseph B. Justice, Jr., Sherry A. Wages, and Adrian C. Michael
Department of Chemistry
Randy D. Blakely
Department of Biology
Darryl B. Neill
Department of Psychology
Emory University
Atlanta, Ga., 30322

ABSTRACT

A comparison is made of chronoamperometric data recorded from the striatum and chromatographic data obtained from extracellular striatal perfusate. Three specific cases are considered: the initial sampling period in which a decline in the observed oxidation current occurs; the effect of haloperidol, a dopamine receptor blocker; and the effect of amphetamine. The perfusate is analyzed for ascorbic acid (AA), the dopamine metabolites dihydroxyphenylacetic acid (DOPAC) and homovanillic acid (HVA), and the serotonin metabolite 5-hydroxyindoleacetic acid (5-HIAA). Using the relative response of these compounds at a carbon epoxy or carbon paste electrode, and the relative concentration of each in the extracellular fluid, the expected changes in oxidation currents for the three cases mentioned above are calculated. It is shown that the decline in oxidation current during the initial sampling period is due primarily to a decrease in ascorbic acid. It is also shown that different electroactive components of the extracellular fluid are the cause of changing oxidation currents under different stimulus conditions.

INTRODUCTION

Work in our laboratory is directed towards development and application of methods for in vivo chemical analysis of the central nervous system. One promising approach for monitoring extracellular neurochemistry in freely moving animals is voltammetry(1-8). There has been some confusion, however, concerning which compounds in the extracellular fluid contribute to the observed oxidation currents at small electrodes implanted in the brain(9). Adams and Marsden have recently reviewed in vivo electrochemical methods and have discussed the problems of interpretation of in vivo voltammetric data extensively(10). For voltammetric recording in the striatum the major concerns are the degree to which ascorbic acid(AA) contributes to the observed increases in oxidation currents following various stimuli and to what extent dopamine and its metabolites dihydroxyphenylacetic acid (DOPAC) and homovanillic acid (HVA) contribute to the increases. The extent that serotonin and its metabolite 5-hydroxyindoleacetic acid (5-HIAA) contribute to the oxidation current in the striatum has also been unclear. In addition, it is not clear whether it is always the same neurochemicals causing the increased currents or whether different stimuli (such as amphetamine, neuroleptics, electrical stimulation of the nigrostriatal pathway, feeding, etc.) cause different neurochemical changes which are indistinguishable in the voltammetric measurements. In order to resolve some of these

questions we began a series of experiments in which the extracellular fluid of the brain is sampled by dialyzed perfusion and analyzed by high performance liquid chromatography with electrochemical detection. The chromatographic results are discussed relative to voltammetric data obtained under similar conditions.

METHODS

Monitoring System

The on-line monitoring system for chromatographic analysis of dialyzed perfusate consists of the components illustrated in Figure 1. The system has two main parts: the perfusion components and the chromatographic components. These two parts connect at the HPLC injection valve. The perfusion components include a model 975 Harvard infusion pump which has been modified to perform simultaneous push-pull perfusion, a three channel fluid swivel (Alice King Chatham Medical Arts, Los Angeles, CA.) located at the top of the test chamber, and a dialysis cannula for perfusion of local brain regions. Two 2.5 ml Hamilton gas tight syringes are used in the infusion pump. These are fitted with three way valves for filling with solution and for removing air bubbles. Artificial cerebrospinal fluid (CSF) flows from the push syringe through the fluid swivel into the dialysis cannula. Low molecular weight components of the extracellular fluid from the surrounding region cross the dialysis membrane

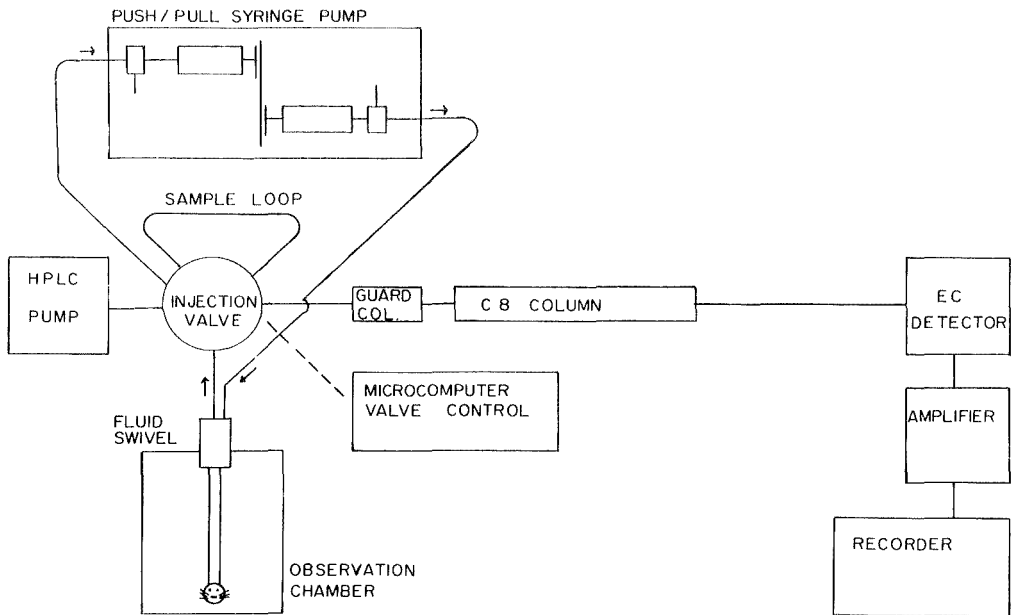


FIGURE 1. Monitoring system for chromatographic analysis of dialyzed perfusate. The pull side of the flow passes through the sample loop of the HPLC system.

and are carried to the sample loop as the flow leaves the cannula and passes through the fluid swivel to the injection valve (Rheodyne 7010). Model studies characterizing the performance of the dialysis cannula have been described previously(11).

Dialysis Cannula Construction

The dialysis cannula (Figure 2) is constructed from Spectrapor HF hollow fiber dialysis tubing with a molecular weight cutoff of 5000 amu and a diameter of 200 μm . To construct the device, the dialysis tubing is cut into 24 mm lengths and

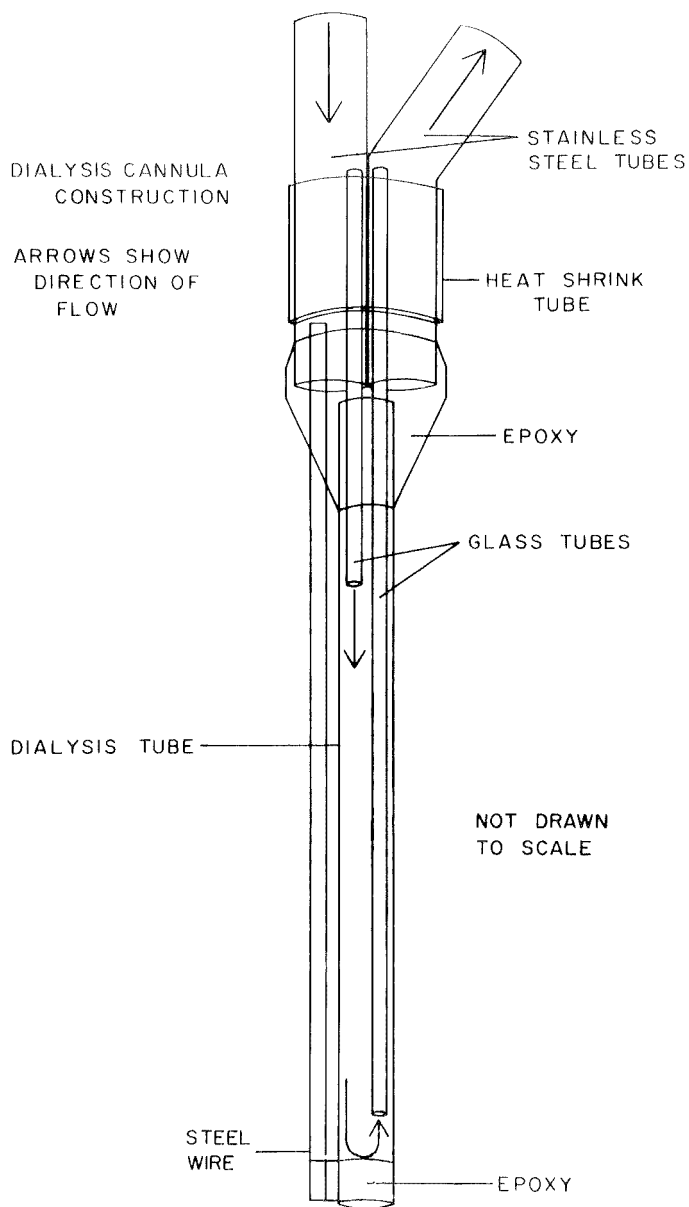


FIGURE 2. Details of the dialysis cannula. Diameter of the cannula is about 200 micrometers. The length depends upon the structure to be perfused. The six pin connector which surrounds the top of the cannula is not shown.

sealed at one end with a cyano-acrylate adhesive. Glass tubing of 2 mm diameter is then pulled over a flame to make glass capillaries of less than 100 μ m diameter. One length of this is inserted into the sealed dialysis tubing to approximately 0.5 mm from the sealed end. A second glass capillary is inserted to 6 mm above the end of the first. The two glass capillaries are then trimmed to extend about 7 mm from the open end of the dialysis tube. To connect the dialysis cannula to the flexible tubing coming from the fluid swivel at the top of the test chamber, 23 gauge stainless steel tubing is cut into two pieces approximately 15 mm in length. One tube is bent at a slight angle about 4 mm from one end to make attachment of the tubing from the swivel easier. The two tubes are then held together with 24 gauge heat-shrinkable teflon tubing, making sure that the bottom ends of the two tubes are flush with each other. The ends of the glass capillaries are then inserted into the flush ends of the stainless steel tubing. This junction is sealed with cyano-acrylate adhesive. In order to reinforce the rather flexible dialysis cannula, a length of fine (0.012 inch) wire 26 mm long is attached at the tip of the cannula and at the junction of the stainless steel tubes. To provide for secure attachment and accurate placement of the cannula, the dialysis cannula is mounted in the center of six pin male connector (Plastic Products, Roanoke, VA.) which has been drilled out in the center to hold the cannula. This connector mates with a six pin female

connector secured to the skull. The female connector contains a central 20 gauge stainless steel guide cannula 15.3 mm long which extends just below the dura.

Dialysis Perfusion Procedure

Male Sprague Dawley rats (Harlan Laboratories) are used in all experiments. Rats are implanted with a cannula guide described above using standard stereotaxic procedures. The lower end of the guide is placed at the following coordinates: AP 8.6, Lat 2.5, height 0.5 mm below dura(12).

After all instrumentation has been turned on and a steady chromatographic baseline achieved, standards of DOPAC, HVA, 5-HIAA (10 ng/100 ul) and AA (100 ng/100 ul) are injected for calibration. Peak heights of samples are compared to peak heights of standards for quantitation. After chromatography of the standards the syringes of the perfusion pump are filled with artificial CSF and the lines checked for air bubbles. The dialysis cannula, which has been previously checked for leaks, is attached to the two lines of the perfusion pump. Before the dialysis cannula is placed in the brain, the animal is lightly anaesthetized with ether to prevent breakage of the cannula during insertion. After the cannula has been inserted and locked in place, the perfusion pump is started at 4 ul/min. The first perfusate injection is made 40 minutes after the start of perfusion, by which time the animal has visibly recovered from

anesthesia. This also allows time for the perfusate to travel to and fill the sample loop. After the first injection, perfusate is injected every thirty minutes.

The first three hours of sampling are used to obtain a baseline. Subsequently, pharmacological or behavioral stimuli are introduced. For the pharmacological experiments, animals are either given the drug of interest or saline. The samples continue to be chromatographed every thirty minutes for the duration of the experiment. At the termination of the experiment, the push-pull lines are disconnected from the cannula, the dialysis cannula is gently removed and the animal is returned to its home cage. The dialysis cannula is examined and the system is cleaned with distilled water. Histology is subsequently done to verify cannula placement.

Chromatography

A Waters model 6000 solvent delivery system is used with a Rheodyne 7010 injection valve. A 100 ul sample loop is used for sample introduction. The detector is an LC-3 amperometric detector from Bioanalytical Systems with a glassy carbon working electrode set at a potential of +0.75 V vs. Ag/AgCl. Peak heights are measured on a Fisher Recordall 5000 strip chart recorder set at 1 V full scale for the neurotransmitter metabolites while the ascorbic acid peak height is measured on a McKee-Pederson recorder set at 10 V full scale.

The analytical column is a 4.6 mm by 25 cm stainless steel 10 μ m Zorbax C8 reverse phase column (DuPont, Wilmington, DE). The analyses are done at ambient temperature with isocratic elution using a 0.05 M phosphate buffer at pH 4.0, containing 3 percent methanol. The mobile phase is prepared by dissolving 6.9 grams sodium phosphate monobasic in 970 ml distilled water. Thirty ml of methanol are then added and the resulting solution is adjusted to pH 4 with 6N HCl. The eluent is filtered through a 0.45 μ m filter before use and is degassed vigorously with helium for approximately 15 minutes prior to use and slowly during the chromatography. The eluent flow rate is 1.6 ml/min.

MATERIALS

All chemicals were purchased from Aldrich (Milwaukee, WI) except for haloperidol (Haldol, MacNeil Laboratories) and d-amphetamine sulfate (Sigma).

Stock solutions of DOPAC, HVA and 5-HIAA were prepared in 0.01 M HCl containing 0.1 percent sodium metabisulfite as an antioxidant. Standard solutions (10 ng/100 μ l) were made from these stocks in artificial CSF on the day of the analysis. The ascorbic acid stock was made up fresh each day in artificial CSF at a concentration of 100 ng/ 100 μ l.

The artificial CSF was made by adding 7.46 g NaCl, 0.190 g KCl, 0.140 g CaCl_2 , and 0.189 g MgCl_2 to one liter distilled water, as described in (13).

RESULTS AND DISCUSSION

The system illustrated in Figure 1 was built to provide additional information to aid in the interpretation of in vivo voltammetric data. Several approaches to the problem of interpretation of voltammetric data obtained in brain tissue have been used, including differential pulse voltammetry and semidifferential pulse voltammetry(14,15,16). We have taken a different approach in which the extracellular fluid of the striatum is sampled for chromatographic analysis. This allows us to determine which electroactive compounds in the extracellular fluid of the striatum contribute to the changes in oxidation currents observed following the administration of various drugs and during certain behaviors such as feeding. The results reported here concern the initial period of sampling and the drugs amphetamine and haloperidol.

The dialysis/chromatography system illustrated in Figure 1 has several advantages for analysis of extracellular fluid. The chromatography is aided because the sample is prepurified of any protein which could degrade column performance. This allows elimination of protein precipitating agents which obscure early eluting compounds such as ascorbic acid. Removal of protein very early in the sampling process also eliminates enzymatic degradation of compounds in the perfusate. In addition, tissue damage is minimized because the fluid flow and associated turbulence are contained within the dialysis tube. Because slow

flow rates can be used, and the device has a relatively large surface area, recoveries are high. Dialyzed perfusion has been shown to be suitable for analysis of amino acids and for monitoring dopamine release in freely moving rats (17,18).

One of the main difficulties in the analysis, aside from the difficulty in obtaining samples, was finding chromatographic conditions which would resolve all the compounds of interest. While suitable conditions could be found for the neurotransmitter metabolites, ascorbic acid was obscured by protein precipitating agents such as perchloric acid which eluted in the solvent front. Conditions which were suitable for ascorbic acid (19) were inappropriate for the other compounds. Accordingly, in the initial studies on the effect of amphetamine, the sampled fluid was analyzed for ascorbic acid in one set of experiments (20) and for the neurotransmitters and metabolites in another series(21). Later, with the on-line analysis, it became possible to determine the compounds of interest with one set of chromatographic conditions, as illustrated in Figure 3. The on-line system meant that protein precipitants could be eliminated from the sample.

A consistent observation of in vivo voltammetry is the decline in oxidation current from the initial measurement to some steady state baseline after a series of measurements. Figure 4 illustrates this phenomena for four separate recordings from the same electrode every other day over an eight day period. These data were obtained using a one second chronoamperometric pulse of

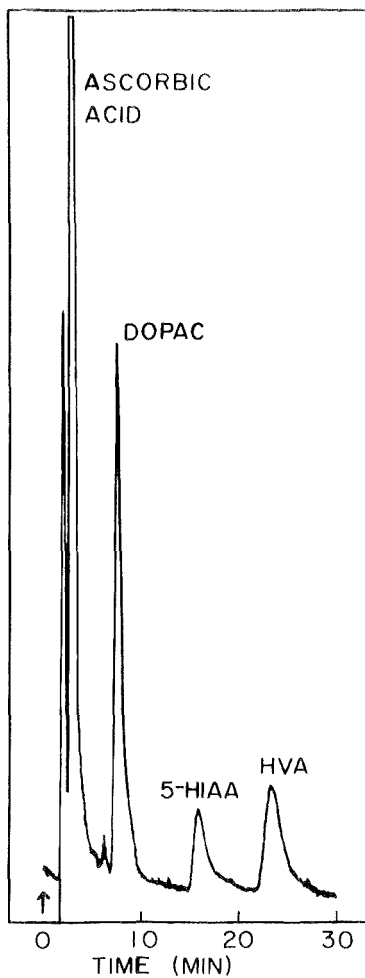


FIGURE 3. Chromatogram of dialyzed perfusate from anterior striatum. Working electrode potential at +0.75 V vs. Ag/AgCl. Mobile phase is pH 4.0 phosphate buffer with 3 percent methanol at a flow rate 1.6 ml/min. The stationary phase is 10 μ m Zorbax C8 reverse phase in a 4.6 mm by 25 cm stainless steel column.

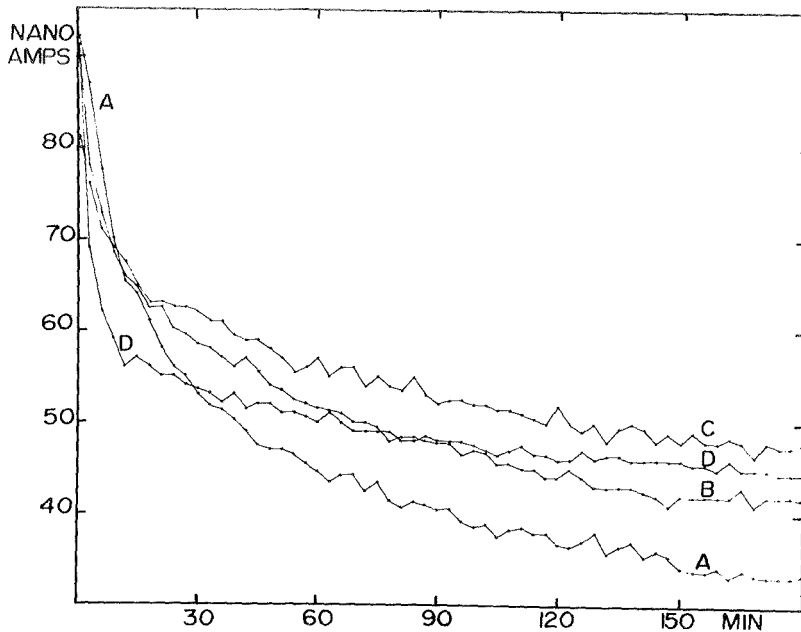


FIGURE 4. Chronoamperometric recordings from anterior striatum of unanesthetized, freely moving rat. Oxidation currents obtained at 100 μ m carbon epoxy electrodes using one second pulses of +0.6 V vs. Ag/AgCl at three minute intervals. Recordings obtained every other day in order A,B,C,D.

+0.6 V vs. Ag/AgCl every three minutes with a 100 μ m diameter carbon-epoxy electrode in the anterior striatum of a freely moving unanaesthetized rat. In each case the oxidation current became progressively smaller until a steady state was established. A model has been proposed to account for these observations(22) in which a small "pool" of extracellular fluid surrounds the electrode tip. As the oxidation at the electrode

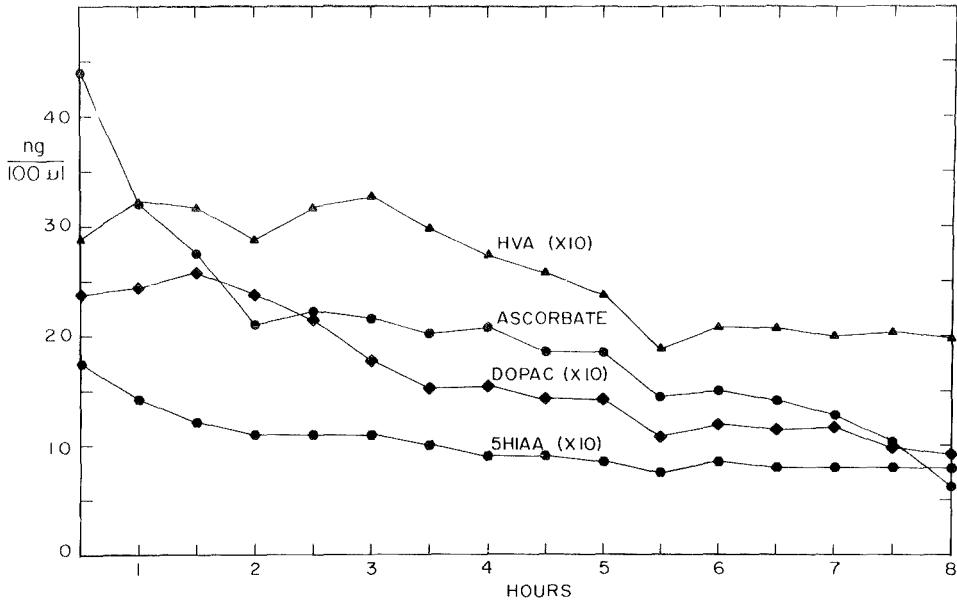


FIGURE 5. Time course of extracellular ascorbic acid, DOPAC, HVA, and 5-HIAA from anterior striatum of unanesthetized, freely moving rat. Samples obtained by dialysed perfusion at 4 μ l/min. The data are expressed per 100 μ l sample.

surface lowers the concentration in this pool, the current becomes progressively smaller and a concentration gradient is established with respect to the surrounding tissue. Eventually, as material flows into the pool as a result of the gradient, a steady state is reached in which consumption at the electrode surface is equalled by influx from the surrounding tissue. The model has been modified(23) to include differences in mass transfer rates for different molecular species. This latter model seems more appropriate as the data of Figure 5 suggest.

The data in this figure were collected during dialyzed perfusion of the anterior striatum of the rat as described in the methods section.

While dialyzed perfusion does not offer the sampling rate of voltammetry, it permits the resolution of the various electroactive components of the extracellular fluid. Thus Figure 5 illustrates the time course of extracellular levels of ascorbic acid, the dopamine metabolites DOPAC and HVA, and the serotonin metabolite 5-HIAA over an eight hour period from the start of perfusion for an N of seven. The interesting observation here is that ascorbic acid is behaving differently from the neurotransmitter metabolites. While the neurotransmitter metabolites appear to be unaffected by the perfusion, there is a considerable decrease in the initial ascorbic acid level to a steady state baseline. This implies that the extracellular level of ascorbic acid is more seriously affected by the sampling method. It may be that the neurotransmitter metabolites are part of a process with a high turnover rate relative to the rate of removal by voltammetry or perfusion and are therefore unaffected by the sampling process, while ascorbic acid has a much slower turnover rate so that the extracellular "pool" of ascorbic acid in the vicinity of the sampling device is apparently seriously affected by the sampling process. This interpretation of course requires additional data before it or any other interpretation can be said to explain the difference.

Using the relative concentrations of the electroactive species present in the extracellular fluid and their change over time, it is possible to predict the change in oxidation current of an electrode in response to changing extracellular concentrations. The additional information needed to calculate such a curve is the relative response of these compounds at a given electrode type. The general form of the equation for the relative oxidation current at time t is:

$$i(t) = \sum (\text{relative response} \times \text{relative concentration}(t))$$

for all compounds electroactive at the applied potential. For a carbon-epoxy electrode and a potential of +0.6 V vs. Ag/AgCl, this equation becomes:

$$i(t) = 0.40(\text{AA}(t)) + 1.0(\text{DOPAC}(t)) + 0.53(\text{HVA}(t)) + \\ 0.85(5\text{-HIAA}(t))$$

where $i(t)$ is the relative current rather than the absolute current, and the abbreviations in parentheses represent relative concentrations. The coefficients were determined by chronoamperometry of 1.0 mM solutions of each component in physiological saline (pH 7.4). To determine the relative concentrations, the nanograms of each component from each 100 μ l

sample were converted to a percent of the baseline for each component. These percentages are then multiplied by the baseline amount of the components to account for the quantities of the components relative to each other. Calculation of an absolute current would require absolute extracellular concentrations, the active area of the electrode and diffusion coefficients in the extracellular matrix.

A comparison of calculated and observed voltammetric data for the initial period of decreasing response is shown in Figure 6. The observed voltammetric data are the four curves of Figure 4, averaged and grouped into periods of fifteen minutes. The data for both the calculated and observed cases are expressed as a percent of the baseline obtained from the three points at the end of each curve. The agreement is surprisingly good given that two different sampling processes are being used. This agreement supports the suggestion that ascorbic acid is the principal source of the initial decline in oxidation current.

The dialysis/perfusion process is analogous to voltammetry in that material is removed, although the rates of removal and geometries are different. An additional difference is that the dialysis/perfusion process removes all compounds with a molecular weight less than the cutoff for the membrane, while the electrode removes only compounds oxidizing at the applied potential. A comparison of the two sampling processes may be made using the geometry and rate of removal for each process. A

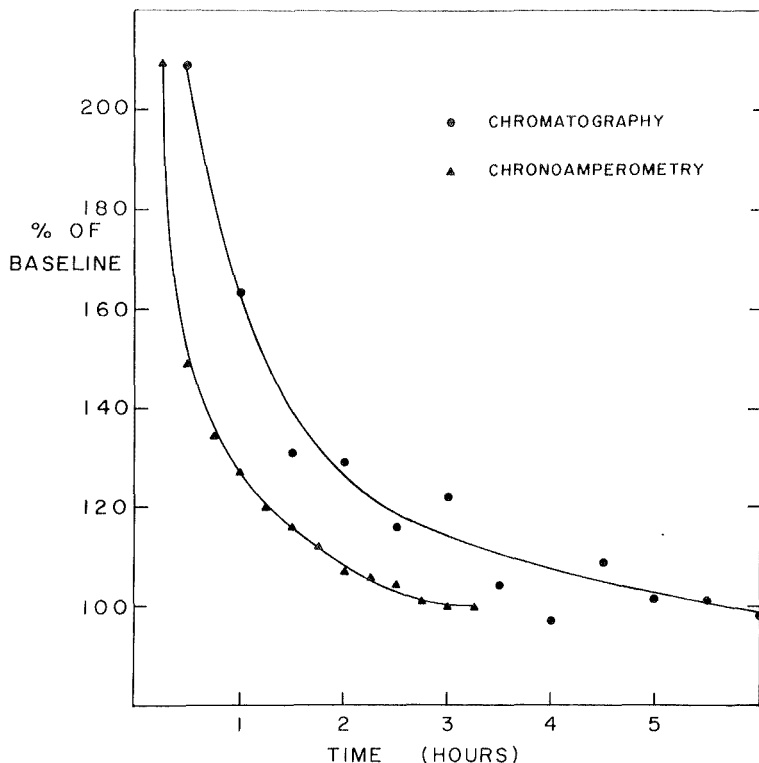


FIGURE 6. Comparison of calculated and observed change in oxidation current during initial period of voltammetry and perfusion. Data are expressed as a percent of the baseline for each curve.

100 μm diameter electrode has a geometric surface area of 0.0008 mm^2 while a dialysis cannula 4 mm long has an area of 2.5 mm^2 . The electrode of Figure 4 has about a 45 nA baseline current for one second chronoamperometry every three minutes. This corresponds to about 0.07 pmoles/min for a two electron oxidation, or $9 \text{ pmoles/min/mm}^2$. For the dialysis cannula, about $2 \text{ pmoles/min/mm}^2$ of ascorbic acid are being removed, with

correspondingly smaller amounts of the neurotransmitter metabolites. Thus the rate of removal per unit area is higher for the electrode than the dialysis cannula. These approximate calculations may help to explain why the observed voltammetric curve decreases more rapidly than the voltammetric curve calculated from the dialysis data.

A calculation similar to that for the initial decrease in current can also be done for the effect of drugs on extracellular levels of electroactive compounds. Haloperidol is a dopamine receptor blocker which leads to increased release of dopamine that in turn increases the level of dopamine metabolites. A 1.0 mg/kg dose i. p. generates the voltammetric curve shown in Figure 7. The data were obtained using chronoamperometry at +0.5 v vs. Ag/AgCl at a carbon paste electrode with one second pulses every one minute in the anterior striatum of anaesthetized rats. Previous work in this laboratory using dialyzed perfusion of the anterior striatum of unanaesthetized rats during a 1.0 mg/kg injection of haloperidol(i. p.) has demonstrated that the dopamine metabolites DOPAC and HVA increase by 226 percent as a result while ascorbic acid and the serotonin metabolite 5-HIAA do not increase(24). Dopamine and serotonin were not detectable under the conditions used and therefore probably does not contribute significantly to the change in oxidation current for this particular pharmacological treatment. The equation for the expected change in oxidation current is:

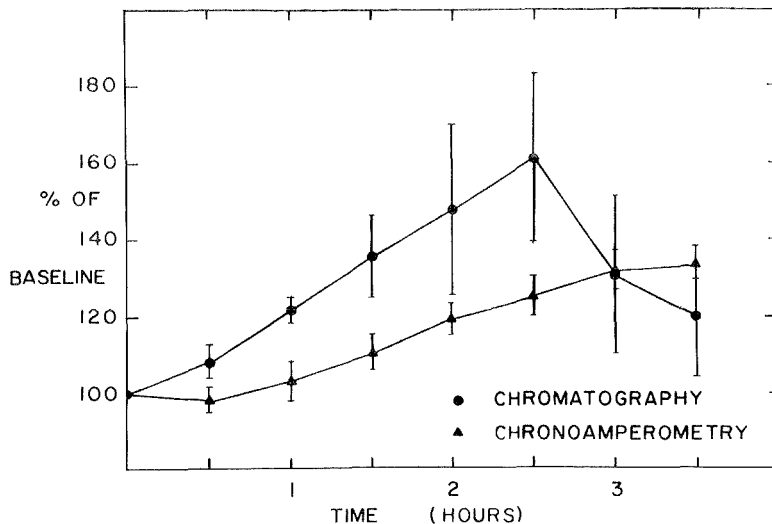


FIGURE 7. Comparison of calculated and observed change in oxidation current following administration(i.p.) of 1.0 mg/kg haloperidol. Three hour baseline preceded drug administration. Chronoamperometry performed with a carbon paste electrode, at +0.5 V vs. Ag/AgCl for one second at one minute intervals.

$$i(t) = 0.40(AA(t)) + 1.0(DOPAC(t)) + 0.24(HVA(t)) + 0.72(5-HIAA(t))$$

where the coefficients are based on chronoamperometry of 1.0 mM solutions of each compound in physiological saline with a carbon paste electrode at +0.5 V vs Ag/AgCl. The perfusion data of Blakely et al.(24), when used in the above equation yield the results of Figure 7. It can be seen that the calculated increase is greater than but similar to the observed increase. The lower increase for the observed voltammetric data may be due to the effect of the anaesthesia.

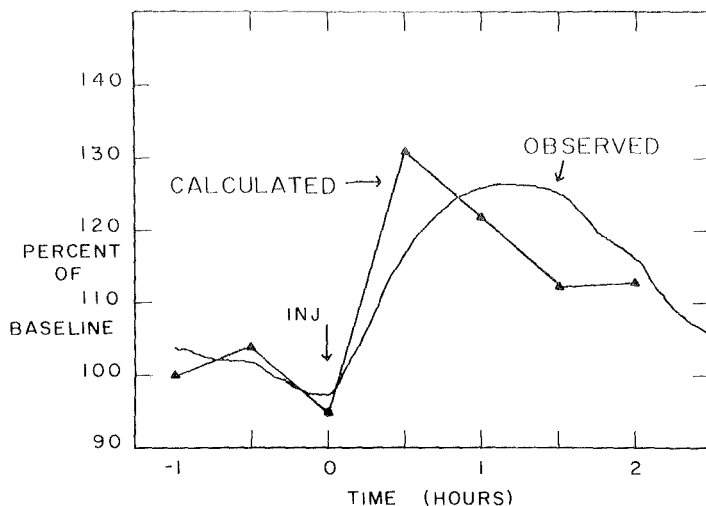


FIGURE 8. Comparison of calculated and observed change in oxidation current following i.p. administration of 1.0 mg/kg amphetamine. Data expressed as percent of baseline. Chronoamperometry done at +0.6 V vs. Ag/AgCl for 1 second at three minute intervals with a carbon-epoxy electrode. Chronoamperometric data collected for 3 hours before administration of 1 mg/Kg d-amphetamine sulfate. All data obtained in anterior striatum.

Amphetamine has been the source of considerable confusion with respect to the changes it causes in extracellular levels of electroactive compounds in the brain. The various voltammetric results have been reviewed by Adams and Marsden(10). Chromatographic data obtained previously with conventional push pull cannulae which demonstrated that amphetamine increases extracellular ascorbic acid in the striatum(20) and that it decreases extracellular DOPAC and HVA (21). A calculation of the expected change in oxidation current can be made from these data.

The results of this calculation are shown in Figure 8, where the calculated change from baseline is superimposed on the observed change in oxidation current. Because the push pull data were obtained from two separate cannulae (and therefore at possibly different exchange rates) and because 5-HIAA was not measured, it is, as with Samuel Johnson's dog, remarkable not that the data agree reasonably well, but that they agree at all. These data support the observations of Dayton et al.(16) and Gonon et al.(6,9).

These experiments demonstrate that different electroactive components of the extracellular fluid are contributing to alterations in the voltammetric signals under different stimulus conditions. They also indicate that in vivo voltammetry can be used to monitor these alterations if independent experiments to interpret the changes in the oxidation currents are conducted.

ACKNOWLEDGEMENTS

Funds from the Emory University Research Fund to JBJ and from the National Science Foundation to JBJ and DBN through Grant BNS-8210773 are gratefully acknowledged.

REFERENCES

1. Adams, R. N., In Vivo Electrochemical Recording--a New Neurophysiological Approach, Trends NeuroSci. 1, 160, 1978.
2. Lane, R. F., Hubbard, A. T., and Blaha, C. D., Brain Dopaminergic neurons: In Vivo Electrochemical Information Concerning Storage, Metabolism, and Release Processes, Bioelectrochem. Bioenerg. 5, 504, 1978.

3. Lane, R. F., Hubbard, A. T., and Blaha, C. D., Application of Semidifferential Electroanalysis to Studies of Neurotransmitters in the Central Nervous System, *J. Electroanal. Chem.*, 95, 117, 1979.
4. Ewing, A. G., Wightman, R. M., and Dayton, M. A., In Vivo Voltammetry with Electrodes that Discriminate between Dopamine and Ascorbate, *Brain Res.*, 249, 361, 1982.
5. Knott, P. J., Hutson, P. H., and Curson, G., Behavioral and Voltammetric Evidence for Serotonergic Inhibition of Caudate Dopamine Release, *Fed. Proc.*, 39, 1810, 1980.
6. Gonon, F., Buda, M., Cespuglio, R., Jouvét, M., and Pujol, J. -F., Voltammetry in the Striatum of Chronic Freely Moving Rats: Detection of Catechols and Ascorbic Acid, *Brain Res.*, 223, 69, 1981.
7. Lindsay, W. S., Herndon, J. G., Blakely, R. D., Justice, J. B., and Neill, D. B., Voltammetric Recording from Neostriatum of Behaving Rhesus Monkey, *Brain Res.*, 220, 391, 1981.
8. Salamone, J. D., Lindsay, W. S., Neill, D. B., and Justice, J. B., Behavioral Observation and Intracerebral Electrochemical Recording Following Administration of Amphetamine in Rats, *Pharmacol. Biochem. and Behav.*, 17, 445, 1982.
9. Gonon, F., Buda, M., Cespuglio, R., Jouvét, M., and Pujol, J. -F., In Vivo Electrochemical Detection of Catechols in the Neostriatum of Anaesthetized Rats: Dopamine or DOPAC? *Nature* 286, 902, 1980.
10. Adams, R. N., Marsden, C. A., Electrochemical Detection Methods for Monoamine Measurements In Vitro and In Vivo, *Handbook of Psychopharmacology*, 15, 1-74, ed. by L. L. Iverson, S. D. Iverson and S. H. Snyder, Plenum, 1982.
11. Johnson, R. D., and Justice, J. B., Model Studies for Brain Dialysis, *Brain Res. Bull.*, 10, 1983, in press.
12. Pellegrino, L. J. and Cushman, A. J., A Stereotaxic Atlas of the Rat Brain. New York, Appleton-Century-Crofts, 1967.
13. Myers, R. D., *Methods in Psychobiology*, vol II, ed. by R. D. Myers, 169-211, London, Academic Press, 1972.
14. Lane, R. F., Hubbard, A. T., Fukunaga, K., and Blanchard, R. J., Brain Catecholamines: Detection In Vivo by Means of Differential Pulse Voltammetry at Surface-Modified Platinum Electrodes, *Brain Res.* 114, 346, 1976.

15. O'Neill, R. D., Grunewald, R. A., Fillenz, M., and Albery, W. J., Linear Sweep Voltammetry with Carbon Paste Electrodes in the Rat Striatum, *Neuroscience*, 7, 1945, 1982.
16. Dayton, M. A., Ewing, A. G., and Wightman, R. M., Evaluation of Amphetamine Induced in Vivo Electrochemical Response, *Eur. J. Pharmacol.*, 75, 141, 1981.
17. Tossman, U. and Ungerstedt, U., Neuroleptic Action of Putative Amino Acid Neurotransmitters in the Brain Studied with a New Technique of Brain Dialysis. *Neurosci. Lett. Suppl.* 7, S479, 1981.
18. Zetterstrom, T., Herrera-Marschitz, M., and Ungerstedt, U., Simultaneous Estimation of Dopamine Release and Rotational Behaviour Induced by alpha-Amphetamine in 6-OH-DA Denervated Rats. *Neurosci. Lett. Suppl.* 7, S27, 1981.
19. Dozier, J. C., Salamone, J. D., Neill, D. B., and Justice, J. B., LCEC Determination of Extracellular Ascorbic Acid in Brain, *Curr. Sep.*, 4, 1, 1982.
20. Salamone, J. D., Neill, D. B., Hamby, L. M., and Justice, J. B., Release of Ascorbic Acid in Striatum Following Systemic Amphetamine, in prep.
21. Salamone, J. D., Saraswat, L. D., Neill, D. B., and Justice, J. B., Decrease in Endogenous Extracellular Striatal DOPAC and HVA Following Systemic Amphetamine, in prep.
22. Cheng, H. -Y., Schenk, J., Huff, R., and Adams, R. N., In Vivo Electrochemistry: Behavior of Microelectrodes in Brain Tissue, *J. Electroanal. Chem.* 100, 23, 1979.
23. Cheng, H. -Y., Compartment Model for Chronoamperometric Measurement in Vivo, *J. Electroanal. Chem.*, 135, 145, 1982.
24. Blakely, R. D., Wages, S. Justice, J. B., Neill, D. B., and Herndon, J., Effects of Haloperidol on Rat Striatal Levels of Ascorbic Acid and Biogenic Amines: HPLC Analysis of Dialyzed Perfusates, submitted, *Brain Res.*

HIGH PERFORMANCE LIQUID CHROMATOGRAPHIC
DETERMINATION OF PHENYLENEDIAMINES
IN AQUEOUS ENVIRONMENTAL SAMPLES

R. M. Riggin and C. C. Howard

Battelle, Columbus Laboratories
505 King Avenue
Columbus, Ohio 43201

ABSTRACT

The use of high performance liquid chromatography (HPLC) for the determination of phenylenediamines has been studied. Detection limits using both ultraviolet (UV) and electrochemical (EC) detectors have been determined and EC is superior in most cases. Chromatographic conditions and sample preparation procedures are described for many phenylenediamines of environmental significance.

INTRODUCTION

Diaminobenzenes (herein the term "phenylenediamines" will be used) are of considerable environmental significance because of the carcinogenic properties of many of these compounds (1). These compounds are currently in widespread use as industrial chemicals for the production of dyes and pigments as well as polyurethane resins. Consequently there is a great need for routine methods for determining these compounds in environmental media.

Unfortunately the highly reactive and nonvolatile nature of the phenylenediamines makes gas chromatographic (GC) determination difficult, although a few studies have used GC for the

determination of relatively high levels of certain phenylenediamines (2). HPLC is therefore the most suitable method for determining phenylenediamines and several studies have been reported (3-5). However, none of these studies have examined the separation, detection, and sample preparation parameters for determining a large number of phenylenediamines.

The objective of the study described herein was to establish suitable separation and detection parameters for the determination of as many phenylenediamines in commercial use as possible.

EQUIPMENT

All HPLC studies were performed using a modular system consisting of an Altex 100A pump, a Spherisorb ODS, 5 μ m particle diameter, 250 x 4.6 mm stainless steel column, and a Rheodyne 7120 injector valve. Two detection systems were used; (1) an LDC Model 1203 fixed wavelength (254 nm) UV detector and (2) a Bioanalytical Systems Model LC-2A electrochemical detector with a glassy carbon working electrode.

MATERIALS

All reagents were "analytical reagent" grade conforming with ACS specifications unless otherwise stated. Solvents were "distilled-in-glass" quality from Burdick and Jackson Laboratories. Analytical standards were the highest purity available and were checked for purity using HPLC.

Reagent water was obtained from a Mill-Q water purification system consisting of reverse osmosis, ion-exchange, and activated carbon treatment modules. HPLC mobile phases were filtered through a Nucleopore 0.22 μ m polyester membrane filter and degassed by heating in a loosely covered erlenmeyer flask before use. Strong cation exchange resin (AG 50W-x8) was purchased from Biorad Laboratories.

Sample Preparation Procedures

Two sample preparation approaches were employed for the determination of the full range of phenylenediamines. The first procedure involved solvent extraction of the water sample and was found to be suitable for most of the compounds of interest. However, the unsubstituted phenylenediamines (i.e. o-, m-, p-phenylenediamine) were not efficiently extracted and an alternate scheme involving ion-exchange isolation of the compounds was developed.

The solvent extraction scheme involved the following steps. An aliquot (500 mL) of the water sample was adjusted to pH 7 with 0.4 M Na_3PO_4 or 0.4 M phosphoric acid. The sample was then extracted serially with 100 mL, 50 mL, and 50 mL portions of methylene chloride. The extracts were combined and concentrated to ~1 mL on a Kuderna-Danish (K-D) evaporator. Four milliliters of acetonitrile was added to the extract followed by re-concentration to ~0.5 mL. The extract was then placed in a 25 mL volumetric flask, diluted to the mark with HPLC mobile phase, and analyzed by HPLC.

The ion-exchange sample preparation procedure was conducted as follows. One gram of AG 50-X8 (sodium form) was hydrated with 3 mL of reagent water. The resin was then transferred to a disposable plastic column and eluted with 15 mL of 0.05 M, pH 3, NaH_2PO_4 . The sample was adjusted to pH 3 with 2 M phosphoric acid and a 10 mL aliquot eluted through the ion-exchange column. The column was then rinsed with 5 mL of 0.05 M, pH 3, NaH_2PO_4 . Finally the compounds of interest were eluted using 10 mL of 30/70 methanol/pH 5.5, 0.5 M sodium acetate buffer. The eluate was then analyzed using HPLC.

RESULTS AND DISCUSSION

Comparison of UV and EC detection limits immediately demonstrated the superiority of EC for this application. Figure 1

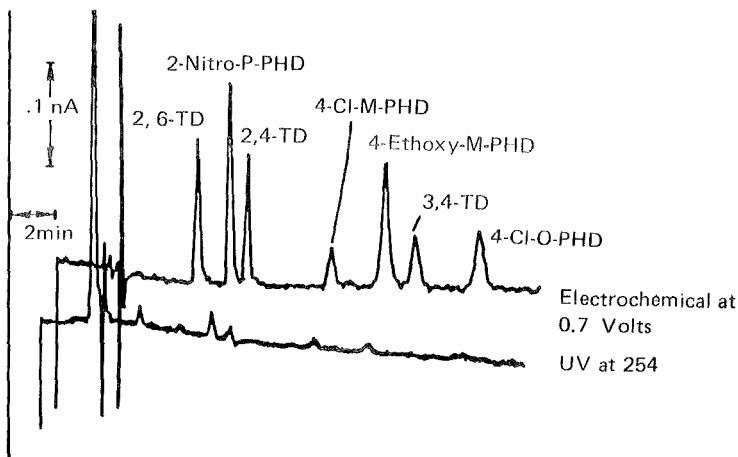


FIGURE 1. HPLC Separation of Various Phenylenediamines

Represents 0.8 ng on column for each PHD with the exception of 4-Cl-m-PHD 0.9 ng and 4-ethoxy-m-PHD (30 ng). See Table 1 for HPLC conditions.

graphically illustrates the 10-50 fold lower detection limit for EC compared to UV. Obviously the EC detector has the additional advantage of greater selectivity. The EC selectivity can be improved for selected compounds by reducing the detection potentials below that chosen for this study (700 mV). However, the nitro- and halogen-substituted compounds are not detected at lower potentials. Table 1 lists the retention and detection parameters for the various phenylenediamines of interest in this study. In general detection limits on the order of 0.2 nanograms injected were obtained for the various compounds. Most of the compounds of interest were chromatographically resolved although, as shown in Table 1, a few compound pairs (e.g. 2,5- and 2,6-toluenediamine) were not adequately resolved for simultaneous determination.

Recovery data for the groups of compounds determined by the two sample preparation procedures are shown in Tables 2 and 3.

TABLE 1

HPLC Retention Times and Detection Limits for Phenylenediamines

Compound	Retention Time (Min.) (a)	Estimated Detection Limit (Nanograms Injected) (b)
p-Phenylenediamine	4.8	0.2
m-Phenylenediamine	5.6	0.2
2,5-Toluenediamine	6.0	0.2
2,6-Toluenediamine	6.2	0.2
2-Methoxy-p-phenylenediamine	6.4	0.6
2-Nitro-p-phenylenediamine	7.8	0.2
2-Chloro-p-phenylenediamine	7.9	0.2
o-Phenylenediamine	8.2	0.2
4-Nitro-o-phenylenediamine	8.4	0.2
2,4-Toluenediamine	8.8	0.2
4-Methoxy-m-phenylenediamine	8.9	0.2
4-Chloro-m-phenylenediamine	12.1	0.7
4-Ethoxy-m-phenylenediamine	15.9	1.2
3,4-Toluenediamine	17.1	0.7
4-Chloro-o-phenylenediamine	18.4	0.6

- (a) HPLC conditions as follows: Column-Spherisorb ODS, 5 μ m particle diameter, 250 x 4.6 mm; Mobile phase - 30/70 methanol/0.1 M, pH 3.5, potassium phosphate with 0.01 M heptane sulfuric acid and 0.02 mM EDTA; Flow rate - 1 mL/min.; Injection Volume 20 μ L; Detector potential - +700 mV vs. Ag/AgCl.
- (b) Using electrochemical detection at 0.7 volts, and a signal to noise ratio of 5.

TABLE 2
 Recovery of Various Phenylenediamines from Aqueous Media Using
 Methylene Chloride Extraction(a)

	2,4- TD	2,5- TD	2,6- TD	3,4- TD	4-Cl-M- PHD	4-Cl-O- PHD	2-NITRO- P-PHD	4-NITRO- O-PHD
Reagent H ₂ O (% recovery)	71 ^(b)	29	65	68	79	87	89	64
Process Blank (ppb)	<3	<3	<2	<6	<5	<5	<2	<2
Wastewater (% recovery)	71	29	50	56	83	NA	NA	NA
Process Blank (ppb)	<2	<2	<1	<3	<2	--	--	--

(a) Aqueous media spiked at the 50 µg/L level.

(b) Average of duplicate analyses.

NA = Not analyzed

TD = Toluenediamine

PHD = Phenylenediamine

TABLE 3

Recovery of m,o,p-Phenylenediamine Spiked at
the 50 $\mu\text{g/L}$ Level from Aqueous Media Using
Ion Exchange Chromatography

	m-PHD	o-PHD	p-PHD
D. I. H ₂ O (% Recovery)	73 \pm 7.8 ^(a)	73 \pm 6.7	62 \pm 1.6
Process Blank (ppb)	<3	<3	<2
Wastewater (% Recovery)	45 \pm 8.3	55 \pm 1.7	46 \pm 3.2
Process Blank (ppb)	<2	<2	2

(a) Data for triplicate analyses.

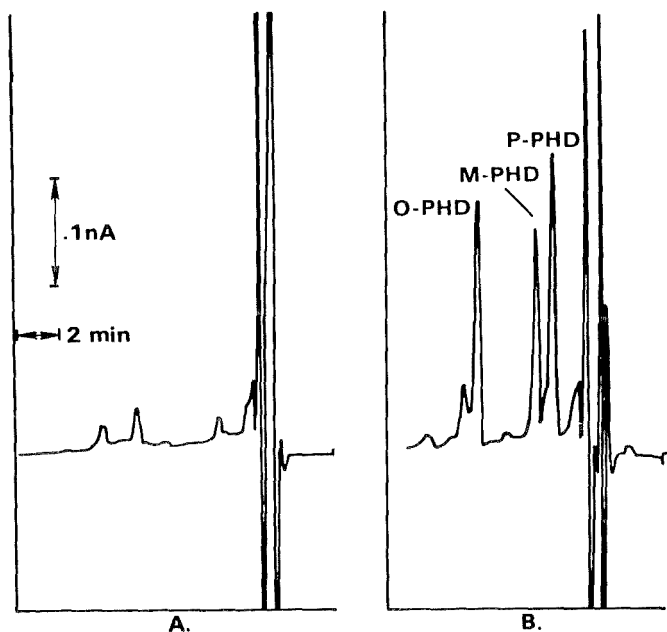


FIGURE 2. Chromatogram of Extracts of Wastewater (A) and of Wastewater Spiked at the 50 ppb Level With o, m, and p-Phenylenediamine (PHD)

As shown in these tables, recoveries were quite good for many of the compounds. However poor recovery (~30 percent) was obtained for 2,5-toluenediamine and only ~50 percent recoveries were obtained for the unsubstituted phenylenediamines from authentic wastewater samples. Figure 2 shows the HPLC separation of the three unsubstituted phenylenediamine isomers spiked into an authentic wastewater sample at the 50 µg/L level. The wastewater referred to in Tables 2 and 3 and Figure 2 is an industrial effluent, after secondary treatment, from a plant producing a variety of substituted aromatic amines.

CONCLUSIONS

While much work needs to be done to improve recoveries for some of the phenylenediamines, this study has demonstrated the clear advantage of using EC detection in conjunction with reversed phase, ion-pair HPLC for this application. Detection limits of a few µg/L were achieved for most of the phenylenediamines studied. This level of detectability is adequate for most environmental applications.

REFERENCES

1. Weisburger, E. K., Russfield, A. B., Homburger, F., Weisburger, J. H., Boger, E., Dougen, C., and Chu, K., Testing of Twenty-one Environmental Aromatic Amines or Derivatives for Long-Term Toxicity or Carcinogenicity. *J. Env. Path. Toxicol.* 2, 325, 1978.
2. Krasuska, E. and Celler, W., Gas Chromatographic Separation of Chloronitrobenzenes, Nitroanilines, and Phenylenediamines. *J. Chrom.* 147, 470, 1978.
3. Unger, P. D. and Friedman, M. A., High Performance Liquid Chromatography of 2,6- and 2,4-Diaminotoluene and its Application to the Determination of 2,4-Diaminotoluene in Urine and Plasma. *J. Chrom.* 174, 379, 1979.

4. Uchoytil, B., Thin-Layer and High Speed Liquid Chromatography of the Derivatives of 1,4-Phenylenediamine. J. Chrom. 93, 447, 1974.
5. Young, P. R. and McNair, H. M., High-Pressure Liquid Chromatography of Aromatic Amines. J. Chrom. 119, 569, 1976.

DUAL ELECTROCHEMICAL DETECTION
OF BIOGENIC AMINE METABOLITES
IN MICRO HIGH-PERFORMANCE LIQUID CHROMATOGRAPHY

Masashi Goto*, Eizo Sakurai and Daido ISHII
Department of Applied Chemistry, Faculty of Engineering,
Nagoya University, Chikusa-ku, Nagoya-shi 464, Japan

ABSTRACT

The dual electrochemical detectors for ordinary and micro high-performance liquid chromatography were briefly reviewed.

The electrochemical behaviors of biogenic amine metabolites were studied by cyclic semi-differential and semi-integral voltammetry with a glassy carbon working electrode. It was found that the electrochemical reactions of many biogenic amine metabolites are quasi-reversible. The dual electrochemical detector based on thin-layer electrolytic cell with two working electrodes (anode and cathode) in series configuration was tested for selective detection of biogenic amine metabolites on their electrochemical quasi-reversibility. The detector was successfully utilized for the simultaneous determination of 3, 4-dihydroxyphenylacetic acid, homovanillic acid and 5-hydroxyindole-3-acetic acid in human urine directly injected by micro high-performance liquid chromatography.

INTRODUCTION

Electrochemical detection in high-performance liquid chromatography (HPLC) has become very popular for the determination of trace amounts of organic substances in biomedical and environmental samples (1-3). An innovative

* Author for correspondence.

approach to electrochemical detection involves the use of two working electrodes operated simultaneously at different potentials. Several dual electrochemical detectors have recently been developed which provide for enhanced performance (4-21). They can basically be classified into the three types in configuration of the two working electrodes with respect to the flow axis, as shown in Figure 1. In the "parallel-adjacent" configuration, the working electrodes are placed adjacent to each other on one side of the rectangular thin-layer channel. In the "series" configuration, the working electrodes are positioned along the flow stream on one side of the channel. In the "parallel-opposed" configuration, the working electrodes are placed opposed to one another on both sides of the channel.

Dual electrochemical detection in HPLC

All dual electrochemical detectors can simultaneously provide two chromatograms of both oxidations or both reductions or oxidation and reduction by using the same or different material and size for each working electrode. Glassy carbon is most widely used as the material of working electrodes.

Parallel-adjacent type

The parallel-adjacent dual electrochemical detector (PADEC) is analogous to the dual-wavelength UV absorbance detector, and can provide useful qualitative information from peak current ratios at different potentials. By using PADEC, Roston and Kissinger performed the identification of phenolic constituents in commercial beverages and benzene metabolites by comparison with the standards (8, 16). Shoup and Mayer used PADEC for additional information on peak identity in determination of environmental phenols and biogenic amines and their metabolites (14, 18).

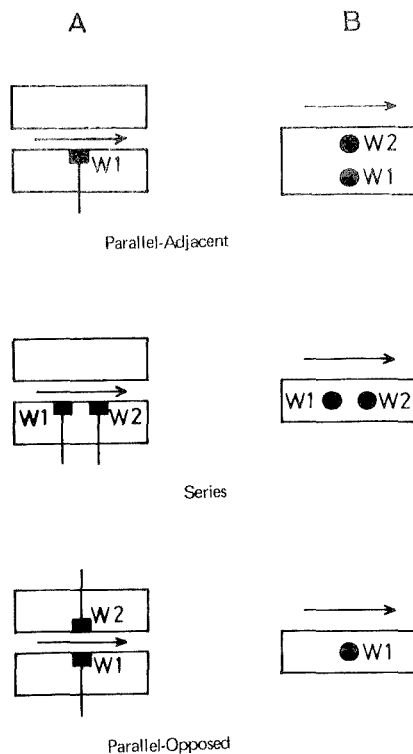


FIGURE 1. Three types in configuration of dual electrochemical detector. (A) Front view, (B) side view. W1 and W2 represent the two working electrodes. The arrows show the direction of flow.

Series type

The series dual electrochemical detector (SDEC) is analogous to the fluorescence detector, and the product of electrode reaction at the upstream working electrode is detected at the downstream working electrode. Blank employed SDEC for instrumental separation of compounds which overlap chromatographically, but have differing electrochemical formal potentials (4). Schieffer reported a series dual coulometric-amperometric detector (6). The upstream coulometric cell was held at lower

potential than the downstream amperometric cell to completely oxidize and make undetectable other species oxidizable at potentials lower than that of the analyte.

MacCrehan and Durst employed SDEC for the downstream oxidative detection of reduction products from the larger upstream mercury amalgam working electrode and demonstrated the detection of analytes with high redox potentials with good sensitivity and selectivity (7). Bratin and Kissinger used SDEC for elimination of oxygen interferences in reductive electrochemical detection (10). Allison and Shoup employed SDEC with mercury amalgam electrodes for simultaneous determination of thiols and disulfides in human blood and citrus leaf homogenate by using their catalytic oxidation of the mercury surface (19).

Roston and Kissinger employed SDEC for the downstream reductive detection of oxidation products from the upstream working electrode and estimated the collection efficiency, the magnitude of fraction of upstream products that are converted at the downstream working electrode, to be less than 0.37 (11). Mayer and Shoup used SDEC for assay of biogenic amines and their metabolites in brain tissue (18).

Parallel-opposed type

The parallel-opposed dual electrochemical detector (PODEC) is analogous to the photomultiplier tube and the product of the electrode reaction at one working electrode can diffuse to the opposite working electrode where starting material may be created. Fenn et al. explored the possibility of PODEC to improve detection limit of catecholamines in blood plasma at flow rates below 0.2 ml/min (5). Kurahashi used PODEC for selective detection of the analyte from peak current difference at different potentials (12). Inoue et al. employed PODEC to lower the background current (17). They applied the same potential to the two working electrodes and monitored the current from only one working electrode. Weber and

Purdy derived the theory concerned with the currents from a coulometric PODEC and approximately confirmed the theory by using a ferricyanide and ferrocyanide redox couple (15). They switched the working electrodes in and out of the current-to-voltage conversion circuit to defeat the large noise current generated by low cell impedance and obtained picogram detection limits for 2,4-toluenediamine in an aqueous methanol solvent.

Dual electrochemical detection in micro HPLC

Goto et al. developed a sub-microliter SDEC suitable for micro HPLC which was used for the downstream reductive detection of oxidation products from the upstream working electrode (9, 13). The detector was successfully utilized for the selective detection of catecholamines in human urine based on their electrochemical reversibility. We obtained the collection efficiencies of 0.68 to 0.78 for catecholamines at a flow rate of 8.3 $\mu\text{l}/\text{min}$. These values are much higher than those of 0.30 to 0.31 obtained in SDEC at a flow rate of 1.6 ml/min in the ordinary HPLC (18).

For slower flow rates, catalytic amplification of detector response for reversible and quasi-reversible analytes may be achieved by recycling the redox couple between the two working electrodes in PODEC. Goto et al. recently developed a coulometric PODEC with small working electrodes for micro HPLC (20, 21). The current amplification in the detector at flow rates of 1.4 to 11.2 $\mu\text{l}/\text{min}$ was investigated by using ferricyanide as analyte. The effective current amplification efficiency, the ratio of anodic (or cathodic) current to coulometric current for oxidant (or reductant), of 19.5 was observed for ferricyanide at the flow rate of 1.4 $\mu\text{l}/\text{min}$ (21). The collection efficiencies from 0.98 to 0.84 were obtained in the flow rate range from 1.4 to 11.2 $\mu\text{l}/\text{min}$ (21). The detector was successfully utilized for the selective and sensitive detection of catecholamines in human serum by micro HPLC (20, 21).

In the present paper, the electrochemical behaviors of biogenic aminemetabolites are investigated and their dual electrochemical detection with SDEC is tried for urine analysis by micro HPLC.

MATERIALS AND METHODS

Apparatus

A cyclic voltammetric instrument (Bioanalytical Systems Co., Model CV-1B) and a home-made analogue semi-differ-integrating circuit were used for cyclic semi-differential and semi-integral voltammetric measurements (22-25). Two x-y recorders (Yokogawa Co., Model 3086) were used to simultaneously record the cyclic semi-derivative and semi-integral voltammograms. A glassy carbon disk of 3 mm diameter was used as the working electrode. A silver/silver chloride electrode and a platinum wire were used for the reference and the counter electrode, respectively.

The micro HPLC system used is schematically shown in Figure 2. A micro feeder (Azuma Denki Co., Model MF-2), a micro syringe (Terumo Co., Model MS-CAN 100) and a three way valve were used to feed the mobile phase. A micro sample injector (Jasco, Model ML-422) with 0.3 μ l loop was used for sample injection. The twin-electrode thin-layer electrolytic cell in series configuration as shown in Figure 2 of the previous paper (9) was used for dual electrochemical detection. The thin-layer cavity was constructed of two fluoro-carbon resin blocks separated by a PTFE sheet 50 μ m thick and 2 mm wide. Two working electrodes were made with glassy carbon disks of 3 mm diameter contained in one of the blocks. The reference electrode, silver/silver chloride electrode, was held in a cylindrical hole in the other block. A platinum tube served both as the counter electrode and the exit line. A dual potentiostat (Nikko Keisoku Co., Model DPGS-2) was employed to control independently the potentials of the two working electrodes and to

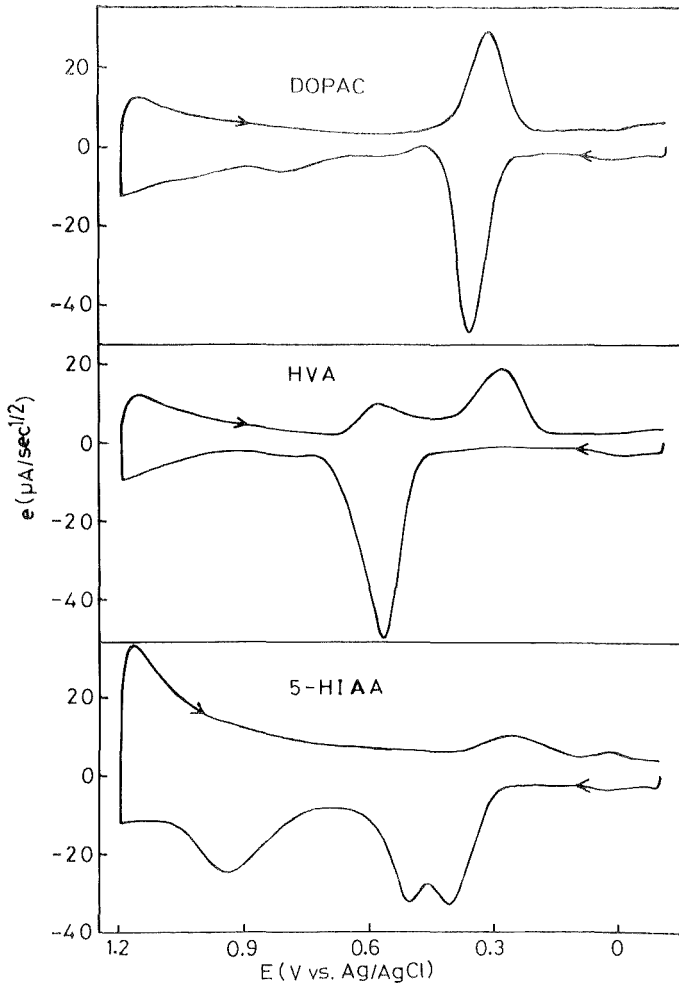


FIGURE 2. Block diagram of the micro HPLC system with series dual electrochemical detector. 1 = Micro feeder, 2 = micro syringe, 3 = three-way valve, 4 = mobile phase, 5 = micro sample injector (0.3 μl), 6 = micro guard column, 7 = micro separation column, 8 = series twin-electrode thin-layer electrolytic cell, 9 = dual potentiostat, 10 = dual pen recorder, 11 = waste.

measure the currents. The anodic and cathodic chromatograms were simultaneously recorded on a dual pen recorder (Yokogawa Co., Model 3056).

The micro guard column and micro separation column were made by packing ODS (Yanapak ODS, 10 μm) in a PTFE tube 2.0 cm x 0.5 mm i. d. and 16.5 cm x 0.5 mm i. d., respectively.

Chemicals

Analytical reagent grade chemicals were used without further purification. All solutions were prepared from distilled and deionized water. For standard samples, 3, 4-dihydroxyphenylacetic acid (DOPAC), vanillylmandelic acid (VMA), homovanillic acid (HVA), serotonin (5-HT) and 5-hydroxyindole-3-acetic acid (5-HIAA) were dissolved in Britton-Robinson (B-R) buffer of pH 1.8 to prepare the stock solutions. The mobile phase used for analysis was B-R buffer of pH 3.6 containing 10 % methanol, 50 mM sodium perchlorate and 0.1 mM EDTA (disodium salt).

Procedures of urine analysis

Typically only 0.3 μl of supernatant of raw human urine was injected into the micro HPLC system. The biogenic amine metabolites were separated at the flow rate of 8.3 $\mu\text{l}/\text{min}$. For dual electrochemical detection, the upstream working electrode was held at + 0.80 V (vs. Ag/AgCl) while the downstream working electrode was done at - 0.05 V. The quantitation was performed selectively by using the response of the downstream electrode.

RESULTS AND DISCUSSION

Electrochemical behaviors of biogenic amine metabolites

By means of the cyclic semi-differential and semi-integral voltammetry (22-25), the electrochemical behaviors of biogenic amine metabolites were studied in

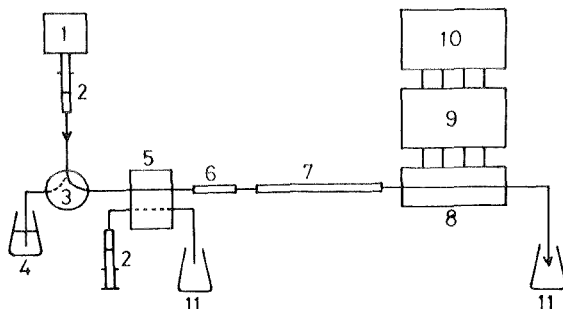


FIGURE 3. Cyclic semi-derivative voltammograms of 1.0 mM DOPAC, HVA and 5-HIAA in the B-R buffer of pH 3.6 containing 10 % methanol, 50 mM sodium perchlorate and 0.1 mM EDTA (disodium salt) at a scan rate of 100 mV/sec.

the mobile phase of micro HPLC, the B-R buffer of PH 3.6 containing 10 % methanol, 50 mM sodium perchlorate and 0.1 mM EDTA (disodium salt). Figure 3 shows the cyclic semi-derivative voltammograms, which are the semi-derivative of current, i , versus electrode potential, E , curves, for DOPAC, HVA and 5-HIAA. VMA and 5-HT showed the roughly similar cyclic semi-derivative voltammograms as HVA and 5-HIAA, respectively. All the species investigated showed oxidation and re-reduction peaks. It is interesting that three successive oxidation steps were observed for 5-HIAA, while only one oxidation step was substantially observed for DOPAC and HVA. On the other hand, two re-reduction steps were observed for HVA and 5-HIAA, while only one re-reduction step was observed for DOPAC. These facts indicate that the electrode reaction of DOPAC is nearly reversible, while those of HVA, VMA, 5-HIAA and 5-HT are quasi-reversible in this medium. For selective detection of biogenic amine metabolites, the potentials (vs. Ag/AgCl) of + 0.80 V and - 0.05 V were chosen as the suitable potentials of the upstream and down stream working electrode, respectively, from Figure 3.

Figure 4 shows the semi-integral voltammograms, the semi-integral of current, m , versus E curves, of 1.0 mM

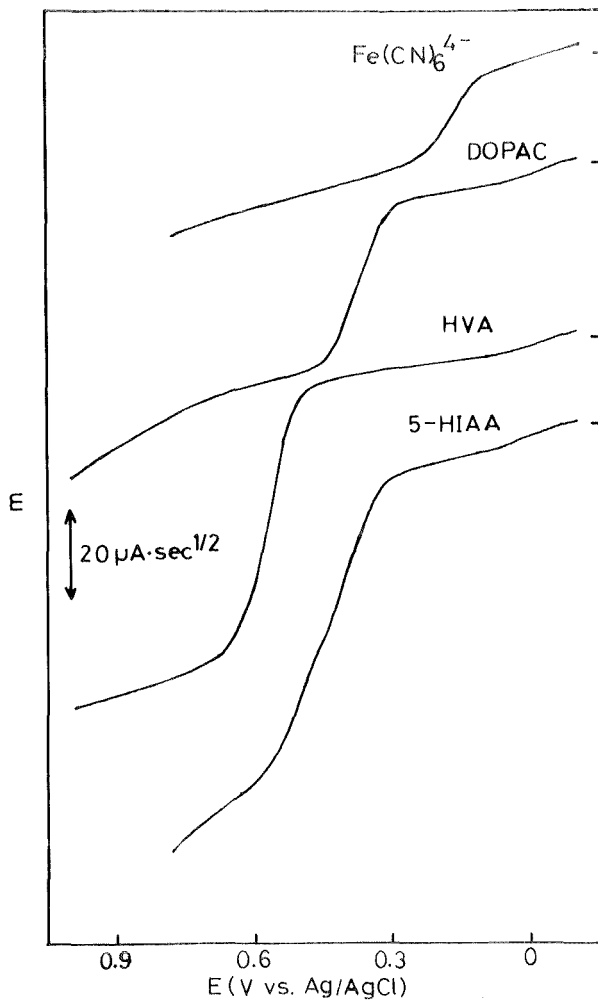


FIGURE 4. Semi-integral voltammograms of 1.0 mM $\text{Fe}(\text{CN})_6^{4-}$, DOPAC, HVA and 5-HIAA in the B-R buffer of pH 3.6 containing 10 % methanol, 50 mM sodium perchlorate and 0.1 mM EDTA (disodium salt) at a scan rate of 100 mV/sec.

each of biogenic amine metabolites and ferricyanide for anodic process. It is clear that the electron transfer number for each oxidation reaction at + 0.8 V is two for DOPAC, four for HVA and four for 5-HIAA, on comparison of their wave heights with that of ferricyanide, whose electrode reaction is one electron transfer, in the semi-integral voltammograms.

Chromatography and quantitation

The retention of biogenic amine metabolites in reversed-phase chromatography was investigated in order to attain a good separation. Figure 5 shows the effect of pH of the mobile phase on retention time. The retention of three biogenic amine metabolites investigated decreased with increasing pH, while that of 5-HT tended to increase with increasing pH. In this study, pH 3.6 was chosen as the suitable pH value of mobile phase for urine analysis.

Figure 6 shows typical chromatograms of a standard solution of VMA, 5-HT, DOPAC, 5-HIAA and HVA by the micro HPLC system with SDEC. Parts A and B are, respectively, the anodic and cathodic chromatograms. The peak separation is satisfactory, and both the anodic and cathodic peak currents were linear with the amounts of species injected, with correlation coefficients better than 0.99, as shown in Table 1. The detection limits ($S/N = 2$) of biogenic amine metabolites by this system were 10 pg for DOPAC, 20 pg for 5-HIAA and 20 pg for HVA, respectively, and the range of linearity was about 1000. The relative standard deviations for repetitive determination of 3 ng level by using the cathodic response in the system were 1.5 % for DOPAC, 1.8 % for 5-HIAA and 1.2 % for HVA, respectively.

The collection efficiencies in the system were found to be 0.61 for DOPAC, 0.20 for 5-HIAA and 0.30 for HVA, respectively, at the flow rate of 8.3 $\mu\text{l}/\text{min}$. It should be noted that these values are much larger than those of 0.31 for DOPAC, 0.05 for 5-HIAA and 0.05 for

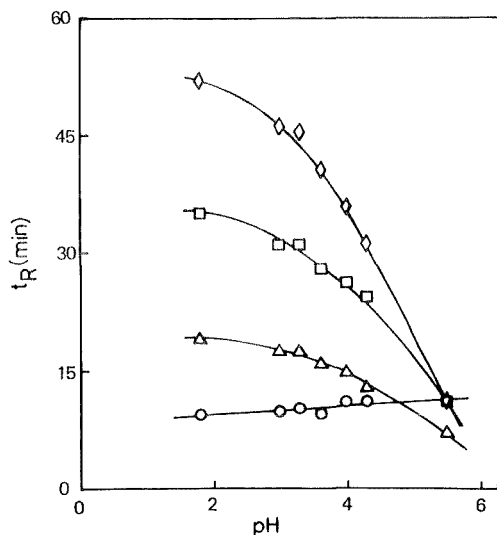


FIGURE 5. Effect of pH of the mobile phase on the retention time of 5-HT(O), DOPAC(Δ), 5-HIAA(\square) and HVA(\diamond). Mobile phase: B-R buffer containing 10 % methanol. Solid sodium hydroxide was used to get the desired pH. Flow rate of mobile phase: 8.3 μ l/min. Separation column: silica-ODS (16.5 cm x 0.5 mm i. d.).

TABLE 1

Relationship between Anodic and Cathodic Peak Height and Amount of Species Injected
 Potentials (V vs. Ag/AgCl): anode + 0.80, cathode - 0.05, flow rate of mobile phase: 8.3 μ l/min.

Species		Relationship*	Correlation coefficient
VMA	Anodic	$y = -11.00x - 0.96$	0.998
	Cathodic	$y = 0.76x + 0.37$	0.991
5-HT	Anodic	$y = -7.25x$	1.000
	Cathodic	$y = 1.08x + 0.07$	0.999
DOPAC	Anodic	$y = -7.49x - 0.05$	1.000
	Cathodic	$y = 4.53x + 0.23$	1.000
5-HIAA	Anodic	$y = -6.63x - 0.28$	0.999
	Cathodic	$y = 1.30x + 0.28$	0.998
HVA	Anodic	$y = -3.33x - 0.17$	0.999
	Cathodic	$y = 0.97x + 0.13$	0.999

* y = peak height measured in nA, x = amount of species measured in ng.

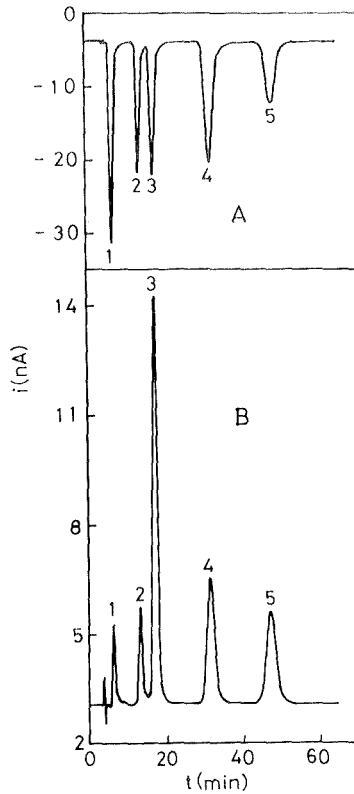


FIGURE 6. Typical chromatograms of a standard solution by the micro HPLC system with SDEC. (A) Anodic response, (B) cathodic response. Peaks: 1 = VMA, 2 = 5-HT, 3 = DOPAC, 4 = 5-HIAA, 5 = HVA. Potentials (V vs. Ag/AgCl): anode + 0.80, cathode - 0.05. Mobile phase: B-R buffer of pH 3.6 containing 10 % methanol, 50 mM sodium perchlorate and 0.1 mM EDTA (disodium salt). Flow rate of mobile phase: 8.3 μ l/min.

HVA, respectively, obtained in SDEC at the flow rate of 1.6 ml/min (18).

Selective detection of DOPAC, 5-HIAA and HVA in human urine

Typical chromatograms for the simultaneous determination of DOPAC, 5-HIAA and HVA in 0.3 μ l of human urine directly injected without any pretreatment in the micro HPLC

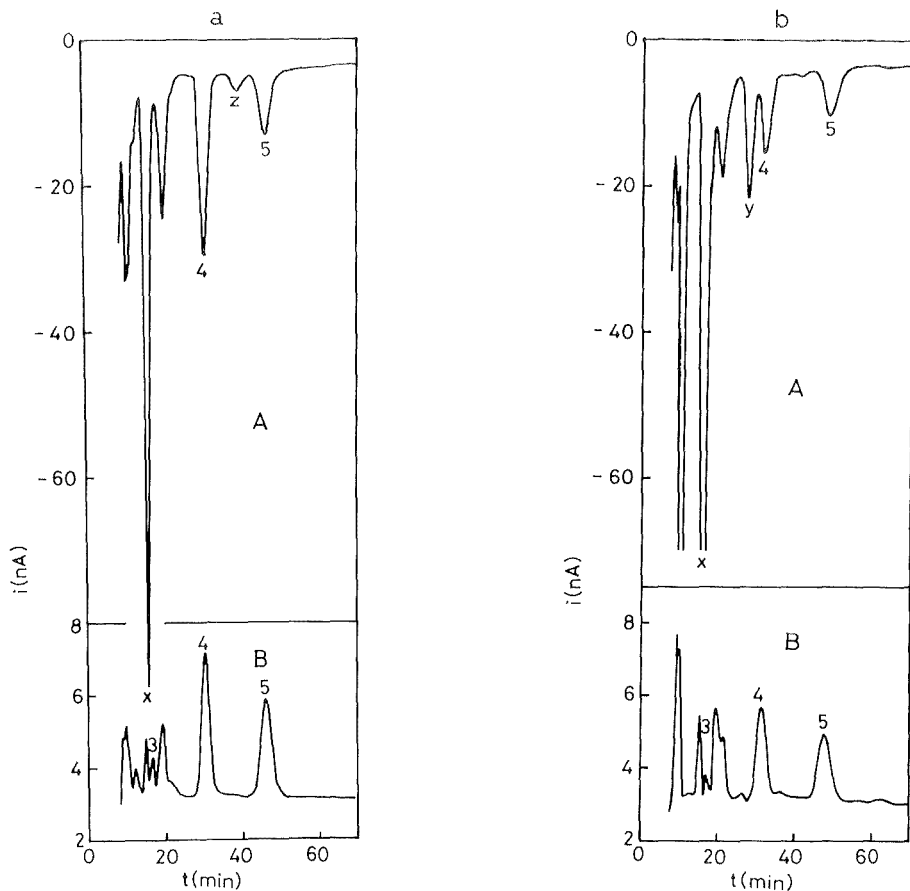


FIGURE 7. Chromatograms of directly injected urines from three healthy individuals to the micro HPLC system. (A) Anodic response, (B) cathodic response. Peaks: 3 = DOPAC, 4 = 5-HIAA, 5 = HVA. Potentials (V vs. Ag/AgCl): anode + 0.80, cathode -0.05. Sample: 0.3 μ l of human urine. Other conditions are the same as in FIGURE 6.

system are shown in Figure 7. Parts A and B are, respectively, the anodic and cathodic chromatograms. Figure 7 a, b and c correspond to the urine from three different healthy individuals, respectively. Peaks 3, 4 and 5 are due to DOPAC, 5-HIAA and HVA in urine, respectively. These were identified by the retention time and/or the peak current

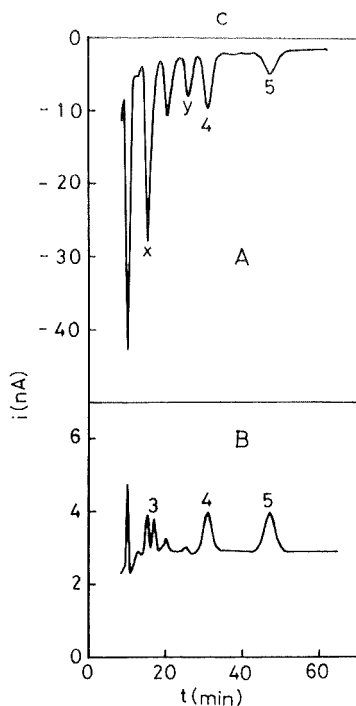


FIGURE 7C

TABLE 2

Analytical Results of DOPAC, 5-HIAA and HVA in Human Urine from Healthy Individuals

Sample number	Concentration ($\mu\text{g/ml}$)		
	DOPAC	5-HIAA	HVA
1	0.29	9.53	8.77
2	0.24	5.93	6.13
3	0.25	2.40	1.73
4	0.31	8.00	8.27
5	0.28	19.00	5.93
6	0.47	4.07	4.33
7	0.41	2.10	3.30

ratio of cathodic to anodic by comparing with the standards. Of particular interest is the peaks of x, y and z in parts A of Figure 7. By recording the cathodic response, it was shown that there were essentially no cathodic peaks corresponding to the anodic peaks of y and z, suggesting that the compound or compounds producing the anodic peaks are irreversibly oxidized. Since the main compounds responsible to the anodic peak of x were also irreversibly oxidized, DOPAC could be selectively detected on the cathodic chromatograms, as shown in part B in Figure 7.

Human urine from seven healthy individuals was analyzed from the linear regression equations in Table 1 using the cathodic chromatograms. The results are shown in Table 2. The concentrations for DOPAC, 5-HIAA and HVA in Table 2 are within the range of results reported in the literature for normal human urines (26-29).

The present system appears to be the first method which simultaneously determines DOPAC, 5-HIAA and HVA with reasonable precision in human urine directly injected without any pretreatment into the micro liquid chromatograph.

CONCLUSION

The series dual electrochemical detector with anode and cathode is a powerful tool for selective detection of reversible and/or quasi-reversible species for micro HPLC, because the collection efficiency increases with decreasing the flow rate of mobile phase. The parallel-opposed dual electrochemical detector with anode and cathode may provide an enhancement in sensitivity by recycling oxidation and re-reduction between the two working electrodes at slow flow rates of mobile phase. Thus the PODEC is the most advantageous type of detector for reversible and/or quasi-reversible species in micro HPLC (20, 21).

The simultaneous determination of DOPAC, 5-HIAA and HVA in healthy human urine could be performed on direct injection of only 0.3 μ l by using the micro HPLC system with SDEC.

REFERENCES

1. Kissinger, P. T., Amperometric and Coulometric Detectors for High Performance Liquid Chromatography, *Anal. Chem.*, 49, 447A, 1977.
2. Heineman, W. R. and Kissinger, P. T., Analytical Electrochemistry: Methodology and Applications of Dynamic Techniques, *Anal. Chem.*, 52, 138R, 1980.
3. Majors, R. E., Barth, H. G. and Lochmüller, Column Liquid Chromatography, *Anal. Chem.*, 54, 32R, 1982.
4. Blank, C. L., Dual Electrochemical Detector for Liquid Chromatography, *J. Chromatogr.*, 117, 35, 1976.
5. Fenn, R. J., Siggia, S. and Curran, D. J., Liquid Chromatography Detector Based on Single and Twin Electrode Thin-layer Electrochemistry: Application to the Determination of Catecholamines in Blood Plasma, *Anal. Chem.*, 50, 1067, 1978.
6. Schieffer, G. W., Dual Coulometric-Amperometric Cells for Increasing the Selectivity of Electrochemical Detection in High-Performance Liquid Chromatography, *Anal. Chem.*, 52, 1994, 1980.
7. MacCrehan, W. A. and Durst, R. A., Dual-Electrode, Liquid Chromatographic Detector for the Determination of Analytes with High Redox Potentials, *Anal. Chem.*, 53, 1700, 1981.
8. Roston, D. A. and Kissinger, P. T., Identification of Phenolic Constituents in Commercial Beverages by Liquid Chromatography with Electrochemical Detection, *Anal. Chem.*, 53, 1695, 1981.
9. Goto, M., Nakamura, T. and Ishii, D., Micro High-Performance Liquid Chromatographic System with Micro Precolumn and Dual Electrochemical Detector for Direct Injection Analysis of Catecholamines in Body Fluids, *J. Chromatogr.*, 226, 33, 1981.
10. Bratin, K. B. and Kissinger, P. T., Reductive LCEC of Organic Compounds, *J. Liq. Chromatogr. Suppl.*, 4, 321, 1981.
11. Roston, D., Kissinger, P.T., Series Dual-Electrode Detector for Liquid Chromatography/Electrochemistry, *Anal. Chem.*, 54, 429, 1982.
12. Kurahashi, T., Twin-Electrode Voltammetric Detector, *The Yanaco News*, 11, 8, 1982.
13. Goto, M., Sakurai, E. and Ishii, D., Dual Electrochemical Detector for Micro High-Performance Liquid

- Chromatography and Its Application to the Selective Detection of Catecholamines, *J. Chromatogr.*, 238, 357, 1982.
14. Shoup, R. E. and Mayer, G. S., Determination of Environmental Phenols by Liquid Chromatography/Electrochemistry, *Anal. Chem.*, 54, 1164, 1982.
 15. Weber, S. G. and Purdy, W. C., Electrochemical Detection with a Regenerative Flow Cell in Liquid Chromatography, *Anal. Chem.*, 54, 1757, 1982.
 16. Roston, D. A. and Kissinger, P. T., Isolation and Identification of Benzene Metabolites in Vitro with Liquid Chromatography/Electrochemistry, *Anal. Chem.*, 54, 1798, 1982.
 17. Inoue, K., Otake, T. and Kyogoku, K., High Sensitivity Analysis of D-Penicillamine in the Human Blood by Use of High-Performance Liquid Chromatography (HPLC) with Twin-Electrode Voltammetry Detector (T-VMD), *Yakugaku Zasshi*, 102, 1041, 1982.
 18. Mayer, G. S. and Shoup, R. E., Simultaneous Multiple Electrode Liquid Chromatographic-Electrochemical Assay for Catecholamines, Indoleamines and Metabolites in Brain Tissue, *J. Chromatogr.*, 225, 533, 1983.
 19. Allison, L. A. and Shoup, R. E., Dual Electrode Liquid Chromatography Detector for Thiols and Disulfides, *Anal. Chem.*, 55, 8, 1983.
 20. Goto, M., Zou, G. and Ishii, D., Determination of Catecholamines in Human Serum by Micro High-Performance Liquid Chromatographic System with Micro Precolumn and Dual Electrochemical Detector, *J. Chromatogr.*, in press.
 21. Goto, M., Zou, G. and Ishii, D., Current Amplification in Dual Electrochemical Detection for Micro High-Performance Liquid Chromatography, *J. Chromatogr.*, submitted.
 22. Goto, M. and Ishii, D., Semidifferential Electroanalysis, *J. Electroanal. Chem.*, 61, 361, 1975.
 23. Dalrymple-Alford, P., Goto, M. and Oldham, K. B., Peak Shapes in Semidifferential Electroanalysis, *Anal. Chem.*, 49, 1390, 1977.
 24. Grenness, M. and Oldham, K. B., Semiintegral Electroanalysis: Theory and Verification, *Anal. Chem.*, 44, 1121, 1972.
 25. Goto, M. and Oldham, K. B., Semiintegral Electroanalysis: Shapes of Neopolarograms, *Anal. Chem.*, 45, 2043, 1973.

26. Felice, L. J. and Kissinger, P. T., Determination of Homovanillic Acid in Urine by Liquid Chromatography with Electrochemical Detection, *Anal. Chem.*, 48, 794, 1976.
27. Mitchell, J. and Coscia, C. J., Application of Paired-Ion High-Pressure Liquid Column Chromatography to the Analysis of L-3, 4-Dihydroxyphenylalanine Metabolites, *J. Chromatogr.*, 145, 295, 1978.
28. Joseph, M. H., Kadam, B. V. and Risby, D., Simple High-Performance Liquid Chromatographic Method for the Concurrent Determination of the Amine Metabolites Vanillylmandelic Acid, 3-Methoxy-4-Hydroxyphenylglycol, 5-Hydroxyindoleacetic Acid, Dihydroxyphenylacetic Acid and Homovanillic Acid in Urine Using Electrochemical Detection, *J. Chromatogr.*, 226, 361, 1981.
29. Yoshida, A., Yoshioka, M., Sakai, T. and Tamura, Z., Simple Method for the Determination of Homovanillic Acid and Vanillylmandelic Acid in Urine by High-Performance Liquid Chromatography, *J. Chromatogr.*, 227, 162, 1982.

LC NEWS

GPC COLUMNS FOR POLYMER ANALYSIS & TESTING offer ultra-resolution at low cost and high speed for detection of subtle differences between polymer samples that can significantly influence polymer processability. The columns are available in 500, 1,000, 10,000, and 100,000 angstroms nominal exclusion as well as a mixed-bed column that provides resolution from 100 Daltons to well over 20 million. They are available packed in any of several commonly used GPC solvents and in many polymer solvents not generally available with GPC columns. Jordi Associates, Inc., JLC/83/10, 397 Village Street, Millis, MA, 02054, USA.

EC/LC FLOW CELL FOR AMPEROMETRIC DETECTION features negligible dead volume, minimum IR drop, improved detection limit, and better peak shape. IBM Instruments, Inc., JLC/83/10, Orchard Park, Box 332, Danbury, CT, 06810, USA.

CELL DEBRIS REMOVER is a modified cellulose formulated to remove contaminants from crude animal, microbial, or plant extracts. It binds cell debris, nucleic acids, polar lipids, many colorants, and other unwanted components more effectively than standard filtration and centrifugation techniques. It provides clarified protein solutions with lower viscosities, while improving column life. Whatman, Inc., JLC/83/10, 9 Bridewell Place, Clifton, NJ, 07014, USA.

DETERMINATION OF GOLD in gold plating baths by ion chromatography also includes speciation between Au(1+) and Au(3+). This is important, as an increase in Au(3+) content can lower plating efficiencies. Dionex Corp., JLC/83/10, 1228 Titan Way, Sunnyvale, CA, 94086, USA.

AUTOMATED GRADIENT CONTROLLER allows automatic control of external accessories such as valves and fraction collectors for sensitivity, selectivity and speed; isocratic to ternary compositional and flow control of up to 3 solvent delivery systems. A CRT display is used to guide the operator thru setup and operation. Up to ten methods may be stored for instant recall. Waters Associates, Inc., JLC/83/10, 34 Maple Street, Milford, MA, 01757, USA.

THIN-LAYER CELL FOR ELECTROCHEMICAL DETECTION allows placement of the auxilliary electrode both downstream and across from the working electrode. A highly polished stainless steel top extends cell life, permits compatibility with new "high speed" columns, and allows for connection of low dead volume fittings for use with micro columns. Bioanalytical Systems, Inc., JLC/83/10, 1205 Kent Avenue, Purdue Research Park, West Lafayette, IN, 47906, USA.

LIQUID PROCESSING UNIT can be used to feed most analytical instruments. It performs all of the crucial sample pickup, mixing and dispensing operations. A pair of syringes whose plungers are driven by a stepper motor and precision ball lead screws, a mixing chamber, and a hand-held control unit are the principal working parts. A computer program directs all operations. Processing parameters such as time, volume, ratios, and increments are entered thru the control unit and become a part of an individual routine program. Hamilton Company, JLC/83/10, P. O. Box 10030, Reno, NV, 89510, USA.

BINARY GRADIENT HPLC CAPABILITIES include easy setting of flow rate, initial and final solvent composition, and times for equilibration, gradient, and hold steps directly from the front panel. The controller also includes the necessary connections for automated operation with many auto samplers and data handling devices. Perkin-Elmer Corp., JLC/83/10, Main Avenue, Mail Station 12, Norwalk, CT, 06856, USA.

PROGRAMMABLE UV-VIS DETECTOR FOR HPLC may be optionally equipped with fast scanning and wavelength capabilities. It is capable of wavelength speeds up to 100 nm per second. The system is microprocessor-based and accessed via an HP-41 programmable calculator. Automatic baseline zero is featured for offsetting wavelength-induced baseline shift. Kratos Analytical Instruments, Inc., JLC/83/10, 170 Williams Drive, Ramsey, NJ, 07446, USA.

PNEUMATIC CLAMPING SYSTEM is for use with HPLC columns and cartridges. No-fault connections ensure consistent results. Columns are added or removed easily by relatively untrained operators without altering analytical integrity. They are useful to 5000 psi. EM Science, Inc., 480 Democrat Rd., Gibbstown, NJ, 08027, USA.

PUMP PRIMING VALVE is designed to simplify purging of HPLC pumps when change of solvent is made. When fitted between pump and injector, it permits new solvent to be purged through the pump to waste via a drain tube. Only half a turn is required to open the valve fully. Negretti & Zambra (Aviation), Ltd., JLC/83/10, The Airport, Southampton, SO9 3FR, Hampshire, England.

UNIVERSAL HPLC SOLVENT CLARIFICATION MEMBRANE accomplishes filtration of all commonly used HPLC solvents. The membranes have

an extensive range of chemical compatibility, are hydrophilic, and do not require a pre-wetting step. They also exhibit an extremely low extractables content, thereby eliminating concern of contamination from the membrane. Millipore Corp., JLC/83/10, 80 Ashby Road, Bedford, MA, 01730, USA.

HPLC FILTER is made of a new fluoropolymer membrane and is housed in solvent resistant polypropylene. It is pressure rated at 75 psi and is available in a 0.45 micron pore size. Gelman Sciences, Inc., JLC/83/10, 600 S. Wagner Rd., Ann Arbor, MI, 48106, USA.

FLAME IONIZATION DETECTOR FOR LC is said to overcome general limitations of prior "universal" LC detectors. A rotating disc, "ringed" by a fibrous quartz belt, conducts samples to a dual-flame ionization detector for analysis. Volatile solvent is vaporized and removed by vacuum. Solutes are carried into the FID, and residual sample is then removed by hotter hydrogen/oxygen cleaning flames. Tracor Instruments, JLC/83/10, 6500 Tracor Lane, Austin, TX, 78721, USA.

HPLC REAGENTS & COLUMNS are described in a new brochure. Included are buffers, ion pair reagents, derivatizing reagents, hardware, and solvents. Fisher Scientific Co., JLC/83/10, 711 Forbes Ave., Pittsburgh, PA, 15219, USA.

LAB AUTOMATION SYSTEM FOR SAMPLE PREPARATION combines robotics and lab stations to automate procedures. The controller interfaces the operator with the robot. Software is menu-based and uses familiar laboratory terms. Zymark Corp., JLC/83/10, Zymark Center, Hopkinton, MA, 01748, USA.

APPLICATIONS GUIDE deals with sample preparation, highlighting background, principles, and techniques of solid phase extraction. The guide contains over 40 detailed procedures for preparing environmental, pharmaceutical, biological, food, and cosmetic samples, such as priority pollutants, crude oil, trace metals, aflatoxins, steroids, etc. J. T. Baker Chem. Co., JLC/83/10, 222 Red School Lane, Phillipsburg, NJ, 08865, USA.

HPTLC/TLC BIBLIOGRAPHY SERVICE is available free of charge. Publications may be included by mailing to the publisher. Applied Analytical Industries, Inc., JLC/83/10, Route 6, Box 55, Wilmington, NC, 28405, USA.

DETERGENT REMOVING GEL is an affinity chromatographic support that selectively removes detergents from protein solutions, with proteins being recovered in virtually 100% yields. The support can be regenerated for repeated use. Pierce Chemical Co., JLC/83/10 P. O. Box 117, Rockford, IL, 61105, USA.

LC CALENDAR

1983

AUGUST 10-12: 22nd Canadian High Polymer Forum, Univ. of Waterloo, Canada. Contact: A. Garton, NRC of Canada, Div. of Chem., Ottawa, Ont., Canada, K1A 0R6.

AUGUST 14-19: 25th Rocky Mountain Conference, Denver Convention Complex, Denver, Colorado. Contact: E. A. Brovsky, Rockwell International, P. O. Box 464, Golden, CO, 80401, USA.

AUGUST 15-19: Coal Science: 1983 Int'l Conference, Pittsburgh, PA. Contact: N. Maceil, JWK Int'l Corp., 275 Curry Hollow Road, Pittsburgh, PA, 15236, USA.

AUGUST 22-26: 7th Australian Symposium on Analytical Chemistry, Adelaide, Australia. Contact: D. Patterson, AMDEL, P.O.Box 114, Eastwood S.A. 5063, Australia.

AUGUST 26 - SEPTEMBER 2: Int'l. Symp. on Solvent Extraction, Denver, CO. Contact: D. Nowak, AIChE, 345 E. 47th St., New York NY, 10017, USA.

AUGUST 28 - SEPTEMBER 2: 11th World Petroleum Congress, London. Contact: Amer. Petrol. Inst., 2101 L St., N.W., Washington, DC, 20037, USA.

AUGUST 28 - SEPTEMBER 2: ACS 186th Nat'l Meeting, Washington, DC. Contact: A. T. Winstead, ACS, 1155 16th St., NW, Washington, DC, 20036, USA.

AUGUST 29 - SEPTEMBER 2: 4th Danube Symposium on Chromatography & 7th Int'l. Sympos. on Advances & Applications of Chromatography in Industry, Bratislava, Czech. Contact: Dr. J. Remen, Anal. Sect., Czech. Scientific & Technical Soc., Slovnaft, 823 00 Bratislava, Czechoslovakia.

SEPTEMBER 22-23: Symposium: "Columns in High Performance Liquid Chromatography," Lady Mitchell Hall, University of Cambridge. Contact: A. G. W. Mulders, Hewlett-Packard, GmbH, Postfach 1280, D-7517 Waldbronn 2, West Germany.

SEPTEMBER 25-30: Federation of Anal. Chem. & Spectroscopy Societies (FACSS) Conf., Franklin Plaza Hotel, Philadelphia. Contact: M. O'Brien, Merck, Sharp & Dohme Res. Labs., West Point, PA, 19486, USA.

OCTOBER 2-6: 97th Annual AOAC Meeting, Shoreham Hotel, Washington, DC. Contact: K. Fominaya, AOAC, 1111 N. 19th St., Suite 210, Arlington, VA, 22209, USA.

OCTOBER 3-5: Chemexpo '83, Harbor Castle Hilton Hotel, Toronto, Ont., Canada. Contact: ITS Canada, 20 Butterick Rd., Toronto, Ont., Canada, M8W 3Z8.

OCTOBER 3 - 6: Advances in Chromatography: 20th Int'l Symposium, Amsterdam, The Netherlands. Contact: A. Zlatkis, Chem. Dept., University of Houston, Houston, TX, 77004, USA.

OCTOBER 12-13: 8th Annual Baton Rouge Anal. Instrum. Disc. Grp. Sympos., Baton Rouge, LA. Contact: G. Lash, P. O. Box 14233, Baton Rouge, LA, 70898, USA.

OCTOBER 12-14: Analyticon'83 - Conference for Analytical Science, sponsored by the Royal Society of Chemistry and the Scientific Instrument Manufacturers' Ass'n of Great Britain, Barbican Centre, London. Contact: G. C. Young, SIMA, Leicester House, 8 Leicester Street, London WC2H 7BN, England.

NOVEMBER 3-4 ACS 18th Midwest Regional Meeting, Lawrence, Kansas. Contact: W. Grindstaff, SW Missouri State Univ., Springfield, MO, 65802, USA.

NOVEMBER 9-11: ACS 34th SE Regional Meeting, Charlotte, NC. Contact: J. M. Fredericksen, Chem. Dept., Davidson College, Davidson, NC, 28036, USA.

NOVEMBER 10-11: Electrofocusing and Electrophoresis Workshop, Birmingham, AL, USA. Contact: Workshop Registrar, LKB Instruments, Inc., 9319 Gaither Rd., Gaithersburg, MD, 20877, USA.

NOVEMBER 14-16: 3rd Int'l. Sympos. on HPLC of Proteins, Peptides and Polynucleotides, Monte Carlo, Monaco. Contact: S. E. Schlessinger, 400 East Randolph, Chicago, IL, 60601, USA.

NOVEMBER 16-18: Eastern Analytical Symposium, New York Statler Hotel, New York City. Contact: S. David Klein, Merck & Co., P. O. Box 2000, Rahway, NJ, 07065, USA.

NOVEMBER 22-23: Short Course: "Sample Handling in Liquid Chromatography," sponsored by the Int'l. Assoc. of Environmental and Biological Samples in Chromatography, Palais de Beaulieu, Lausanne, Switzerland. Contact: Dr. A. Donzel, Workshop Office, Case Postale 130, CH-1000 Lausanne 20, Switzerland.

NOVEMBER 24-25: Workshop: "Handling of Environmental and Biological Samples in Chromatography," sponsored by the Int'l. Assoc. of Environmental Anal. Chem., Palais de Beaulieu, Lausanne, Switzerland. Contact: Dr. A. Donzel, Workshop Office, Case Postale 130, CH-1000 Lausanne 20, Switzerland.

NOVEMBER 29-30: Electrofocusing and Electrophoresis Workshop, San Francisco, CA, USA. Contact: Workshop Registrar, LKB Instruments, Inc., 9319 Gaither Road, Gaithersburg, MD, 20877, USA.

DECEMBER 6-7 and 8-9: Electrofocusing and Electrophoresis Workshop, Los Angeles, CA, USA. Contact: Workshop Registrar, LKB Instruments, Inc., 9319 Gaither Road, Gaithersburg, MD, 20877, USA.

1984

FEBRUARY 12-16: 14th Australian Polymer Symposium, Old Ballarat Travel Inn, Ballarat, Australia, sponsored by the Polymer Div., Royal Australian Chemical Inst. Contact: Dr. G. B. Guise, RACI Polymer Div., P. O. Box 224, Belmont, Victoria 3216, Australia.

APRIL 8-13: National ACS Meeting, St. Louis, MO. Contact: Meetings, ACS, 1155 16th Street, NW, Washington, DC, 20036, USA.

MAY 20 - 26: 8th Intl. Symposium on Column Liquid Chromatography, New York Statler Hotel, New York City. Contact: Prof. Cs. Horvath, Yale University, Dept. of Chem. Eng., P. O. Box 2159, Yale Stn., New Haven, CT, 06520, USA.

JUNE 18-21: Symposium on Liquid Chromatography in the Biological Sciences, Ronneby, Sweden, sponsored by The Swedish Academy of Pharmaceutical Sciences. Contact: Swedish Academy of Pharmaceutical Sciences, P. O. Box 1136, S-111 81 Stockholm, Sweden.

AUGUST 26-31: National ACS Meeting, Philadelphia, PA. Contact: Meetings, ACS, 1155 16th Street, NW, Washington, DC, 20036, USA.

OCTOBER 1-5: 15th Int'l. Sympos. on Chromatography, Nuremberg, West Germany. Contact: K. Begitt, Ges. Deutscher Chemiker, Postfach 90 04 40, D-6000 Frankfurt Main, West Germany.

1985

FEBRUARY 11-14: Polymer 85, Int'l Symposium on Characterization and Analysis of Polymers, Monash University, Melbourne, Australia, sponsored by the Polymer Div., Royal Australian Chemical Inst. Contact: Polymer 85, RACI, 191 Royal Parade, Parkville Victoria 3052, Australia.

APRIL 28 - MAY 3: 189th National ACS Meeting, Miami Beach. Contact: A. T. Winstead, ACS, 1155 16th Street, NW, Washington, DC, 20036, USA.

SEPTEMBER 8-13: 190th National ACS Meeting, Chicago. Contact: A. T. Winstead, ACS, 1155 16th Street, NW, Washington, DC, 20036, USA

1986

APRIL 6-11: 191st National Am. Chem. Soc. Mtng., Atlantic City, NJ. Contact: A. T. Winstead, ACS, 1155 16th Street, NW, Washington, DC, 20036, USA.

SEPTEMBER 7-12: 192nd National Am. Chem. Soc. Mtng., Anaheim, Calif. Contact: A. T. Winstead, ACS, 1155 16th Street, NW, Washington, DC, 20036, USA

1987

APRIL 5-10: 193rd National Am. Chem. Soc. Mtng., Denver, Colo. Contact: A. T. Winstead, ACS, 1155 16th Street, NW, Washington, DC, 20036, USA.

AUGUST 30 - SEPTEMBER 4: 194th National Am. Chem. Soc. Mtng., New Orleans, LA. Contact: A. T. Winstead, ACS, 1155 16th Street, NW, Washington, DC, 20036, USA.

The Journal of Liquid Chromatography will publish announcements of interest to liquid chromatographers in every issue of the Journal. To be listed in the LC Calendar, we will need to know: Name of the meeting or symposium, sponsoring organization, when and where it will be held, and whom to contact for additional details. You are invited to send announcements to Dr. Jack Cazes, Editor, Journal of Liquid Chromatography, P. O. Box 1440-SMS, Fairfield, CT, 06430, USA.

INSTRUCTIONS FOR PREPARATION OF MANUSCRIPTS FOR DIRECT REPRODUCTION

Journal of Liquid Chromatography is a bimonthly publication in the English language for the rapid communication of liquid chromatographic research.

Directions for Submission

One typewritten manuscript suitable for direct reproduction, carefully inserted in a folder, and two (2) copies of the manuscript must be submitted. Since all contributions are reproduced by direct photography of the manuscripts, the typing and format instructions must be strictly adhered to. Noncompliance will result in return of the manuscript to the authors and delay its publication. To avoid creasing, manuscripts should be placed between heavy cardboards and securely bound before mailing.

Manuscripts should be mailed to the Editor:

Dr. Jack Cazes
Journal of Liquid Chromatography
P. O. Box 1440-SMS
Fairfield, Connecticut 06430

Reprints

Owing to the short production time for articles in this journal, it is essential to indicate the number of reprints required upon notification of acceptance of the manuscript. Reprints are available in quantities of 100 and multiples thereof. For orders of 100 or more reprints, twenty (20) free copies are provided. A reprint order form and price list will be sent to the author with the notification of acceptance of the manuscript.

Format of Manuscript

1. The general format of the manuscript should be as follows: title of article; names and addresses of authors; abstract; and text discussion.

2. Title and Authors: The entire title should be in capital letters and centered on the width of the typing area at least 2 inches (5.1 cm) from the top of the page. This should be followed by three lines of space and then by the names and addresses of the authors in the following way (also centered):

A SEMI-AUTOMATIC TECHNIQUE FOR THE
SEPARATION AND DETERMINATION OF
BARIUM AND STRONTIUM IN SURFACE WATERS
BY ION EXCHANGE CHROMATOGRAPHY AND
ATOMIC EMISSION SPECTROMETRY

F. D. Pierce and H. R. Brown
Utah Biomedical Test Laboratory
520 Wakra Way
Salt Lake City, Utah 84108

3. Abstract: Three lines below the addresses, the title ABSTRACT should be typed (capitalized and centered on the page). This should be followed by a single-spaced, concise, abstract comprising less than 10% of the length of the text of the article. Allow three lines of space below the abstract before beginning the article itself.

4. Text Discussion: Whenever possible, the text discussion should be divided into such major sections as INTRODUCTION, MATERIALS, METHODS, RESULTS, DISCUSSION, ACKNOWLEDGMENTS, and REFERENCES. These major headings should be separated from the text by two lines of space above and one line of space below. Each heading should be in capital letters, centered, and underlined. Secondary headings, if any, should be flush with the left margin, underscored, and have the first letter of all main words capitalized. Leave two lines of space above and one line of space below secondary headings.

5. Paragraphs should be indented five (5) typewriter spaces.

6. Acknowledgment of collaboration, sources of research funds, and address changes for an author should be listed in a separate section at the end of the paper.

7. References (including footnotes) in the text will be numbered consecutively by numbers in parentheses. All references (and footnotes) should then be aggregated in sequence at the end of the communication. No footnotes should be shown at the bottom of pages. The reference list follows immediately after the text. The word REFERENCES should be capitalized and centered above the reference list. It should be noted that all reference lists should contain initials and names of all authors; *et al.* will not be used in reference lists. Abbreviations of journal titles and styles of reference lists will follow the American Chemical Society's Chemical Abstracts List of Periodicals. References should be typed single-spaced with one line space between each reference.

8. Each page of manuscript should be numbered lightly at the bottom of the sheet with a light blue pencil.

9. Only standard symbols and nomenclature approved by the International Union of Pure and Applied Chemistry should be used.

10. Any material that cannot be typed, such as Greek letters, script letters, and structural formulae, should be drawn carefully in black India ink (do not use blue ink).

Typing Instructions

1. The manuscript must be typewritten on good quality white bond paper measuring approximately 8½ x 11 inches (21.6 cm x 27.9 cm). Do not use Corrisable bond or its equivalent. The typing area of the article opening page, including the title, should be 5½ inches wide by 7 inches deep (14 cm x 18 cm). The typing area of all other pages should be no more than 5½ inches wide by 8½ inches deep (14 cm x 21.6 cm).

2. In general, the chapter title and the abstract, as well as the tables and references, are typed single-spaced. All other text discussion should be typed 1½-line spaced, if available, or double-spaced. Prestige elite characters (12 per inch) are recommended, if available.

3. It is essential to use black typewriter ribbon (carbon film is preferred) in good condition so that a clean, clear impression of the letters is obtained. Erasure marks, smudges, creases, etc., may result in return of the manuscript to the authors for retyping.

4. Tables should be typed as part of the text but in such a way as to separate them from the text by a three-line space at both top and bottom of each table. Tables should be inserted in the text as close to the point of reference as possible, but authors must make sure that one table does not run over to the next page, that is, no table may exceed one page. The word TABLE (capitalized and followed by an Arabic number) should precede the table and be centered on the page. The table title should have the first letters of all main words in capitals. Titles should be typed single-spaced. Use the full width of the type page for the table title.

5. Drawings, graphs, and other numbered figures should be professionally drawn in black India ink (do not use blue ink) on separate sheets of white paper and placed at the end of text. Figures should not be placed within the body of the text. They should be sized to fit within the width and/or height of the type page, including any legend, label, or number associated with them. Photographs should be glossy prints. A typewriter or lettering set should be used for all labels on the figures or photographs; they may not be hand drawn. Captions for the pictures should be typed single-spaced on a separate sheet, along the full width of the

type page, and preceded by the word FIGURE and a number in arabic numerals. All figures and lettering must be of a size to remain legible after a 20% reduction from original size. Figure numbers, name of senior author, and arrow indicating "top" should be written in light blue pencil on the back or typed on a gummed label, which should be attached to the back of the illustration. Indicate approximate placement of the illustrations in the text by a marginal note in light blue pencil.

6. The reference list should be typed single-spaced although separated from one another by an extra line of space. Use Chemical Abstract abbreviations for journal titles. References to journal articles should include (1) the last name of all author(s) to any one paper, followed by their initials, (2) article title, (3) journal, (4) volume number (underlined), (5) first page, and (6) year, in that order. Books should be cited similarly and include (1) author, surname, first and middle initials, (2) title of book, (3) editor of book (if applicable), (4) edition of book (if any), (5) publisher, (6) city of publication, (7) year of publication, and (8) page reference (if applicable). E.g., Journals: Craig, L. C. and Konigsber, W., Use of Catechol Oxygenase and Determination of Catechol, *Chromatogr.*, 10, 421, 1963. Books: Albertsson, P. A., *Partition of Cell Particles and Macromolecules*, Wiley, New York, 1960. Article in a Book: Walter, H., *Proceedings of the Protoplasts of Biological Fluids, XVth Colloquium, Ptecters.*, H., eds., Elsevier, Amsterdam, 1968, p. 367.

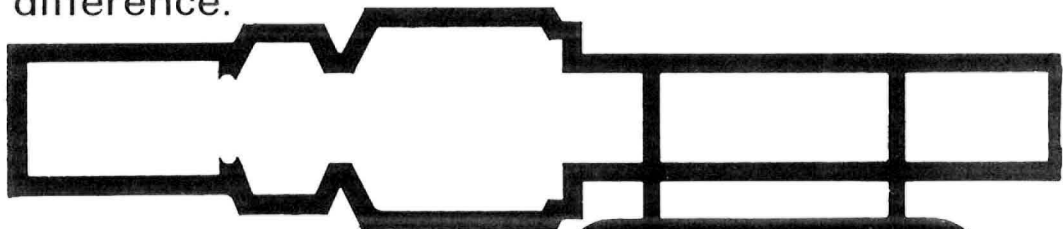
Custom packing HPLC columns has become our specialty. Any length, several ID's (including 3.2mm) and almost any commercially available packing material may be specified. We'll supply the column others won't.

With each column, you will receive the original test chromatogram plus a vial of the test mixture. Our advanced technology and computer testing is your assurance of a quality product.

When custom packing and testing is your special concern, we make the difference.

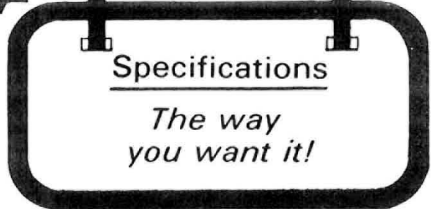
**Each
one
is
our
special
concern**

**CUSTOM
PACKED
HPLC
COLUMNS**



For further information contact:

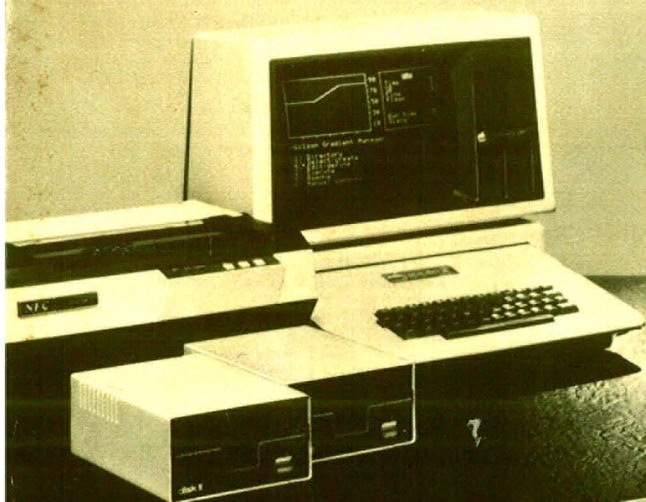
ALLTECH ASSOCIATES, INC.
2051 Waukegan Road
Deerfield, Illinois 60015
312/948-8600



ALLTECH ASSOCIATES

GILSON HPLC

**adds up to
the right system
at the right price.**



Going with Gilson can add up to this.
Gilson Gradient System with Apple-
base gradient Controller, Data Master
for peak analysis and programmable
201 fraction collector.

*...all for less than \$21,000.**

Modularity makes it work. Our add-on approach lets you match the right system to your application. And expansion through hardware and software additions will enhance your system's capabilities without costly duplication. Let Gilson modularity work for you. Contact us for complete information.



GILSON
INTERNATIONAL

Box 27, 3000 W. Beltline, Middleton, WI 53562
Telephone (608) 836-1551

B.P. No. 45, 95400, Villiers-le-Bel, France
Telephone (3) 990.54.41

**U.S. shipments only*